

Doctoral thesis

**Runoff event characteristics and their controls
for different runoff generation mechanisms**

submitted in satisfaction of the requirements for the degree of
Doctor of Science in Civil Engineering
of the Vienna University of Technology, Faculty of Civil Engineering

as part of the
Vienna Doctoral Programme on Water Resource Systems

by

Xiaofei Chen

Student registration number: 1428833

Kalsplatz 13, 1040 Vienna, Austria

under the supervision of

Prof. Günter Blöschl & Prof. Juraj Parajka

Institute of Hydraulic Engineering and Water Resources Management

Vienna University of Technology

Vienna, 2020

.....
Xiaofei Chen

Dissertation

Eigenschaften und Einflussgrößen von Abflussereignissen für unterschiedliche Abflussbildungsprozesse

ausgeführt zum Zwecke der Erlangung des akademischen Grades einer Doktorin
der technischen Wissenschaft

eingereicht an der Technischen Universität Wien Fakultät für Bauingenieurwesen
von

Xiaofei Chen

Matrikelnummer: 1428833

Karlsplatz 13, 1040 Wien, Österreich

unter der Leitung von

Prof. Günter Blöschl und Prof. Juraj Parajka
Institut für Wasserbau und Ingenieurhydrologie
Technische Universität Wien

Wien, 2020

.....
Xiaofei Chen

Examiners

Examiners

Univ. Prof. Dipl.-Ing. Dr. Günter Blöschl

Institute of Hydraulic Engineering and Water Resources Management, Department of Civil Engineering, Vienna University of Technology
Karlsplatz 13/222, 1040 Vienna, Austria

Ao. Univ. Prof. Dipl.-Ing. Dr. Matthias Zessner

Research Unit for Water Quality Management, Institute for Water Quality and Resource Management, Department of Civil Engineering, Vienna University of Technology
Karlsplatz 13/226, 1040 Vienna, Austria

Prof. Dipl.-Ing. Dr. Ralf Merz

Department Catchment Hydrology, Helmholtz-Centre for Environmental Research – UFZ
Theodor-Lieser-Str. 4, 06120 Halle (Saale), Germany

Gutachter

Gutachter

Univ. Prof. Dipl.-Ing. Dr. Günter Blöschl

Institut für Wasserbau und Ingenieurhydrologie, Fakultät für Bauingenieurwesen, Technische Universität Wien

Karlsplatz 13/222, 1040 Wien, Österreich

Ao. Univ. Prof. Dipl.-Ing. Dr. Matthias Zessner

Forschungsbereich Wassergütewirtschaft, Institut für Wassergüte und Ressourcenmanagement, Fakultät für Bauingenieurwesen, Technische Universität Wien

Karlsplatz 13/226, 1040 Wien, Österreich

Prof. Dipl.-Ing. Dr. Ralf Merz

Abteilung Einzugsgebietshydrologie, Helmholtz-Zentrum für Umweltforschung - UFZ

Theodor-Lieser-Str. 4, 06120 Halle (Saale), Deutschland

Abstract

Understanding the factors controlling event runoff and its variability in space and time is essential for solving many practical and scientific problems related to engineering design, flood risk prediction, water and agricultural management and the diagnostic evaluation of runoff generation processes.

Previous investigations have shown that the controls on event runoff differ between spatial scales. While infiltration rate, change in soil water storage and spatial connectivity are the main controls of the runoff response at the plot and hillslope scales, climate, physiographic characteristics and the runoff regime are the main controls at the regional scale. The event runoff characteristics at the small catchment scale are, however, still not fully understood.

The objective of this thesis is thus: (a) to investigate the spatial and temporal variability of event runoff characteristics at the small catchment scale; (b) to identify and evaluate the factors that control their variability; (c) to examine the role of different runoff generation mechanisms and subsurface hydrogeological characteristics in runoff response.

The thesis is organized into five chapters. Chapter 1 introduces the research context and the main objectives of the thesis. Chapter 2 examines the spatial and temporal variability of event runoff characteristics at the small catchment scale. The analysis is based on detailed hydrological observations at nine streamflow gauging stations in the Hydrologic Open Air Laboratory (HOAL, Petzenkirchen, Austria), where the gauged subcatchments represent different runoff generation systems. The results show that the runoff coefficients (R_c) and their variability tend to be largest for the tile drainages (mean $R_c=0.09$) and the main outlet (mean $R_c=0.08$). The magnitude of R_c for the tile drainage catchments is more than two times higher than in natural drainage systems and varies between the seasons. The recession time constants (T_c) do not differ much between different runoff generation systems and tend to be largest at the main outlet (mean $T_c =6.5$ hrs) and smallest for the tile drainages (mean $T_c=4.5$ hrs). The evaluation of the role of event precipitation, soil moisture and groundwater levels on the event runoff characteristics indicates that groundwater levels explain the temporal variability of R_c and T_c better than soil moisture or precipitation. These findings suggest an essential role of shallow flow paths for event runoff generation at the small catchment scale.

Chapter 3 identifies factors that control the variability of event R_c and T_c in the HOAL. Evaluation of the relative importance of the controls in individual runoff generation systems is based on three regression-based machine-learning techniques, i.e. Random Forests, Gradient Boost Decision Trees and Support Vector Machines (SVM). The results show that the SVM algorithm obtains the best model performance, and the performance is larger for R_c than that for T_c . The assessment of the relative importance of the explanatory variables suggests that R_c of the tile drainage systems is more strongly controlled by the weather conditions than by the catchment state. In contrast, the opposite is true for natural drainage systems. Overall, model performance at the small catchment scale strongly depends on the runoff generation type.

Although geology is often cited as an important factor driving event runoff response at the catchment scale, missing detailed field geological observations often limit the attribution of event runoff response to subsurface and geological conditions. The aim of Chapter 4 is to link the variability of event runoff to climate and geology characteristics in small and medium catchments. The role of climate (i.e. event precipitation volume, precipitation intensity and

antecedent precipitation) and runoff regime (i.e. initial flow before runoff event and event duration) characteristics in the context of the seasonal dynamics of runoff response is examined in different hydro-geological settings by detailed field mapping. The results show that the hydro-geological mapping helps to explain and attribute the characteristics of runoff response. The largest R_c , largest event peaks and the fastest recessions are observed in the catchment with the largest precipitation, lowest permeability, steep hillslopes, and with a large proportion of areas characterized by shallow interflow processes. In contrast, catchments that are drier and have a significant portion of deep groundwater flow and largest permeability are characterized by the lowest R_c , lowest event peaks and longest T_c .

The final part of the thesis provides a synthesis of the findings, an outlook to future research and the conclusions. Overall, the findings of the thesis complement the current understanding of the variability of event runoff characteristics at the small catchment scale. While previous studies have showed that climate and mean annual precipitation controls runoff response at the regional scale, at the small catchment scale the event runoff response is predominantly related to the main runoff generation mechanism. The thesis demonstrates that in small agricultural catchments, groundwater levels explain the variability of runoff response better than soil moisture or precipitation, suggesting an important role of connectivity and the location of flow paths. The use of field mapping of hydro-geological flow paths has shown the importance and usefulness of such information for interpreting the spatial and temporal variability of event runoff characteristics. The thesis provides illustrative examples of the link between geology, climate and runoff response. It demonstrates the value of detailed long term hydrological observations and field hydro-geological mapping for understanding the runoff response at the medium catchment scale, which provides an avenue toward improving predictions of event runoff and transferring them to a regional scale.

Kurzfassung

Das Verständnis der Faktoren, die das Verhalten und die raum-zeitliche Variabilität von Abflussereignissen beeinflussen, ist für viele praktische und wissenschaftliche Problemstellungen notwendig, wie etwa die wasserbauliche Bemessung, Hochwasserrisikovorhersage, Wasser- und Landmanagement, oder die diagnostische Bewertung von Abflussbildungsprozessen.

Bisherige Untersuchungen haben gezeigt, dass sich die Einflussfaktoren der Abflussbildungsprozesse je nach räumlicher Skala unterscheiden. Während vorwiegend Infiltrationsrate, Änderungen der Bodenfeuchtigkeit und Konnektivität die lokalen Abflussbildungsprozesse beeinflussen, sind es auf der regionalen Skala das Klima, die physiographischen Eigenschaften und das Abflussregime. Das Abflussverhalten auf der Skala von kleinen Einzugsgebieten ist allerdings noch nicht vollständig erforscht.

Diese Dissertation stellt sich daher die folgenden Ziele: (a) die räumliche und zeitliche Variabilität des Abflussverhaltens während Niederschlagsereignissen auf der Skala von kleinen Einzugsgebieten zu untersuchen; (b) die Faktoren, die die Variabilität des Abflussverhaltens beeinflussen, zu identifizieren; (c) die Rolle verschiedener Abflussbildungsprozesse und unterirdischer hydrogeologischer Eigenschaften bei der Abflussbildung zu analysieren.

Die Dissertation ist in fünf Kapitel gegliedert. Kapitel 1 beschreibt das Ziel und den Kontext der Arbeit. Kapitel 2 untersucht die räumliche und zeitliche Variabilität der Eigenschaften der Abflussereignisse in einem kleinen Einzugsgebiet. Die Untersuchung basiert auf umfangreichen hydrologischen Beobachtungen an neun Pegeln im Hydrologic Open Air Laboratory (HOAL, Petzenkirchen, Österreich), deren Kleinsteneinzugsgebiete verschiedene Abflussbildungsprozesse repräsentieren. Die Ergebnisse zeigen, dass die Abflussbeiwerte (R_c) und ihre Variabilität am höchsten sind in den drainagierten Gebieten (durchschnittlicher $R_c=0.09$) und am Gebietsauslass (durchschnittlicher $R_c=0.08$). Die R_c der drainagierten Gebiete sind oft mehr als zweimal größer als die der natürlichen Gebiete, und R_c ändert sich je nach Jahreszeit. Die Rezessionszeitkonstanten (T_c) unterscheiden sich nur gering zwischen den Abflussbildungsprozessen. Sie sind am größten für den Gebietsauslass (durchschnittliches $T_c=6.5$ Stunden) und am kleinsten in den drainagierten Gebieten (durchschnittliches $T_c=4.5$ Stunden). Die Ergebnisse zeigen, dass der Grundwasserspiegel die zeitliche Variabilität von R_c und T_c besser erklärt, als die Bodenfeuchte oder der Niederschlag. Diese Ergebnisse weisen auf die wichtige Rolle der oberflächlichen Fließwege bei den Abflussbildungsprozessen in kleinen Einzugsgebieten hin.

In Kapitel 3 werden Faktoren identifiziert, die die Variabilität von R_c und T_c im HOAL steuern. Die relative Bedeutung der Einflussgrößen auf R_c und T_c für unterschiedliche Abflussbildungsprozesse wird mit drei regressionsbasierten Machine-Learning Techniken evaluiert, Random Forests, Gradient Boost Decision Trees und Support Vector Machines (SVM). Die Ergebnisse zeigen, dass der SVM Algorithmus die besten Ergebnisse liefert, und die Ergebnisse für R_c besser sind als für T_c . Die Bewertung der relativen Wichtigkeit der Erklärungsvariablen zeigt, dass R_c der drainagierten Gebiete von der Wettersituation stärker beeinflusst wird als vom hydrologischen Zustand des Einzugsgebiets. Das Gegenteil trifft für die natürlichen Gebiete zu. Insgesamt hängt die Modellgüte in diesem kleinen Einzugsgebiet stark von den Abflussbildungsprozessen ab.

Obwohl die Geologie häufig als wichtiger Faktor für die Abflussbildung und Abflusskonzentration genannt wird, ist es wegen des Mangels an detaillierten geologischen Feldmessungen nicht einfach, das Abflusssignal den unterirdischen und geologische Bedingungen zuzuordnen. Das Ziel des Kapitels 4 ist es, die Variabilität von Abflussereignissen in kleinen und mittleren Einzugsgebieten mit dem Klima und der Geologie zu verknüpfen. Es untersucht daher den Einfluss von Klima (das Niederschlagsvolumen während der Ereignisse, die Niederschlagsintensität und der Vorregen) und Abflussregime (der initiale Abfluss vor einem Ereignis und die Ereignisdauer) auf die saisonale Dynamik der Abflussreaktion von Einzugsgebieten mit unterschiedlichen hydrogeologischen Eigenschaften, die durch Feldbeobachtungen charakterisiert wurden. Die Ergebnisse zeigen, dass die hydrogeologischen Feldbeobachtungen helfen können, die Reaktion des Einzugsgebiets auf Niederschläge zu erklären und ihren Ursachen zuzuordnen. Das Einzugsgebiet mit dem höchsten Niederschlagsvolumen, der niedrigsten Durchlässigkeit, steilen Hängen und dem höchsten Anteil von Flächen mit oberflächlichem Zwischenabfluss hat die größten R_c , die höchsten Abflussspitzen und die schnellste Reaktion. Die Einzugsgebiete, die trockener sind und einen hohen Anteil von Flächen mit tiefem Grundwasser haben, besitzen hingegen die kleinsten R_c , die kleinsten Abflussspitzen und das längste T_c .

Das letzte Kapitel präsentiert eine Synthese der Ergebnisse, einen Ausblick auf die zukünftige Forschung und die Schlussfolgerungen. Insgesamt erweitern die Ergebnisse dieser Dissertation unser Verständnis der Variabilität der Eigenschaften des Abflusses bei Niederschlagsereignissen in kleinen Einzugsgebieten. Während frühere Studien gezeigt haben, dass das Klima und der mittlere Jahresniederschlag den Abfluss auf der regionalen Skala beeinflussen, sind es auf der Skala von kleinen Einzugsgebieten primär die Abflussmechanismen. Die Dissertation zeigt, dass der Grundwasserspiegel die Variabilität der Abflussbildung in kleinen landwirtschaftlichen Einzugsgebieten mehr beeinflusst als der Niederschlag und die Bodenfeuchte. Dieses Ergebnis weist auf die bedeutende Rolle der Konnektivität und der Lage der Fließwege hin. Die Verwendung von hydrogeologischen Feldbeobachtungen kann sehr hilfreich sein für die Interpretation der räumlichen und zeitlichen Eigenschaften des Abflusses bei Niederschlagsereignissen. Die Dissertation gibt illustrative Beispiele der Zusammenhänge zwischen Geologie, Klima und Abflussbildung. Sie demonstriert den Wert von langfristigen hydrologischen und hydrogeologischen Feldbeobachtungen, die wesentlich sind, um die Abflussbildung in mittleren Einzugsgebieten besser zu verstehen. Damit entsteht eine Grundlage für genauere Abflussvorhersagen und für die Skalierung auf die regionale Skala.

Funding information

Funding information

This work has been conducted as part of the following research projects:

Vienna Doctoral Programme on Water Resource Systems (DK W1219-N28) of the Austrian Science Funds (FWF).

China Scholarship Council (CSC) (201406710002)

Acknowledgements

I would like to express my great appreciation and respect to Prof. Günter Blöschl and Prof. Juraj Parajka, who supervised my PhD thesis and supported my research with a lot of patience during these years. They have provided me with many constructive and valuable suggestions on both my research and writing skills. I am also grateful for the precious chance provided by Prof. Günter Blöschl to study in Vienna.

I would like to thank my colleagues in Petzenkirchen, who also gave me a lot of support on my field work and my research. They generously share lots of data in Petzenkirchen with me which has made my research more precise and comprehensive.

I would like to thank my colleagues at the TU Wien, especially Borbála Széles and Rui Tong for providing a harmonious environment of corporation. Borbála Széles is always warm-hearted and has kept a serious attitude towards my questions regarding my research progress. Rui Tong has always been happy to exchange research methods and ideas with me. The inspiration from the discussions with them has been very valuable for me.

I would also like to thank the students of the Vienna Doctoral Programme on Water Resources Systems for organizing a symposium every year and for providing many chances to exchange research results with other PhD studies.

Finally, I would like to express my deep gratitude to my parents and friends who have given me great love and tolerance to support my studies in Vienna.

Content

Examiners 3

Gutachter 4

Abstract 5

Kurzfassung 7

Funding information 9

Acknowledgements 10

Content 11

1. Introduction 14

2. Spatial and temporal variability of runoff event characteristics in a small agricultural catchment 18

 2.1. General 18

 2.2. Key points 18

 2.3. Abstract 18

 2.4. Introduction 18

 2.5. Study area and data 20

 2.6. Methodology 23

 2.7. Results 26

 2.7.1. Runoff responses for various runoff generation mechanisms 26

 2.7.2. Seasonal variability of runoff event characteristics and potential controllers 27

 2.7.3. Effects of potential controllers on spatial variability of runoff response 31

 2.8. Discussion 38

 2.8.1. Spatial and seasonal variability of runoff event characteristics 38

 2.8.2. Process controls on runoff event characteristics 38

 2.9. Conclusions 39

3. Controls on event runoff coefficients and recession time constants for different runoff generation mechanisms identified by three regression methods 40

 3.1. General 40

 3.2. Key Points 40

 3.3. Abstract 40

 3.4. Introduction 41

 3.5. Study area and data 42

 3.6. Methodology 46

 3.6.1. Estimation of event runoff coefficients and recession time constants 46

3.6.2.	Ensemble learning techniques for regression	47
3.6.2.1.	Random Forests (RF).....	47
3.6.2.2.	Gradient Boost Decision Trees (GBDT)	48
3.6.2.3.	Support Vector Machines (SVM).....	48
3.6.3.	Calibration and validation performance of the non-linear regression models	49
3.7.	Results	49
3.7.1.	Evaluation of the runoff event characteristics and their potential controls	49
3.7.2.	Parameter sensitivities of the three non-linear regression models.....	52
3.7.2.1.	RF model (<i>n_{tree}</i> and <i>m_{try}</i>).....	52
3.7.2.2.	GBDT model (<i>n.trees</i>)	54
3.7.2.3.	SVM model (γ , ϵ and <i>C</i>).....	55
3.7.3.	Temporal calibration and validation performance of regression models.....	56
3.7.4.	Spatial calibration and validation performance of regression models	58
3.7.5.	Linear correlations of <i>R_c</i> and <i>T_c</i> with the explanatory variables	59
3.7.6.	Importance of explanatory variables for <i>R_c</i> and <i>T_c</i>	60
3.8.	Discussion	61
3.9.	Conclusions	62
4.	Impact of climate and geology on runoff event characteristics at the regional scale	64
4.1.	General	64
4.2.	Key points	64
4.3.	Abstract	64
4.4.	Introduction	65
4.5.	Study area and data	66
4.5.1.	Study areas	66
4.5.2.	Meteorological and hydrological data	68
4.6.	Methodology	69
4.6.1.	Estimation of event runoff characteristics	69
4.6.2.	Potential impact variables of runoff response.....	70
4.7.	Results	71
4.7.1.	Spatial and temporal variability of runoff response.....	71
4.7.2.	Distributions of event and precipitation characteristics.....	73
4.7.3.	Effects of event and precipitation characteristics on runoff response.	77
4.8.	Discussion	82
4.9.	Conclusions	84

5. Summary and conclusions	85
References.....	88
Appendix A1.....	95
Appendix A2.....	95
Appendix A3.....	98

1. Introduction

Runoff response to precipitation is a fundamental process analysed by many hydrologists since the earliest days of hydrological research. The runoff coefficient, recession time constant, and peak flow are three main characteristics of a runoff event, which have been widely applied in runoff simulation and prediction, engineering design of flood control and regulation, silt carrying management and erosion management. Representing the complex transformation of precipitation into the runoff, event runoff coefficient is defined as the ratio of precipitation volume that becomes quick/direct runoff (*Gottschalk and Weingartner, 1998; Longobardi et al., 2003; Penna et al., 2011*). For characterizing the recession rate after the runoff event peak, event recession time constants are used by hydrologists as an indicator of catchment aquifer storage (*Krakauer and Temimi, 2011; Patnaik et al., 2015; Vogel and Kroll, 1996*). In the single linear reservoir model, both runoff coefficient and recession time constant are critical parameters controlling the event runoff hydrographs for a specific precipitation event. *Merz et al. (2006)* have estimated them by using runoff observations in 337 Austrian catchments. Runoff event peak flow is a significant engineering indicator for evaluating the flood risk. *Villarini and Smith (2010)*, for example, have examined them for the regional distribution of annual maximum peak discharge in 572 stations of the United States.

The spatial and temporal dynamics of event runoff characteristics have been relevant questions for a long time. Although spatial patterns of mean event based runoff coefficients have been shown to be consistent with climate indicators (*Merz and Blöschl, 2009; Norbiato et al., 2009*), the impact of catchments characteristics and runoff generation mechanism on event runoff characteristics are still not well understood. Depending on the runoff generation mechanisms, the seasonal dynamics of event based runoff coefficient can be significantly different (*Tarasova et al., 2018a*). There is only a limited knowledge on how event precipitation, soil moisture, groundwater or infiltration characteristics control the seasonal dynamics of runoff response in various runoff generation systems. Additionally, the spatial patterns of event based recession time constants are rarely studied, but its variability across recession events have been shown to be connected to catchment storage (*Patnaik et al., 2015*). *Biswal and Nagesh Kumar (2014a)* have proposed that the spatial dynamics of runoff event recession could also be related to rainfall variations. However, how runoff event recession and peak flow vary between runoff generation systems, and what are the controlling factors of this variability needs to be further investigated.

A significant role of climate in shaping the spatial variability of runoff coefficients has been shown by a number of studies (*Del Giudice et al., 2012; Merz and Blöschl, 2009; Norbiato et al., 2009*). For example, a large spatial variation of runoff coefficient in 12 cropland hillslopes of the United States has been observed by *Chen et al. (2019)* under the same climate conditions. This phenomenon implies that the spatial variability of runoff coefficient is also influenced by subsurface characteristics (like saturated conductivity, soil properties, topography, geological structures etc.) after eliminating climate variations. *Gottschalk and Weingartner (1998)* have found that quick drainage tends to be larger for steeper catchment slopes in pre-alpine catchments, resulting in higher runoff coefficients. Additionally, storm runoff coefficients may decrease as slope length increases, which has been examined by *Wainwright and Parsons (2002)*. Similarly, based on the analysis of three catchments with similar slope gradients, soil types and land use, *Cerdan et al. (2004)* have concluded that, as the area increases, runoff coefficients decrease. For catchments with various geological structures, *Norbiato et al. (2009)* point out that

subsurface permeability may be a relevant control on runoff coefficients when the mean annual precipitation is less than 1200 mm. All in all, subsurface characteristics, such as infiltration rate, soil water storage, subsurface structure etc., directly influence the dominant runoff generation mechanisms and further indirectly impact the spatial variations of event based runoff coefficients (Scherrer *et al.*, 2007). Therefore a comparison of runoff coefficients between different runoff generation mechanisms would give us new insights into their physical controls. Part of this thesis will focus on the relations between runoff generation and event based runoff coefficients.

From the point of view of the seasonal change of event based event runoff coefficients for a specific catchment, summer event based runoff coefficients are often lower than those in other seasons because of drier subsurface conditions and higher evapotranspiration rates (Merz and Blöschl, 2009; Rodríguez-Blanco *et al.*, 2012; Tian *et al.*, 2012). For some high alpine catchments, a summer decrease of runoff coefficient could be delayed because of late snowmelt, as evidenced by a significant effect of snowmelt on the seasonal dynamics of runoff events (Merz and Blöschl, 2009). In a subsurface dominated catchment in Spain, Rodríguez-Blanco *et al.* (2012) showed that the seasonal variability of event runoff coefficient is controlled both by soil moisture and rainfall amount. However, Norbiato *et al.* (2009) indicate that the effect of soil moisture is relatively large only in basins with intermediate subsurface storage capacities. Although runoff coefficients seem to be consistently lower in summer, the magnitude of the variability and exact period of low values are different for catchments dominated by different runoff generation mechanisms. Even in one catchment such as the Blue River basin, runoff generation could change with time. Tian *et al.* (2012) confirmed three processes (surface depressions, canopy interception and soil cracking) which could explain a runoff coefficient drop between spring and summer. Runoff generation mechanisms therefore influence both the spatial and the temporal variations of runoff coefficients. It will be interesting to test whether the effects of subsurface wetness and precipitation on runoff coefficients are consistent for various runoff generation mechanisms.

Runoff event recession processes reflect not only the relationship between storage and discharge but also travel pathways of subsurface water. Drainage of water storage could be retarded in different ways by various geological structures (Blume *et al.*, 2007; Tallaksen, 1995). Besides, Tallaksen (1995) also indicates that different flow paths, including surface flow, unsaturated/saturated interflow and groundwater flow, have different storage residence times, and the recession of groundwater flow tends to be slower than other flow paths. Therefore runoff generation mechanisms are significant factors influencing the spatial distribution of runoff event recessions. These will be further discussed in this thesis in diverse catchments. Furthermore, subsurface conditions, such as hydrological and geological properties of the aquifer, soil moisture and texture etc., are critical considerations for analyzing runoff generation mechanisms. As for specific aquifer features, Dewandel *et al.* (2003) show that aquifer thickness and hydrodynamic parameters (such as the aquifer permeability) control the stream and spring recession forms. In impervious areas with extremely low permeability, runoff event recession tends to be faster, and peak magnitude tends to be larger (Burns *et al.*, 2005). Moreover, the variability of recession rate tends to be decrease with spatial scale in nested basins under similar geophysical and climate conditions (Chen and Krajewski, 2015). This thesis will further discuss the recession features of various runoff generation mechanisms in catchments with the same and different geological structures and discuss the principle controls of the spatial variability of runoff event recession.

Runoff event early-time recession processes can be nonlinear with more variability than the late-time recession process (*Blume et al., 2007; Chen and Krajewski, 2015*). Its relationship with antecedent catchment storage has been studied by many researchers, because recession water not only directly drains rainfall/snowmelt during a runoff event, but also past stored water (*Biswal and Nagesh Kumar, 2014a; b; Patnaik et al., 2015; Shaw et al., 2013*). Event runoff recession tends to be faster in summer, which is thought to be caused by increased evapotranspiration (*Federer, 1973*), but *Shaw et al. (2013)* find stronger linkages between recession and catchment storage in at least nine catchments instead of with evapotranspiration. Furthermore, the relationship between recession and past average discharge (as an index of catchment storage) is controlled by topographical characteristics (*Patnaik et al., 2015*). Another potential factor influencing the relationship between catchment storage and runoff event recessions is precipitation, and precipitation could also indirectly influence such relations by controlling runoff event peaks, as identified by *Biswal and Nagesh Kumar (2014a)*. All in all, functions of potential controls on event runoff recessions vary with different topographical and climate conditions. In individual catchments, however, the impact of storage and precipitation on the temporal dynamics of event recessions still needs to be investigated in more detail.

The overall objective of this thesis is to investigate spatial and temporal variability of event runoff characteristics (i.e. runoff coefficient, recession time constant and peak flow) and to identify and evaluate the factors that control their variability at the small catchment scale. The intention is to advance the understanding of the role of different runoff generation systems and hydrogeological characteristics in the formation of runoff response of small catchments.

The research part of the thesis is organized into three chapters (Chapter 2-4). Chapter 2 explores the spatial and temporal variability of event runoff characteristics at the small catchment scale. The analysis is based on detailed hydrological observations at nine streamflow gauging stations in the Hydrologic Open Air Laboratory (HOAL, Petzenkirchen, Austria), where the gauged sub-catchments represent different runoff generation systems. This part of the thesis compares the runoff event characteristics between the sub-catchments and the main outlet for various magnitudes of flood peaks, event precipitation, antecedent soil moisture and groundwater levels.

To evaluate the relative importance of the controls in individual runoff generation systems, Chapter 3 builds explanatory regression models to predict runoff event runoff coefficients and recession time constants. The models are based on three regression-based machine-learning techniques, i.e. Random Forests, Gradient Boost Decision Trees and Support Vector Machines (SVM).

Although geology is often cited as an important factor modulating event runoff response at the catchment scale, missing detailed field geological observations often limit the attribution of event runoff response to subsurface and geological conditions. In order to explore a wider range of geologies than that present in the HOAL, Chapter 4 investigates four other Austria catchments from small to median scale with the aim to link the variability of event runoff response to climate and geology characteristics in small and medium catchments. The chapter examines the role of climate (i.e. event precipitation volume, precipitation intensity and antecedent precipitation) and runoff regime (i.e. initial flow before a runoff event and event duration) on the seasonal dynamics of runoff response in different hydro-geological settings using detailed field mapping.

Finally, Chapter 5 concludes the thesis with a summary of the key findings and discusses potential future extensions of the research to further advance the understanding of runoff

response dynamics in small headwater catchments, and to identify the role of runoff generation systems for improving the predictions of runoff hydrographs.

2. Spatial and temporal variability of runoff event characteristics in a small agricultural catchment

2.1. General

The goal of this chapter was to understand the role of runoff generation mechanisms on runoff response under the same climate conditions.

The chapter investigates the spatial and temporal variability of runoff event characteristics for different runoff generation mechanisms. We explore the controlling process of runoff event characteristics, such as soil moisture, flow paths and precipitation, for different runoff generation mechanisms.

The present chapter is based on the following scientific publication:

Chen, X., Parajka, J., Széles, B., Strauss, P., & Blöschl, G. (2020). Spatial and temporal variability of event runoff characteristics in a small agricultural catchment. *Hydrological Sciences Journal*, 65(13), 2185-2195. doi:10.1080/02626667.2020.1798451

2.2. Key points

1. Tile drainage runoff events generally have larger ratios of discharge than other discharges due to the better discharge conditions as a consequence of underground pipes.
2. Runoff event characteristics are generally more influenced by initial conditions than event precipitation volume in a small agricultural catchment.
3. The dynamics of pre-event groundwater levels can better explain the temporal variability of event based runoff coefficients and recession time constants than antecedent soil moisture.

2.3. Abstract

The objective of this study is to investigate the factors that control event runoff characteristics at the small catchment scale. The study area is the Hydrological Open Air Laboratory, Lower Austria. Event runoff coefficient (R_c), recession time constant (T_c) and peak discharge (Q_p) are estimated from hourly discharge and precipitation data for 298 events in the period 2013-2015. The results show that the R_c and their variability tend to be largest for the tile drainages (mean $R_c = 0.09$) and the main outlet (mean $R_c = 0.08$) showing larger R_c in January/February and smaller R_c in July/August. T_c does not vary much between the systems and tends to be largest at the main outlet (mean $T_c = 6.5$ hrs) and smallest for the tile drainages (mean $T_c = 4.5$ hrs). Groundwater levels explain the temporal variability of R_c and T_c more than soil moisture or precipitation, suggesting a role of shallow flow paths.

2.4. Introduction

Formation of runoff during rainfall events is controlled by climate and physiographic catchment characteristics and depends on the runoff generation processes. The infiltration excess mechanism is mainly controlled by precipitation intensity and infiltration capacity while the saturation excess mechanism is mainly controlled by precipitation volume and soil depth (*Tian et*

al., 2012). Both affect event runoff characteristics such as the runoff coefficient, the recession time constant and the runoff peaks (*Merz et al.*, 2006; *Ruggenthaler et al.*, 2015).

Event runoff coefficient indicates the ratio of direct flow volume to total event rainfall, so it is an important parameter in engineering design (*Blume et al.*, 2007; *A. Viglione et al.*, 2009). It indirectly reflects not only hydrological conditions but also catchment characteristics and different runoff generation mechanisms. Especially in agricultural catchments, understanding factors controlling runoff coefficient is an essential information for management agricultural practices and preventing erosion (*García-Ruiz et al.*, 2008). The runoff recession time constant is a measure of the time required after rainfall for streams to return to their base flow levels (*Czikowsky and Fitzjarrald*, 2004). It is usually described by a simple linear reservoir model and indicates the interaction between groundwater and surface flow (*Merz et al.*, 2006). Understanding the factors controlling recession flows is critical mainly for water supply, irrigation, water quality and erosion. Besides, the magnitude of event peak flow is an important hydrological characteristic used in flood risk and design estimation (*Gottschalk and Weingartner*, 1998; *La Torre Torres et al.*, 2011).

Previous studies examining event runoff characteristics found that the controlling factors differ with the spatial scale. The connectivity between the ‘infiltrating’ and ‘runoff producing’ areas explains variability of event runoff characteristics from plot to small catchments scales, and as found by *Joel et al.* (2002) and *Cerdan et al.* (2004), event runoff coefficient at this scale tends to significantly decrease with increasing catchment size. The differences in connectivity of flow paths can explain the differences in runoff response between plot and small catchment scale, but are less important for larger catchments. In small catchments, land use plays an important role (*Cerdan et al.*, 2004) and may have significant impact on streamflow recession by increasing recession constant with increasing percentage of impervious areas (*Burns et al.*, 2005) and affect the variability in frequency, seasonality and magnitude of runoff event peaks (*García-Ruiz et al.*, 2008).

Evaluation of event runoff characteristics at the plot and hillslope scale based on experiments show that the main controls depend on the interactions between infiltration rate, change in soil water storage and drainage of the soil water (*Ruggenthaler et al.*, 2015; *Scherrer et al.*, 2007). At the catchment scale, runoff formation is less understood, mainly because of the large spatial variability of the environment and the connectivity of runoff flow paths (*Cerdan et al.*, 2004; *James and Roulet*, 2007; *Silasari et al.*, 2017; *Western et al.*, 1998). Statistical analyses of flow data in medium and large catchments show that the main controls of the spatial variability of event runoff characteristics at the regional scale are mean annual precipitation and the runoff regime (*Merz et al.*, 2006), physiographic catchment characteristics (*Gottschalk and Weingartner*, 1998) and antecedent soil moisture (*Norbiato et al.*, 2009). Often, similarly to the plot scale (*Ruggenthaler et al.*, 2015), only a weak correlation between event runoff characteristics and soil type or land use has been found at the regional scale (*Merz et al.*, 2006).

Temporal changes in event runoff characteristics at the regional scale are mostly related to the volume of rainfall and pre-event soil moisture (*Chiffard et al.*, 2018; *La Torre Torres et al.*, 2011; *Penna et al.*, 2011; *Tarasova et al.*, 2018a; *Tarasova et al.*, 2018b). The runoff coefficients tend to be high in winter and spring when soil moisture is high and lower in summer when catchments are dryer (*Merz and Blöschl*, 2009). The role of pre-event soil moisture at the plot scale depends on the subsurface storage of the catchments and the dominant runoff generation

processes (Rodríguez-Blanco *et al.*, 2012; Scherrer *et al.*, 2007). In regions with poorly developed soils, the relationship between runoff coefficients and pre-event soil moisture tends to be strongly nonlinear, while permeable soils tend to exhibit more linear relationships (Tarasova *et al.*, 2018a; Tarasova *et al.*, 2018b).

The results of previous studies on event runoff characteristics indicate that there is a scale gap between plot experiments and comparative regional analyses of medium to large catchments. The objective of the study is thus to investigate the spatial and temporal variability of event runoff characteristics at the small catchment scale. The aim is to identify and evaluate the factors that control the variability of the event runoff coefficient, the recession time constant and the peak discharge in a small agricultural catchment where the individual tributaries are characterized by different runoff generation systems. The investigation evaluates the role of event precipitation, soil moisture and groundwater for event runoff characteristics of the different runoff generation systems.

2.5. Study area and data

The study area is a small experimental catchment, the Hydrological Open Air Laboratory (HOAL) in Petzenkirchen, Lower Austria (Figure 1). HOAL is an agricultural catchment situated approximately 100 km west of Vienna (48°9'N, 15°9'E). The main land use is arable land (87%), forest and pastures. The size of the catchment is 66 ha and the elevation varies between 268 and 323 m a.s.l. The main stream is approximately 620 m long and has a medium slope of 2.4% (Blöschl *et al.*, 2016).

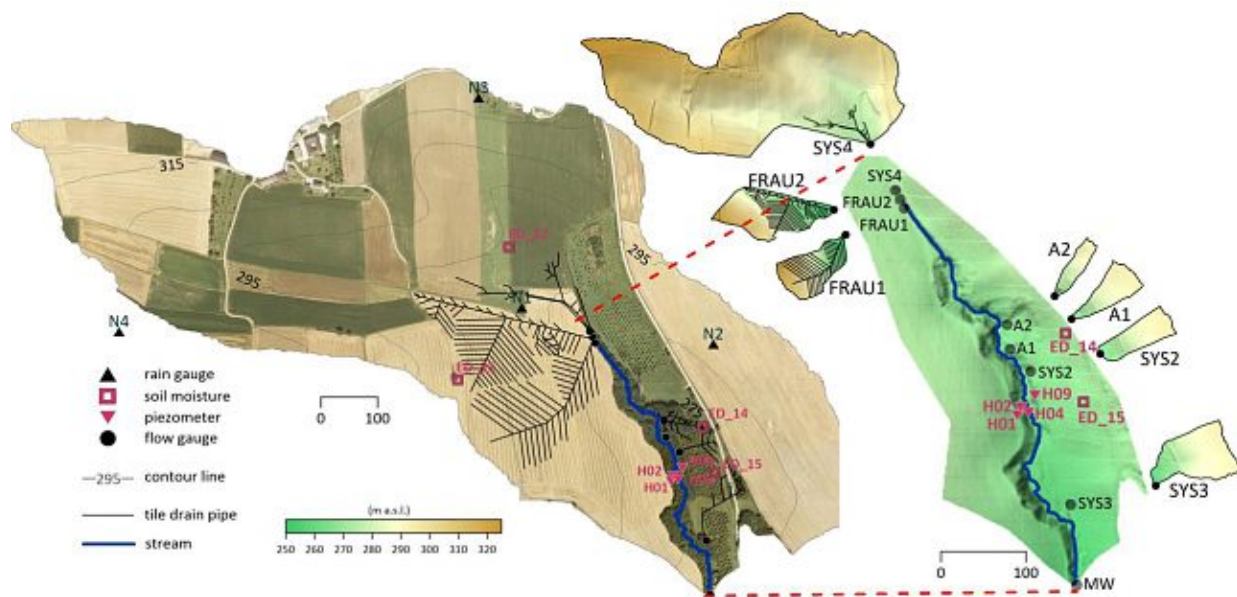


Figure 1. Study area and location of the rain gauges (black triangles), soil moisture sensors (squares), groundwater piezometers (red triangles) and stream gauges (circles) Left: orthophoto of the HOAL catchment and location of the tile drainage system. Right: zoom in to the tributary catchments and their topography.

The climate of the region is classified as warm and temperate (Cfb class of The Köppen-Geiger climate classification) with a mean annual temperature of 9.3°C, a mean annual precipitation of

around 750 mm and a mean annual flow of about 4 L/s (*Blöschl et al.*, 2016). The main geology classes of the HOAL consist of Tertiary fine sediments and fractured siltstone of the Molasse zone and the dominant soil types are Cambisols (57%), Kolluvisol (16%), Planosols (21%) and Gleysols (6%) (*Blöschl et al.*, 2016).

The observation period analysed in this chapter is 2013-2015. Rainfall is measured by four OTT Pluvio raingauges within or near the catchment (Figure 1). Streamflow is measured by calibrated H-flumes with pressure transducers (Figure 1). Both measurements are carried out at 1 min temporal resolution. The gauged tributaries represent different runoff generation systems (Table 1). The contributions from the wetland areas in the south-eastern part of the catchment are measured at sites A1 and A2. While Sys2 and Sys3 are perennial streams and contribute to the flow of the main stream throughout the whole year, Frau1, Frau2 are ephemeral and mainly consist of tile drains. During low flow conditions, Sys3 behaves as a combination of a tile drain and a wetland as it collects water from saturated areas near the stream. The upper part of the stream is piped and enters the main stream at inlet Sys4. The catchment area and mean flow of each runoff generation system is given in Table 1.

All streamflow data were quality checked and aggregated to an hourly time step. Catchment boundaries were derived from a 1-m digital elevation model (DEM), additionally accounting for the position of the tile drain pipes (*Széles et al.*, 2018).

For the analysis of initial soil moisture, the soil moisture measurements from sensors (ED14, ED15, ED21 and ED22) at 5, 10 and 20 cm depth were integrated over depth to represent the mean profile soil moisture. The soil moisture monitoring started in August 2013, so for the first 15 events, the initial soil moisture information is missing. The sensors used for different sub-catchments are shown in Table 1. For the analysis of the initial groundwater conditions, the mean value of four piezometer readings (H01, H02, H04 and H09) is calculated and used in all sub-catchments and the main outlet. The initial groundwater levels can slightly differ between the sub-catchments as the exact time of event start can be different.

Spatial and temporal variability of runoff event characteristics in a small agricultural catchment

Table 1. Characteristics of HOAL catchment and its sub-catchments used in this chapter. SD: standard deviation.

Gauge	Runoff generation system	Estimated drainage area (ha)	Mean drainage area slope (%)	SD of mean drainage area slope	Forest coverage (ha)	Mean streamflow 2013–2015 (mm/hrs)	SD of mean streamflow	Soil moisture sensor station
A1	Wetland	2.1	8.90	6.56	0.25	0.025	0.036	ED14
A2	Wetland	1.1	11.53	6.55	0.17	0.029	0.024	ED14
FRAU1	Ephemeral tile drain	3.1	7.00	2.21	0.00	0.024	0.053	ED21
FRAU2	Ephemeral tile drain	4.8	9.07	3.74	0.01	0.012	0.028	ED21
SYS2	Natural drainage	2.4	9.73	7.05	0.45	0.026	0.018	ED15
SYS3	Natural drainage (with wetland)	4.3	10.04	6.06	0.61	0.008	0.015	ED15
SYS4	Natural drainage (inlet pipe)	37.4	10.91	5.84	1.73	0.007	0.011	ED22
MW	Outlet system) (aggregated)	65.8	10.65	6.67	6.32	0.023	0.045	Mean of ED14, ED15, ED21 and ED22

2.6. Methodology

The rainfall–runoff events were separated by using the automatic method of *Merz et al.* (2006). Five parameters need to be optimized (see Appendix A1). It consists of estimating the catchment precipitation, determining direct runoff and baseflow, identifying the start and end of the events and calculating the event runoff characteristics, i.e. peak discharge, runoff coefficient and recession time constant. Hourly catchment precipitation was estimated based on measurements at four raingauges by the Thiessen polygon method. The event runoff coefficient relates direct flow volume to total event rainfall, so it was necessary to separate direct quickflow and baseflow. Direct quickflow runoff arises from rainfall that contributes immediately to streamflow during an event, while baseflow contributes to streamflow with a significant delay. Baseflow and direct runoff contributions were determined by the *Chapman and Maxwell* (1996) digital filter. If the ratio of direct runoff and baseflow at time t was larger than a threshold value of parameter q_{drat} and there was no larger flow in the previous and following i_{max} hours, the flow at time t was considered as a peak. The parameters q_{drat} and i_{max} were set to 2 and 12 hrs, respectively, based on sensitivity analyses (not shown here), consistent with the parameters of *Merz et al.* (2006) for Austria. For each peak, the start of the event was searched backwards to find the time when the direct runoff is less than 1% of the direct runoff at the time of the peak. The number of time steps in the backward search (size of the time window) depends on the characteristic time scale of an event (*Merz et al.*, 2006). If no such point in predefined time window is found, a higher limit for minimum direct runoff is allowed (stepwise increased from 1% to 40%). The end time was found in an analogue way by searching forwards. Multi-peak events were identified when the lowest direct runoff between peaks was smaller than a threshold. The runoff coefficient R_c and recession time constant T_c were determined in two steps. In the first step, R_c and T_c values were automatically calibrated by using the shuffled complex evolution optimisation scheme (*Duan et al.*, 1992). The linear reservoir model was fitted to the direct flow by minimizing the root mean square difference between observed and simulated runoff. In the second step, final hydrographs were visually checked and, in some cases, T_c was manually adjusted and fixed to match the form one would separate manually. After fixing, R_c is again automatically optimized until the simulated hydrograph fits the observation. More details on the method are given in *Merz et al.* (2006).

An example of an identified event in October 2014 is shown in Figure 2. The runoff response to precipitation differs between the tributaries, but the linear reservoir model fits the observed streamflow well. For this event, the runoff peaks (in units mm/hrs) of the tile drain systems Frau 1 and Frau2 are noticeably larger than those of the wetlands A1 and A2.

Spatial and temporal variability of runoff event characteristics in a small agricultural catchment

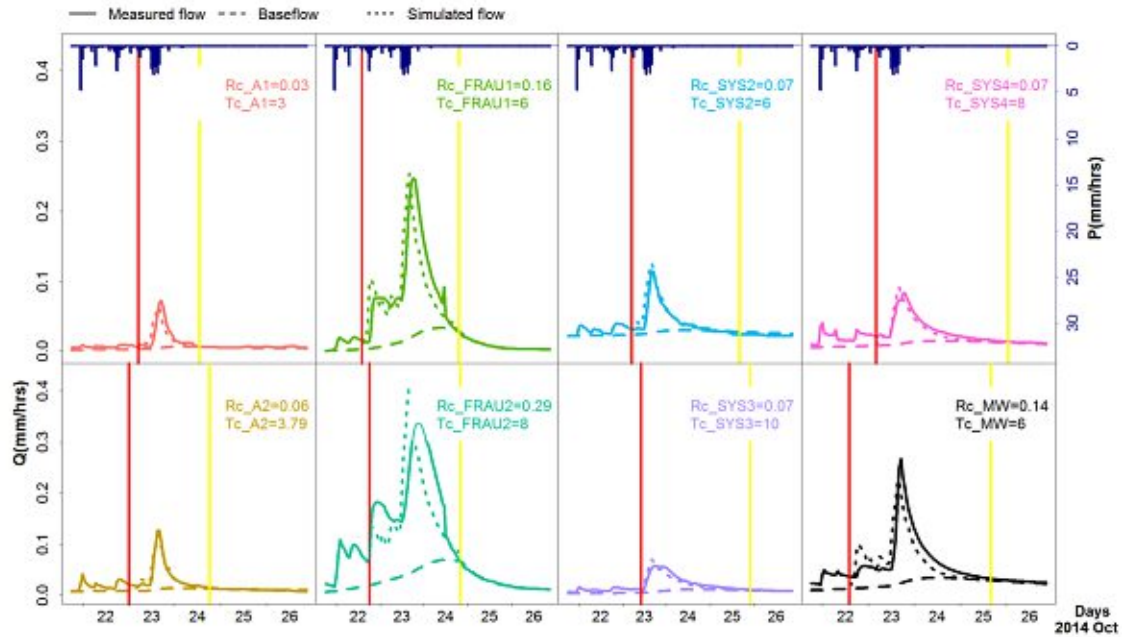


Figure 2. Example of observed and simulated runoff events at the main outlet (MW) and seven tributaries in HOAL catchment in October 2014. Runoff (dotted lines) is simulated by the linear reservoir model. Start and end of the events are plotted by red and yellow vertical lines, respectively.

In total, 57 runoff events were identified at the main outlet in the period 2013-2015. Figure 3 shows the time sequence of these events both at the main outlet (MW) and the seven tributaries (black squares). In case no event was identified at a tributary, but streamflow data were available, grey symbols are plotted. During the second half of 2015 runoff data at A2 is available, but some data were missing. In total 298 event hydrographs were identified at the eight gauges in the HOAL, which are summarized in the Appendix A2 (Table A2.1).

Spatial and temporal variability of runoff event characteristics in a small agricultural catchment

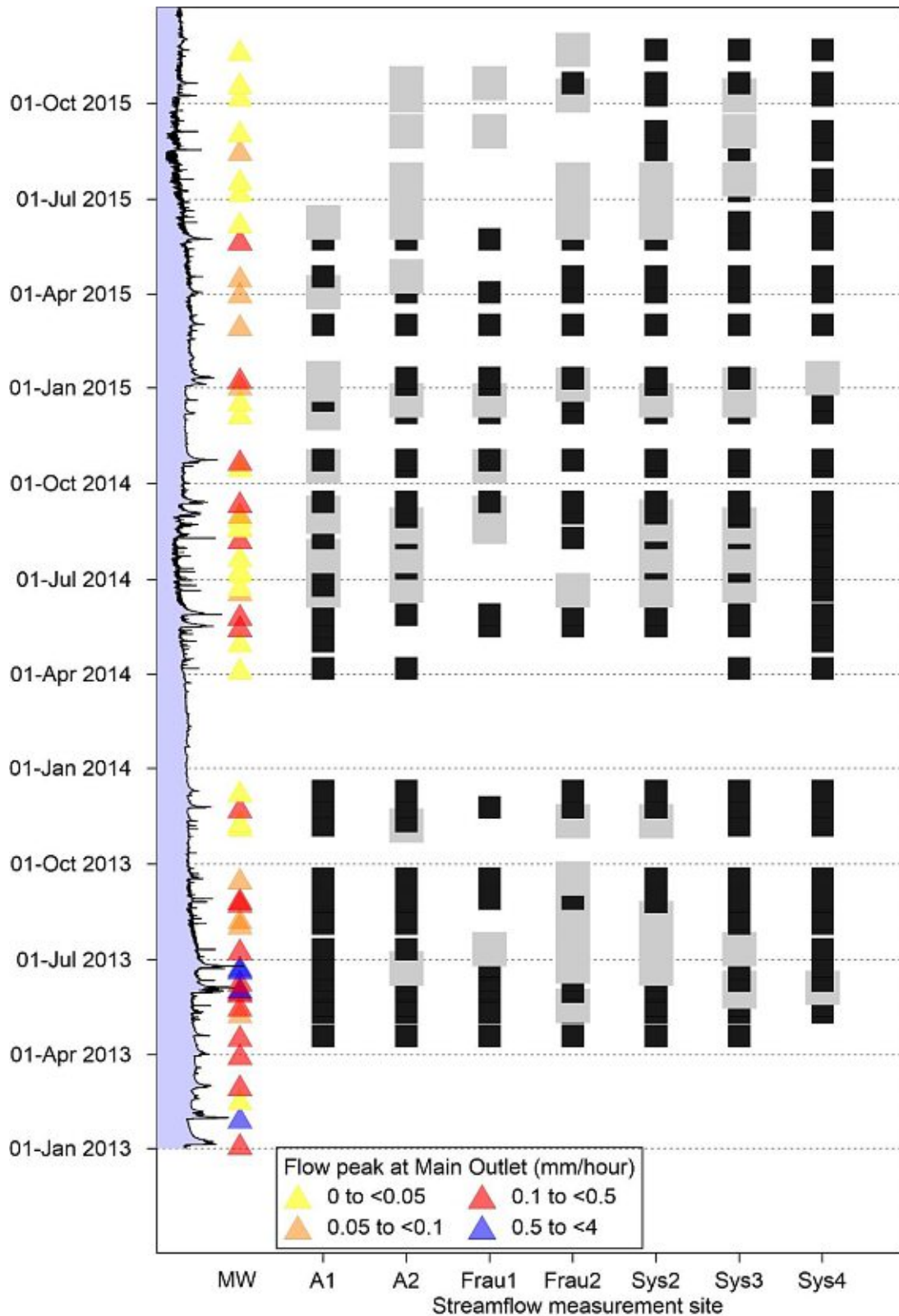


Figure 3. Runoff event peaks at the main outlet (triangles) in the period 2013-2015 and identified runoff events (black rectangles) at the tributaries. Grey symbols indicate available streamflow but no identified runoff event at the tributaries. In case of data gaps at the tributaries because of equipment failure or regular maintenance, no symbol is plotted. On the left side the hydrograph at the main outlet (MW) is presented.

2.7. Results

2.7.1. Runoff responses for various runoff generation mechanisms

Table 2 presents a summary of the event runoff characteristics of the identified event hydrographs. The mean R_c of all hydrographs at the main outlet is less than 0.08 with standard deviation (σ) of 0.09. The mean R_c of the tile drainage systems is somewhat larger (mean R_c is 0.09 and σ is 0.09), while those of the wetlands and natural drainage systems are notably smaller (mean R_c is 0.04 and 0.03, and σ is 0.03 and 0.02, respectively). While the largest mean recession time constant is found at the main outlet (mean $T_c = 6.6$ hrs, $\sigma = 7.6$ hrs), the smallest mean T_c is observed for the tile drainage systems (mean $T_c = 4.2$ hrs, $\sigma = 2.5$ hrs). The largest difference in mean T_c between the systems (2.35) is still smaller than the lowest standard deviation of T_c at the same gauge (2.49 hrs in Frau1). This means that the temporal variation of T_c is larger than the spatial difference in the HOAL. The relative magnitudes of the mean peak discharges (in mm/hrs) of the different systems is similar to those of the runoff coefficients, i.e. compared to wetland systems, mean peaks are larger for the tile drainage systems and smaller for the natural drainage system. At the main outlet the mean peaks are the largest (mean Q_p : 0.2 mm/hrs and σ : 0.4 mm/hrs).

Table 2. Summary of runoff event characteristics in the HOAL in the period 2013–2015. Minimum, maximum, mean and standard deviation (σ) of runoff coefficient (R_c), recession time constant (T_c) and peak discharges (Q_p) evaluated for the different runoff generation systems (wetland, tile drainage, natural drainage and the main outlet MW). The statistical evaluation is based on the events listed in Appendix A2 (Table A2.1)

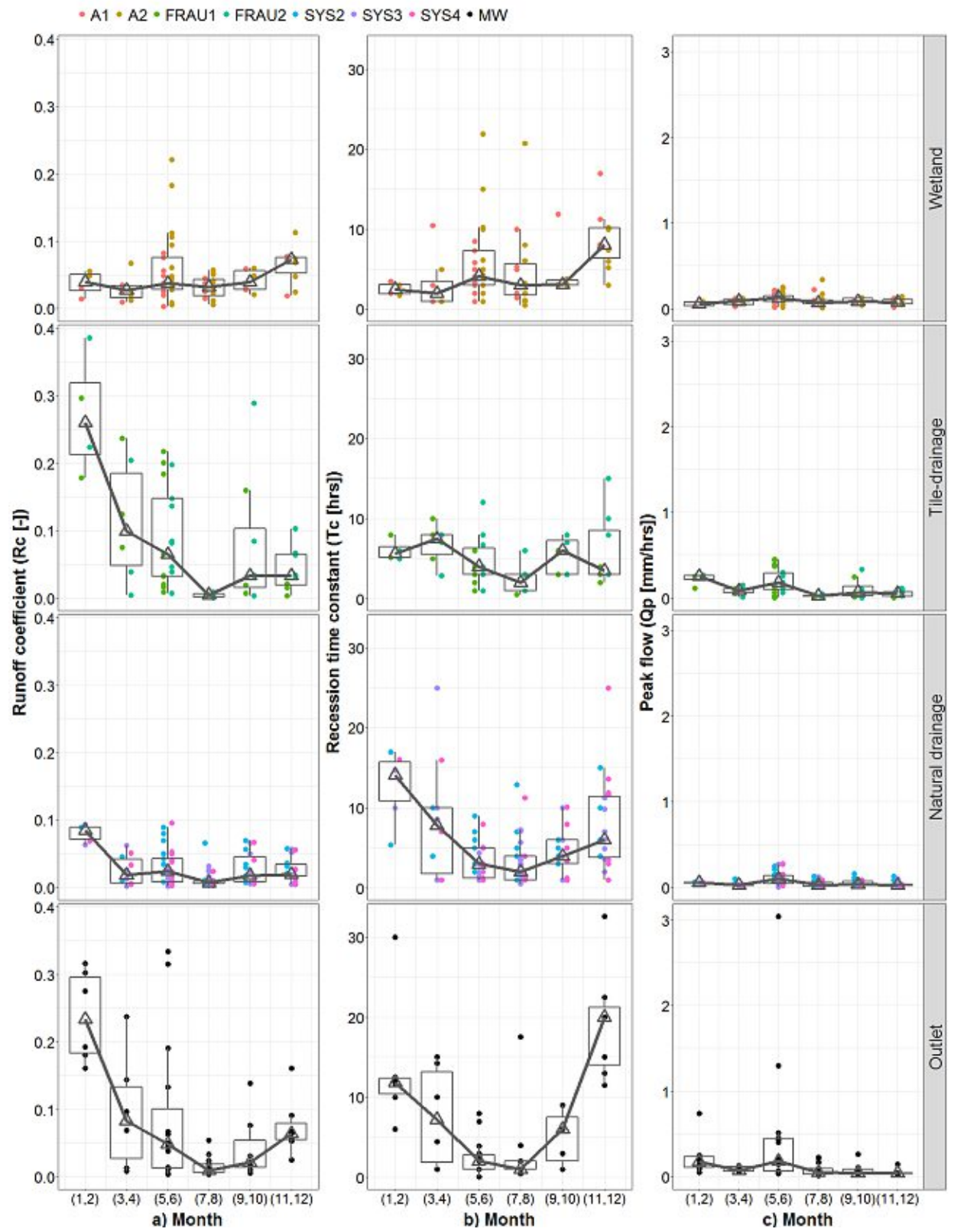
Characteristics of runoff events		Wetland		Tile drainage		Natural drainage			Outlet
		A1	A2	FRAU1	FRAU2	SYS2	SYS3	SYS4	MW
R_c	Min	0.003	0.006	0.001	0.0003	0.006	0.001	0.003	0.004
	Max	0.082	0.222	0.297	0.386	0.089	0.094	0.096	0.334
	Mean	0.038	0.054	0.091	0.086	0.036	0.022	0.021	0.077
	σ	0.021	0.046	0.094	0.095	0.028	0.022	0.022	0.093
T_c (h)	Min	1.00	0.50	0.50	1.00	1.00	0.50	1.00	0.10
	Max	17.0	21.9	10.0	15.0	17.0	25.0	25.0	32.6
	Mean	5.37	5.41	4.22	5.65	5.76	5.44	4.61	6.57
	σ	3.80	5.13	2.49	3.33	3.77	4.78	5.28	7.58
Q_p (mm/hrs)	Min	0.017	0.015	0.004	0.003	0.023	0.004	0.008	0.018
	Max	0.221	0.344	0.454	0.335	0.249	0.267	0.280	3.038
	Mean	0.091	0.107	0.142	0.128	0.087	0.044	0.052	0.198
	σ	0.057	0.067	0.153	0.104	0.055	0.050	0.055	0.436

2.7.2. Seasonal variability of runoff event characteristics and potential controllers

The seasonal variability of the event runoff characteristics is presented in Figure 4. The results of individual events are grouped (for better visual appearance) into bi-monthly classes. The results show that seasonal variability of R_c differs between the systems (Figure 4 (a)). For the main outlet (MW) and the tile drain systems (Frau1 and Frau2) the largest runoff coefficients (median over 0.2) occur in January/February, while from July to October the median is below 0.035. In the wetlands, the runoff coefficients vary only slightly between months with a median between 0.03 and 0.07, and in May/June the scatter is largest. In the natural drainage systems (Sys2, Sys3 and Sys4) the runoff coefficients are largest in January/February (median about 0.08), but in the other months they are rather small and similar to the wetlands. Overall, the runoff coefficients in the HOAL catchments are small, and the median R_c is less than 0.03. There are only five events with R_c larger than 0.3 in sub-catchments and the main outlet, and the largest runoff coefficient ($R_c = 0.38$) is observed in the ephemeral tile drain (Frau 2) in February 2015.

The seasonal variability of the recession time constant T_c (Figure 4 (b)) is the largest in the natural drainage systems and the main outlet. T_c in these two systems are particularly large in January/February when the median exceeds 10 hrs. The smallest T_c is observed in July/August and except wetlands, the median T_c is below 3 hrs. The wetlands have the smallest inter-seasonal variability, and large T_c is mainly observed in May/June and November/December. Interestingly, at MW, the largest T_c occur in November/December, while the largest R_c occur two months later in January/February.

The peak discharge does not vary much seasonally in HOAL catchments with the exception of a number of large events at the main outlet in June.



Die approbierte gedruckte Originalversion dieser Dissertation ist an der TU Wien Bibliothek verfügbar.
The approved original version of this doctoral thesis is available in print at TU Wien Bibliothek.

Figure 4. Seasonal variability of event runoff characteristics in the HOAL in the period 2013-2015. Left, middle and right panels show the runoff coefficient R_c , recession time constant T_c , and peak discharge Q_p , respectively, for four different runoff generation systems (wetland, tile drainage, natural drainage and main outlet). The boxes represent the 25% and 75% quantiles, and the triangles the medians. The lower whisker represents the smallest observation greater than or equal the 25% quantile - $1.5 * IQR$; the upper whisker the largest observation less than or equal the 75% quantile + $1.5 * IQR$ (where IQR is the differences between the 25 and 75% quantiles). Each circle represents an event.

The seasonal variability of selected factors that may control event runoff generation is presented in Figure 5. The largest precipitation volumes (Figure 5 left panel) with a median larger than 25 mm/event occur in May/June. In these months, more than 25% of the events have precipitation volumes larger than 40 mm. Interestingly, the larger precipitation volumes in May/June are not generally reflected in higher groundwater or soil moisture levels (Figure 5 middle and right panels) indicating drier subsurface conditions due to enhanced evaporation, and during summer most of the runoff events are caused by convective rainfall that does not usually saturate the soils. As would be expected in the climate of the HOAL, soil moisture varies strongly seasonally with drier months from May to August. The seasonal variability of the groundwater levels is smaller.

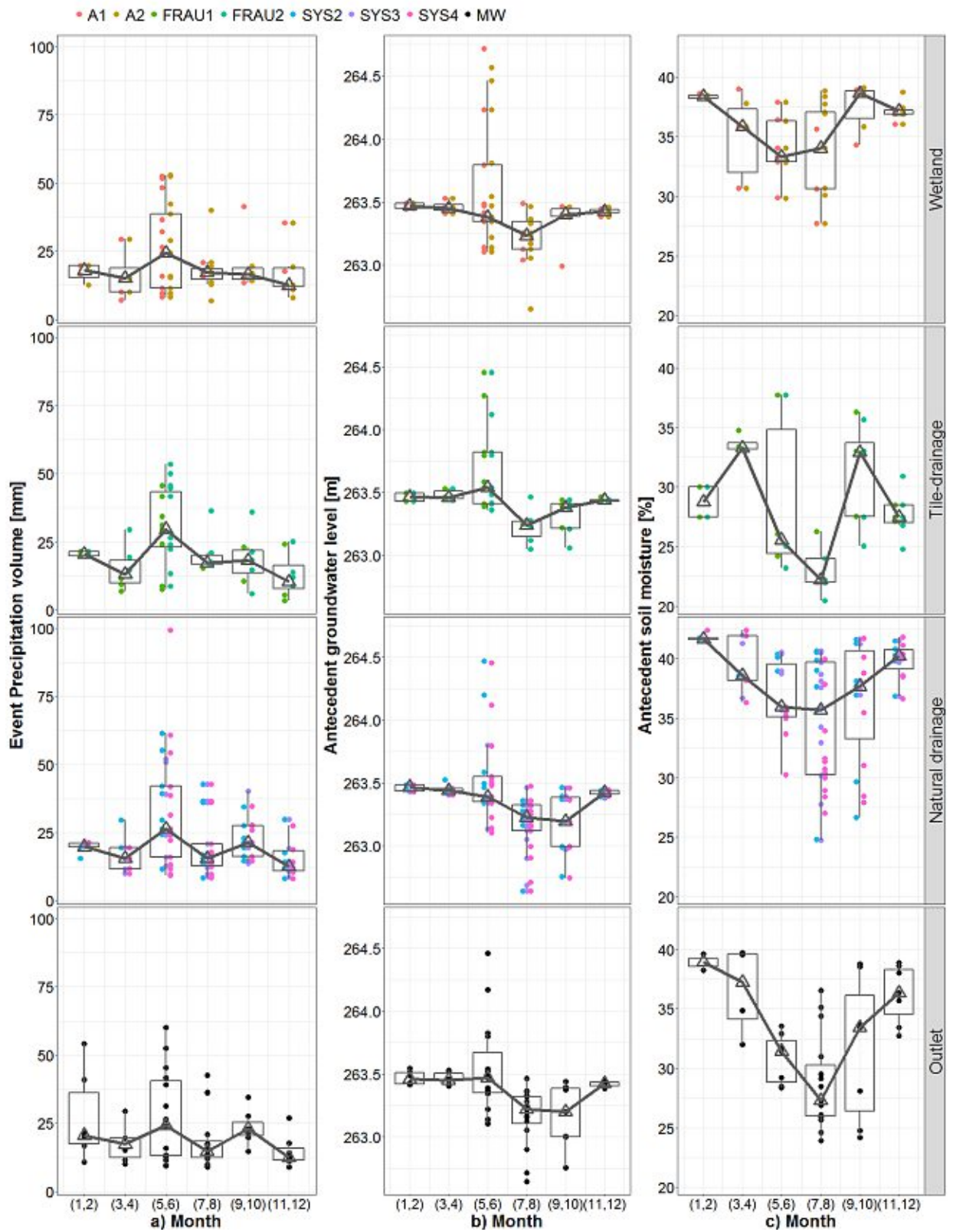


Figure 5. Seasonal variability of selected controls of event runoff characteristics in the HOAL in the period 2013-2015. Left, middle and right panels show the event precipitation volume, initial groundwater level and initial soil moisture, respectively, for four different runoff generation systems (wetland, tile drainage, natural drainage and main outlet). Explanation of boxes see Figure 4.

2.7.3. Effects of potential controllers on spatial variability of runoff response

Figure 6-9 plot the event runoff characteristics of the tributaries against those of the main outlet, with potential controlling factors indicated by the symbol type. Figure 6 (right panels) suggests that the peak discharges of MW are correlated with those of the tributaries as would be expected. While the small peaks of the main outlet tend to be similar to those of the tributaries, some of the large peaks are much larger than those of the tributaries (i.e. much below the 1:1 line). There are only a few events at the tile drainage systems (Frau 1, Frau2) and wetland (A2) where the peaks (in mm/hrs) are larger than those at MW. The runoff coefficient differs for groups classified by the mean runoff event peaks in different sub-catchments (Figure 6 left panels). The median R_c at the main outlet of the events with peaks below and above the mean (0.2 mm/hrs) is 0.03 and 0.14, respectively. The larger R_c associated with larger peaks also occurs for the tile drainage systems (Frau1, Frau2), where the median R_c below and above the mean peak are 0.02 and 0.19 in Frau1, 0.03 and 0.15 in Frau2, respectively. In the natural drainage (Sys2, Sys3, Sys4) and the wetland (A1, A2) systems, R_c is much less related to the magnitude of runoff peaks, and the difference between the median R_c for larger and smaller peaks is very small. Table 3 shows p -values of the Kolmogorov-Smirnov two sample test (KS) indicating differences in the group distributions, when stratifying by different characteristics according to their mean. The R_c has statistically different distributions for smaller and larger Q_p only for wetlands (mainly A2), inlet pipe (Sys4) and main outlet (MW).

Similar patterns can be observed for T_c (middle panels of Figure 6). At the main outlet, the median T_c of the events with small and large peaks is 2 and 3 hours, respectively.

While for the natural drainage systems (Sys2, Sys3, Sys4) the events with larger peaks (i.e. larger than the mean) tend to have larger T_c at both MW and tributaries, this is not the case for the other systems. In the tile drainage systems (Frau1 and Frau2), in fact, the opposite is the case. The median T_c of smaller events (in terms of runoff event peak) at the tributaries corresponds to larger T_c at the MW. The larger events have larger T_c at the tile drainage tributaries, but those events tend to have smaller T_c at the MW. For the wetland systems (A1, A2), the difference between median T_c for larger or smaller peaks at MW is very small, indicating that runoff generation processes are rather disconnected. Table 3 shows that there is no large statistically significant effect on grouping of T_c according to mean Q_p in HOAL.

Table 3. Statistical analysis (P values of a two-sample Kolmogorov-Smirnov test) of the distributions of Rc, Tc and Qp for events with smaller and larger runoff event peaks (Qp), precipitation volumes (Pvol), initial soil moisture (PreSM) and initial groundwater levels (PreWL). The two samples are created by splitting the events according to the mean of Qp, Pvol, PreSM and PreWL of each tributary (open and full circles in Figs 6–9). Variables with significantly different distributions at the 5% level are indicated in bold.

Gauge	Runoff generation system	Qp		Pvol			PreSM			PreWL		
		Rc	Tc	Rc	Tc	Qp	Rc	Tc	Qp	Rc	Tc	Qp
A1	Wetland	0.070	0.472	0.009	0.521	0.000	0.632	0.935	0.124	0.178	0.777	0.533
A2	Wetland	0.015	0.273	0.466	0.813	0.005	0.942	0.977	0.099	0.002	0.147	0.150
Frau1	Ephemeral tile drain	0.094	0.598	0.349	0.435	0.020	0.651	0.519	0.345	0.018	0.011	0.410
Frau2	Ephemeral tile drain	0.588	0.911	0.653	0.900	0.037	0.137	0.377	0.513	0.002	0.006	0.063
Sys2	Natural drainage	0.302	0.477	0.254	1.000	0.001	0.246	0.556	0.345	0.001	0.017	0.227
Sys3	Natural drainage (with wetland)	0.919	0.081	0.155	0.675	0.000	0.001	0.003	0.379	0.037	0.014	0.626
Sys4	Natural drainage (inlet pipe)	0.012	0.407	0.027	0.331	0.000	0.005	0.000	0.207	0.000	0.000	0.334
MW	Outlet (aggregated system)	0.022	0.107	0.081	0.444	0.000	0.081	0.000	0.279	0.000	0.000	0.006

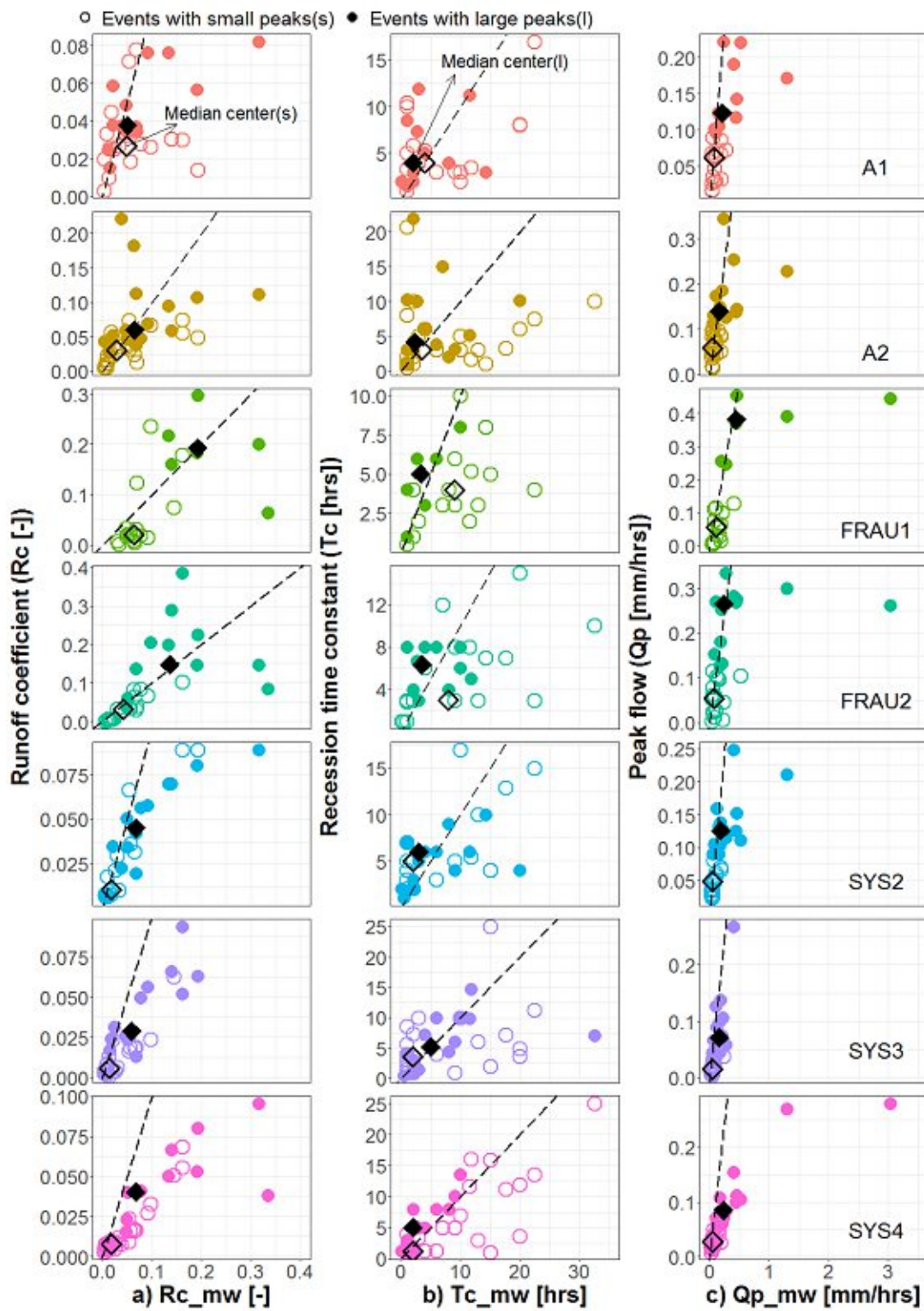


Figure 6. Event runoff characteristics of the tributaries plotted against those of the main outlet. Left, middle and right panels show the runoff coefficient R_c , recession time constant T_c and peak discharges Q_p , respectively. Open and full circles indicate Q_p at the

tributaries smaller and larger than the means, which are 0.09, 0.11, 0.14, 0.13, 0.09, 0.04 and 0.05 mm/hrs in tributaries of A1, A2, FRAU1, FRAU2, SYS2, SYS3 and SYS4, respectively. Open and full diamonds indicate the median centers of the groups smaller and larger than that means, respectively. Dashed line is the 1:1 line.

Event precipitation volume, Pvol, (Figure 7) also has an important effect on the runoff characteristics at MW, and at the tributaries the runoff peaks are clearly stratified by precipitation volume. In the tile drainage systems (Frau1 and Frau2) and in Sys2, the differences of the peaks between the two precipitation groups are particularly large (Figure 7, right panel) indicating a very non-linear runoff generation process triggered by precipitation. The subsurface tile drainage pipes are likely starting to be effective after reaching soil moisture state, which hence can accelerate and enhance hillslope drainage process for larger precipitation volumes. Rc and Tc generally differ less for the two precipitation groups (Figure 7, left and middle panel). Rc for the wetland system A1 for large precipitation events tends to be smaller than Rc at the main outlet. For a few small precipitation events Rc can be larger, but the two groups of Rc (according to their means) are statistically different (Table 3). For Tc, a small difference is observed for the wetland systems between the two precipitation groups, suggesting that precipitation volume is not a relevant factor controlling differences in Tc. The tile drainage systems (Frau1 and Frau2) do indicate larger Rc for the high precipitation group, but Tc actually decreases with precipitation, suggesting a tendency for flashier response for high precipitation events. Sys 2 is similar to the tile drainage systems, but the other natural drainage system Sys3 shows less difference between the two precipitation groups. The KS test indicates that Rc samples split according to the Pvol mean are statistically significant at the 5% level only for A1 and Sys4 and there is no statistically significant difference for Tc in all HOAL catchments (Table 3).

Figure 8&9 evaluate the effect of initial soil moisture and initial groundwater levels on the runoff characteristics. Because of missing soil moisture data from January to July of 2013, several events are not included in Figure 8 compared to Figure 6, 7&9. In the wetland systems (A1, A2), the tile drainage systems (Frau1, Frau2) and at the outlet (MW), groundwater levels stratify Rc more than soil moisture. The differences in the group median of Rc (i.e. difference between open and full diamonds in Figure 8&9) in the wetland, tile drainage and outlet systems is 0.02, 0.05 and 0.06, respectively, which is generally larger than the corresponding differences in the median Rc when stratifying by soil moisture. This is documented also by the results of the KS test (Table 3) where groups based on groundwater levels are statistically different in all tributaries except wetland A1, but soil moisture stratifies Rc only in the natural drainage systems (Sys3 and Sys4).

Similar results are found for Tc. In the wetland, tile drainage and main outlet systems, the differences in the group medians, when stratifying by groundwater, is larger than when stratifying by soil moisture. Interestingly, groundwater levels tend to increase Tc in the wetland systems of A2, but there is little effect of soil moisture on Tc. In the tile drainage systems (Frau1, Frau2), unfortunately, soil moisture data were not available for events with large Tc, so comparisons with soil moisture are not possible. For the natural drainage systems (Sys2, Sys3, Sys4), large soil moisture results in events with large Tc.

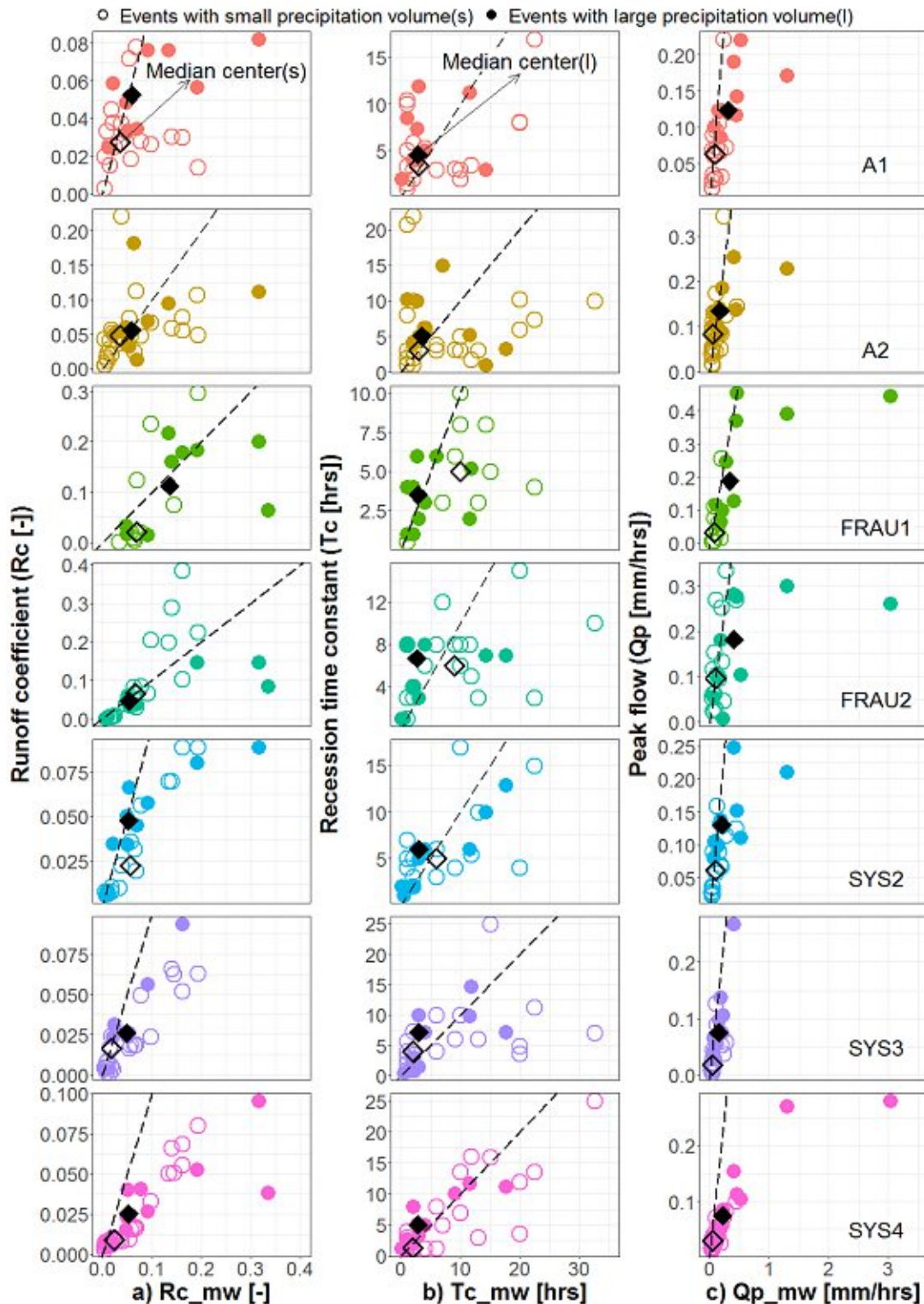


Figure 7. Same as Figure 6, but open and full circles indicate precipitation volumes (Pvol) of the tributaries smaller and larger than the means, which are 22.3, 20.0, 20.9, 25.4, 24.3, 20.0 and 22.5 mm in tributaries of A1, A2, FRAU1, FRAU2, SYS2, SYS3 and SYS4, respectively.

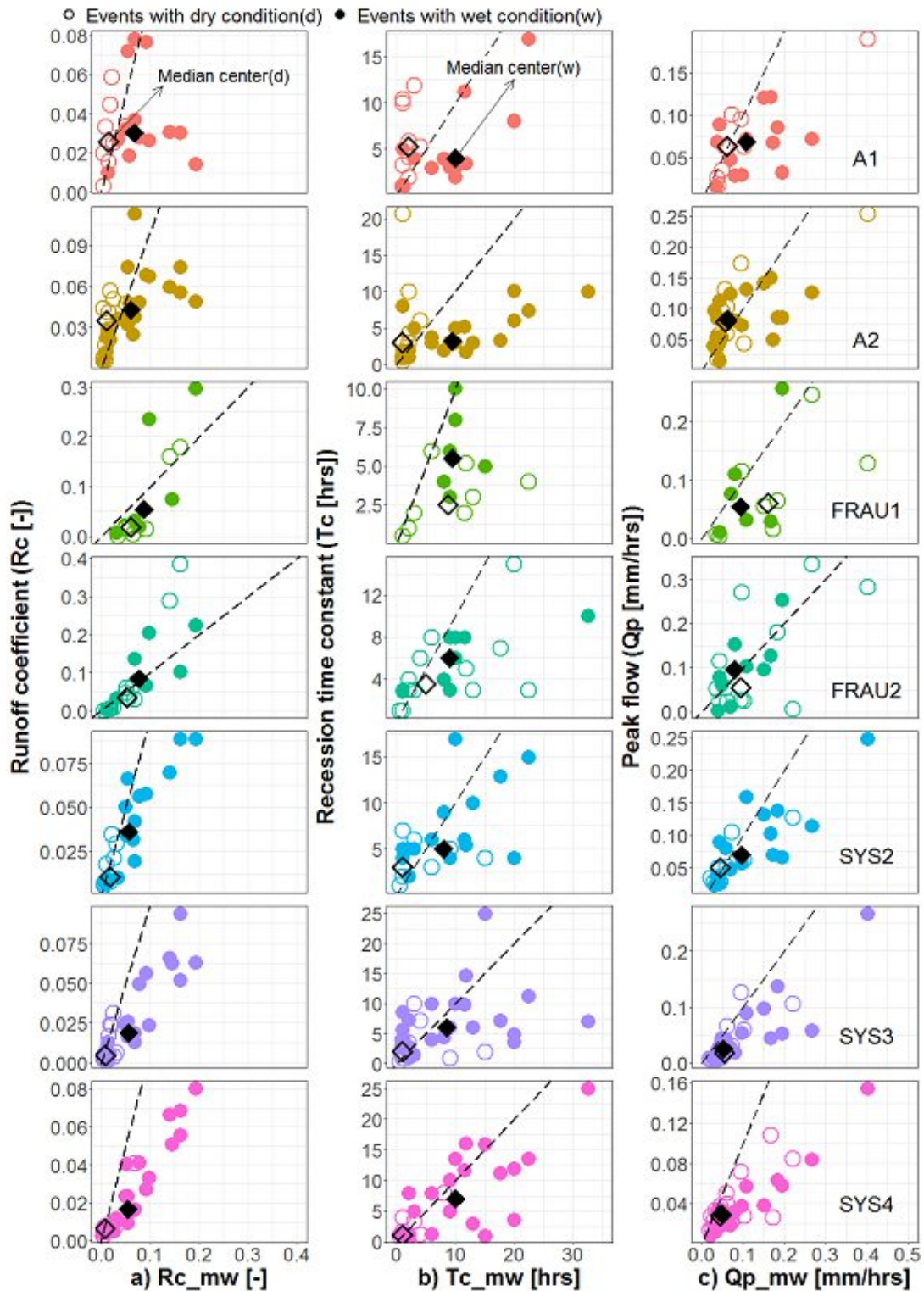


Figure 8. Same as Figure 6, but open and full circles indicate soil moisture prior to the event PreSM of the tributaries smaller and larger than the means, which are 35.2, 35.6, 30.0, 28.1, 38.1, 38.2 and 35.2% in tributaries of A1, A2, FRAU1, FRAU2, SYS2, SYS3 and SYS4, respectively.

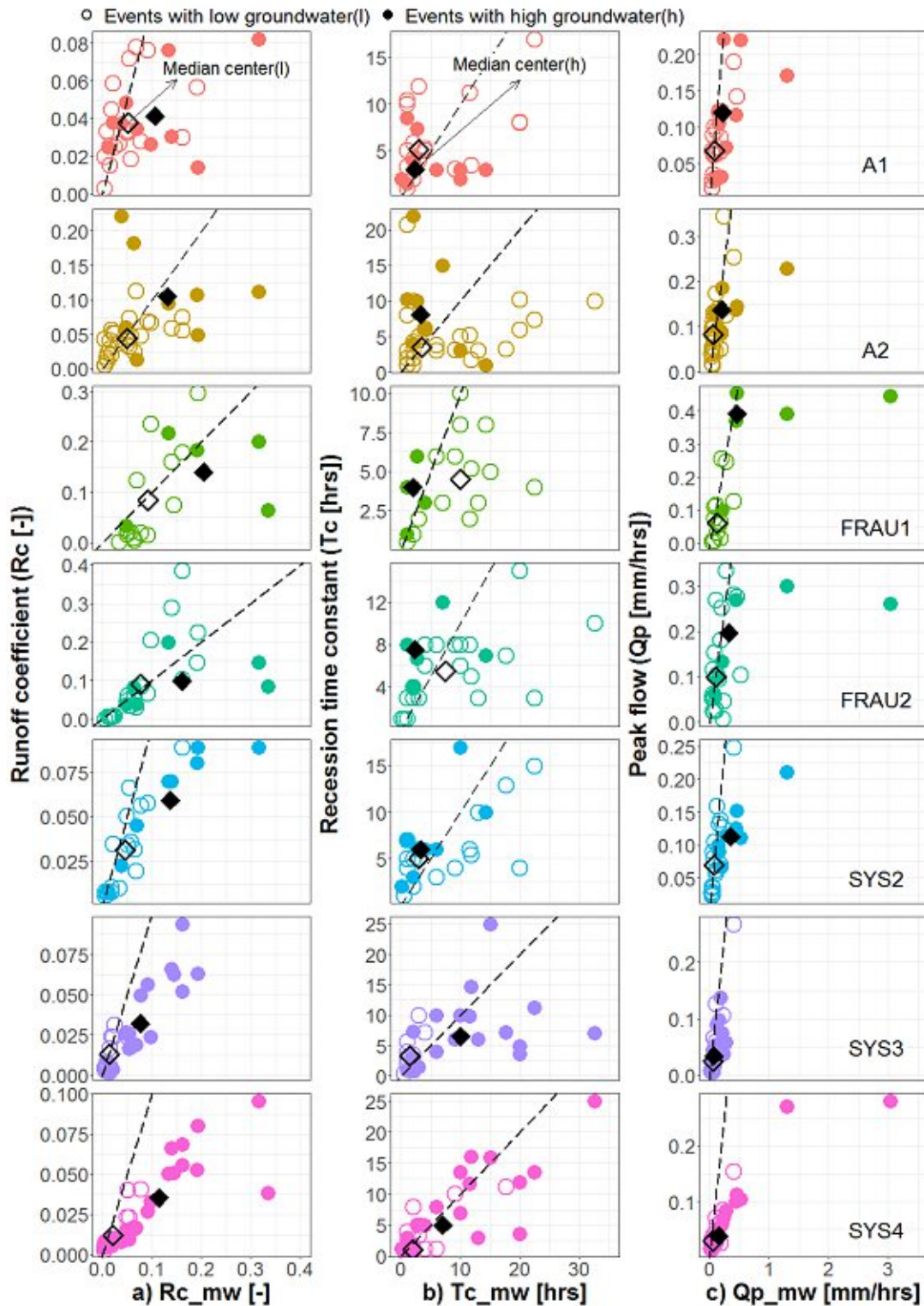


Figure 9. Same as Figure 6, but open and full circles indicate groundwater levels prior to the runoff events PreWL of the tributaries smaller and larger than the means, which are 263.44, 263.47, 263.58, 263.49, 263.45, 263.35 and 263.40 m a.s.l. in tributaries of A1, A2, FRAU1, FRAU2, SYS2, SYS3 and SYS4, respectively.

2.8. Discussion

2.8.1. Spatial and seasonal variability of runoff event characteristics

The results show that the spatial variability of event runoff characteristics is related to the main runoff generation systems represented by different subcatchments. We found that R_c tends to be the largest for the tile drainage systems (mean $R_c = 0.09$, standard deviation $\sigma = 0.09$) and the main outlet (mean $R_c = 0.08$, $\sigma = 0.09$), while it is smaller in the natural drainage systems (mean $R_c = 0.03$, $\sigma = 0.02$). This is consistent with previous assessments in small agricultural catchments (*Blume et al.*, 2007; *Cerdan et al.*, 2004; *Tachecí et al.*, 2013). For example, *Cerdan et al.* (2004) found mean R_c and σ of 0.05 and 0.045, respectively for 90 ha catchment in Normandy or *Tachecí et al.* (2013) found the R_c between 0.03 and 0.06 in 0.6 km² catchment in Czech Republic. The magnitude of R_c in HOAL is smaller than what was found on cropland hillslopes in central Iowa (*Chen et al.*, 2019) where the median over 70 events was 0.22, or as reported in regional assessments of meso-scale catchments in Austria (the median of R_c varies between 0.18 and 0.43) (*Merz et al.*, 2006) or Germany (*Tarasova et al.*, 2018b). The magnitude of R_c is not related to size or surface slope of sub-catchments in HOAL, which is similar as reported in previous studies of *Chen et al.* (2019) or *Cerdan et al.* (2004).

The analysis of recession time constants showed that T_c does not vary much between the systems and the difference between the largest T_c at the main outlet (mean $T_c = 6.6$ hrs, $\sigma = 7.6$ hrs) and the smallest T_c for the tile drainage systems (mean $T_c = 4.2$ hrs, $\sigma = 2.5$ hrs) is around only 2 hours. A comparison with a regional assessment of T_c and runoff event time scales of *Gaál et al.* (2012) shows that the natural drainage and aggregated systems compare well with hotspots of fast response catchments in terms of magnitude and seasonality of T_c . Wetland and tile drainage systems have generally lower T_c which indicates shallower flow paths and higher subsurface connectivity compared to natural drainage systems.

The largest R_c is estimated for the tile drainage systems and the main outlet in January and February and small values of R_c are found between July and October. The seasonal pattern of R_c value is in agreement with previous hillslope or regional studies (*Hewlett and Hibbert*, 1967; *Merz and Blöschl*, 2009; *Norbiato et al.*, 2009; *Rodríguez-Blanco et al.*, 2012) and corresponds to the higher contribution of rainfall to soil moisture changes and to the high evapotranspiration in July and August (*Rodríguez-Blanco et al.*, 2012). A similar seasonal variability is observed for T_c for the main outlet and the natural drainage system with large T_c in January and February and small T_c in July and August. This is consistent with the seasonal dynamics of groundwater levels, which reflect functions of water holding capacity in aquifer structure to recession (*Patnaik et al.*, 2015; *Thomas et al.*, 2015).

2.8.2. Process controls on runoff event characteristics.

The comparison of the runoff responses for different runoff generation systems indicates that groundwater levels explain the temporal variability of R_c and T_c at the main outlet. The sub-catchments with extensive cover of tile drain pipes are characterised by faster runoff response, larger runoff coefficients R_c and shorter recession time constants. The study of *Silasari et al.* (2017) shows that overland flow events do not occur frequently and, in the study area, these are generated mainly by saturation excess mechanisms and the connectivity of runoff flow paths rather than by infiltration excess processes. This is consistent with the impact of initial

groundwater levels on R_c and T_c . The wetland systems tend to be disconnected from the rest of the catchment as R_c and T_c are not explained by groundwater levels or soil moisture and, apparently, by shallower drainage processes.

The results of our study show that, at the small catchment scale, event precipitation volume variability is very small and it does not have an impact on the event runoff characteristics. Event precipitation volume determines the magnitude of runoff peaks, but is not related much to the event runoff coefficients or recession time constants. Neither is precipitation intensity a big control of the variability in runoff response. Our results indicate that precipitation volume in the HOAL plays a role in predicting R_c only for the main outlet. This is in agreement with previous study of *Blume et al. (2007)* who reported an increase in runoff coefficients with total precipitation. *Blume et al. (2007)* attributed this finding not only to the precipitation water volume routed to the stream, but also to the effect of rising groundwater levels, groundwater mounding (increasing hydraulic gradients), pipe flow, and also saturation overland flow. Our results are in line also with previous findings of *Chen et al. (2020b)* who indicates that precipitation characteristics and in particular precipitation duration is a factor controlling prediction of R_c for the tile drainage and outlet systems. The weak correlation with precipitation intensity found in previous studies of *Kostka and Holko (2003)*, *Tachecí et al. (2013)* and *Chen et al. (2020b)* indicate that in small catchments variability in precipitation intensity does not control variability in runoff response. Rainfall amount and intensity are likely important only when the groundwater level is close to the surface as indicated by *García-Ruiz et al. (2008)*.

Our findings indicate that, at the small catchment scale, the impact of different runoff generation systems on the variability of runoff response is significant. In the next studies, we plan to further investigate the scale where geology, climate and runoff generation system interact and have effect on runoff response, i.e. to examine how subsurface structure and rainfall characteristics affect spatial and temporal variability of runoff generation.

2.9. Conclusions

This study presented the role of runoff generation mechanisms on runoff event characteristics in a small agricultural catchment. Through combining high resolution observations of soil moisture and groundwater level, their functions on runoff responses are explored for different runoff generation mechanisms. Our results showed that:

- The spatial variability of runoff event characteristics is highly connected to runoff generation mechanisms in a small agricultural catchment. Event runoff coefficients of tile drainages tend to be the highest, and the mixed outlet flow is in the second place. While runoff event recession time constants of the outlet tend to be the highest due to mixed flow paths.
- In the small agricultural catchment, groundwater level dynamics are the most relevant process of runoff response, reflecting the role of subsurface flow paths in runoff generation.
- Soil moisture dynamics only influence the runoff responses for natural drainages and outlet flow because of the more complex subsurface flow paths and hydrological conditions than tile drainages and wetland.

Controls on event runoff coefficients and recession time constants for different runoff generation mechanisms identified by three regression methods

3. Controls on event runoff coefficients and recession time constants for different runoff generation mechanisms identified by three regression methods

3.1. General

The goal of this chapter was to identify potential controls of runoff event characteristics for different runoff generation mechanisms in a small agricultural catchment.

This chapter aims to estimate runoff event runoff coefficients and recession time constants from 22 event-based explanatory variables representing precipitation, soil moisture, groundwater level and season. The importance of the explanatory variables in the regressions is estimated in order to identify potential controls of event runoff coefficient and recession time constant for different runoff generation mechanisms, such as wetland, tile drainages, natural drainages and outlet flow.

The present chapter is based on the following scientific publication:

Chen, X., Parajka, J., Széles, B., Strauss, P., & Blöschl, G. (2020). Controls on event runoff coefficients and recession coefficients for different runoff generation mechanisms identified by three regression methods. *Journal of Hydrology and Hydromechanics*, 68(2), 155-169. doi: <https://doi.org/10.2478/johh-2020-0008>

3.2. Key Points

1. The validation performances of regressions based on the algorithm of Support vector machine (SVM) are better than those for Random forest (RF) and Gradient Boost Decision Tree (GBDT) methods.
2. The relative importance of the explanatory variables strongly depends on the runoff generation mechanism.
3. The event runoff coefficients for tile drainages are mainly controlled by precipitation variables, while for other runoff generation mechanisms subsurface wetness is more important.

3.3. Abstract

The event runoff coefficient (R_c) and the recession time constant (T_c) are of theoretical importance for understanding catchment response and of practical importance in hydrological design. We analyse 57 event periods in the period 2013 to 2015 in the 66 ha Austrian Hydrological Open Air Laboratory (HOAL), where the seven subcatchments are stratified by runoff generation types into wetlands, tile drainage and natural drainage. Three machine learning algorithms (Random forest (RF), Gradient Boost Decision Tree (GBDT) and Support vector machine (SVM)) are used to estimate R_c and T_c from 22 event based explanatory variables representing precipitation, soil moisture, groundwater level and season. The model performance of the SVM algorithm in estimating R_c and T_c is generally higher than that of the other two methods, measured by the coefficient of determination R^2 , and the performance for R_c is higher than that for T_c . The relative importance of the explanatory variables for the predictions, assessed by a heatmap, suggests that R_c of the tile drainage systems is more strongly controlled by the weather conditions than by the catchment state, while the opposite is true for natural drainage systems. Overall, model performance strongly depends on the runoff generation type.

3.4. Introduction

The event runoff coefficient and the recession time constant are important characteristics of hydrologic response at the event scale. Understanding their controls and their variability is essential for predicting runoff in ungauged basins and for extrapolating hydrologic response to extreme events (*Blöschl et al.*, 2013; *Sivapalan*, 2003; *Tarasova et al.*, 2018a; *Tarasova et al.*, 2018b; *A. Viglione et al.*, 2009).

The event runoff coefficient R_c is defined as the portion of rainfall that becomes direct runoff during an event (*Merz et al.*, 2006). The spatial-temporal variability of R_c has been widely studied (*Hayes and Young*, 2006; *Longobardi et al.*, 2003; *Merz and Blöschl*, 2009; *Merz et al.*, 2006; *Wainwright and Parsons*, 2002). Previous studies show that the magnitude of R_c varies between the regions. While regional assessments of meso-scale catchments in Austria or Germany (*Merz et al.*, 2006; *Tarasova et al.*, 2018a; *Tarasova et al.*, 2018b) indicate the median of R_c between 0.18 and 0.43, R_c in small agricultural catchments tends to be lower and varies between 0.03 and 0.10 (*Blume et al.*, 2007; *Tacheci et al.*, 2013) to more than 0.2 over cropland hillslopes in central Iowa (*Chen et al.*, 2019). The controls on R_c generally depend on the runoff mechanisms. Precipitation intensity tends to be most important when the infiltration excess mechanism dominates, precipitation depth when the saturation excess mechanism dominates, and soil moisture is important for all mechanisms (*Tian et al.*, 2012). *Rodríguez-Blanco et al.* (2012) and *Palleiro et al.* (2014) found that the event runoff coefficient in forested catchments in northwestern Spain depended both on the soil moisture at the start of the event and on rainfall depth, whereas rainfall intensity was less important. They explained this finding by the dominant role of subsurface stormflow in event runoff generation. Based on a comparative study in the eastern Italian Alps, *Norbiato et al.* (2009) suggested that the effect of antecedent soil moisture on the event runoff coefficient might be largest in catchments with intermediate storage capacities. Besides climate and hydrological conditions, *Norbiato et al.* (2009) also verified that the ‘permeability index’ deduced from geology is another considerable control on event runoff coefficient in regions with mean annual precipitation less than 1200 mm. *Gottschalk and Weingartner* (1998) showed that moderate slopes and low geological permeability in the Swiss midlands basins generally lead to events with low event runoff coefficients.

The recession time constant, T_c , is the parameter in a linear function of $(-dQ)/dt=1/T_c Q$ where $(-dQ)/dt$ is the time derivative of runoff Q (*Brutsaert and Nieber*, 1977; *Tallaksen*, 1995). Similarly to the event runoff coefficient, the recession parameter has been widely studied (*Biswal and Nagesh Kumar*, 2014b; *Krakauer and Temimi*, 2011; *Merz et al.*, 2006; *Patnaik et al.*, 2015). *Krakauer and Temimi* (2011) identified soil infiltration capacity and forest cover as important controls on the recession in small catchments in the United States. *Tague and Grant* (2004) and *Gaál et al.* (2012) highlighted the important role of geology for the recession.

One of the challenges in identifying the controls and predicting R_c and T_c is the typically non-linear nature of the relationships between these two parameters and their controls (*Krakauer and Temimi*, 2011; *Merz and Blöschl*, 2009). It is therefore of advantage to use non-linear rather than linear analyses and predictive methods. Machine learning techniques based on regressions are able to capture the non-linearity in the relationship between predictor and prediction (*Cánovas-García et al.*, 2017; *Erdal and Karakurt*, 2013; *Naghbi et al.*, 2017; *Şen and Altunkaynak*, 2006). Three widely used methods are random forests (RF), Gradient Boost Decision Trees (GBDT) and Support vector machines (SVM).

RF (Ho, 1995) are a learning method for classification and regression that consists of a number of decision trees at training time and identifies the class that has the greatest number of votes (classification) or the mean prediction (regression) of the individual trees. Random forests have been applied in numerous surface and subsurface hydrological studies (Baudron *et al.*, 2013; Naghibi *et al.*, 2017; Zimmermann *et al.*, 2014).

GBDT make use of the gradient boosting framework to combine decision trees based on the RF algorithm. GBDT are usually composed of hundreds of decision trees with shallow depth. In this algorithm, every decision tree adjusts and modifies the predicted value, finally resulting in the prediction. The trees are trained sequentially, which improves the prediction accuracy but involves a longer training time (Friedman, 2001; 2002). Naghibi *et al.* (2015) compared boosted regression trees (BRT), classification and regression trees (CART), and RF in producing groundwater spring potential maps according to thirteen hydrological-geological-physiographical factors (Naghibi *et al.*, 2015). (Sachdeva *et al.*, 2018) constructed wildfire susceptibility maps by combining evolutionary optimized gradient boosted decision trees, and showed that they outperformed other machine learning models.

SVM are supervised learning models with associated learning algorithms. Given a set of training examples, the training algorithm builds a model that assigns new examples to one of two categories (Basak *et al.*, 2007; Ben-Hur and Weston, 2010; Vapnik *et al.*, 1997). SVM have a number of advantages: they effectively solve the classification and regression problem for high dimensions; they solve various nonlinear classification and regression problems by means of different kernel functions; they are able to generalize well. However, computational costs are very high when the dimension of the mapping kernel function is large, and they are sensitive to missing data. They have been applied to surface flow, evaporation, droughts, soil moisture and groundwater prediction (Asefa *et al.*, 2006; Hwang *et al.*, 2012; Raghavendra. N and Deka, 2014; Rajib *et al.*, 2010).

The aim of this chapter is (a) to identify factors which control variability of event runoff coefficient (R_c) and the recession time constant (T_c) in small agricultural catchment; (b) to evaluate the relative importance of the control in different subcatchments representing different runoff generation mechanisms and (c) to compare three regression based machine learning techniques, random forests (RF), Gradient Boost Decision Trees (GBDT) and Support vector machines (SVM), in terms of their ability to estimate the event runoff coefficient and the recession time constant from their controls.

3.5. Study area and data

The study is performed in the Hydrological Open Air Laboratory (HOAL). This is a small experimental catchment situated in Lower Austria (Blöschl *et al.*, 2016; Exner-Kittridge *et al.*, 2016; Széles *et al.*, 2018) (Figure 10). The land use is mainly agricultural (82%) and part of the catchment is tile drained. Runoff is recorded at a number of flumes within the catchment at a time step of 1 minute. In this study, eight flumes are used (Table 4). MW is the catchment outlet of the HOAL and has a catchment area of 65.8 ha. All the other flumes are nested in this catchment (Figure 10). The runoff generation mechanisms of the catchments drained by the flumes differ. Sys4 represents a piped stream and is considered as “natural subsurface drainage” here. Frau1 and Frau2 are tile drained. A1 and A2 drain wetland areas. Sys2, Sys3 and Sys4 are classified as natural drainage here, although (Széles *et al.*, 2018) classified them as tile drains.

Controls on event runoff coefficients and recession time constants for different runoff generation mechanisms identified by three regression methods

The reason for the different classification is that the drainage areas of these systems are not fully covered by underground tile pipes and most of the flow is drained from subsurface without tile pipes. All discharge data are processed to remove outliers caused by instrument malfunction and maintenance and aggregated to an hourly time step. Catchment boundaries are identified by analysing a digital elevation model (DEM) and account for the position of tile pipes (Széles *et al.*, 2018). These are used for estimating specific runoff as the ratio of runoff and catchment area and for estimating catchment precipitation (Table 4).

Table 4. Runoff generation mechanism and estimated drainage area of the gauged catchments in the HOAL. Figure 10 shows locations of the gauges. From (Széles *et al.*, 2018).

Gauge	Runoff generation mechanism	Estimated drainage area (ha)	Tile pipe covered area percentage (%)
A1	Wetland	2.1	6.5
A2	Wetland	1.1	11.0
Frau1	Tile drain	3.1	96.6
Frau2	Tile drain	4.8	60.8
Sys2	Natural drainage	2.4	8.7
Sys3	Natural drainage	4.3	10.7
Sys4	Natural drainage	37.4	4.3
MW	Outlet	65.8	12.9

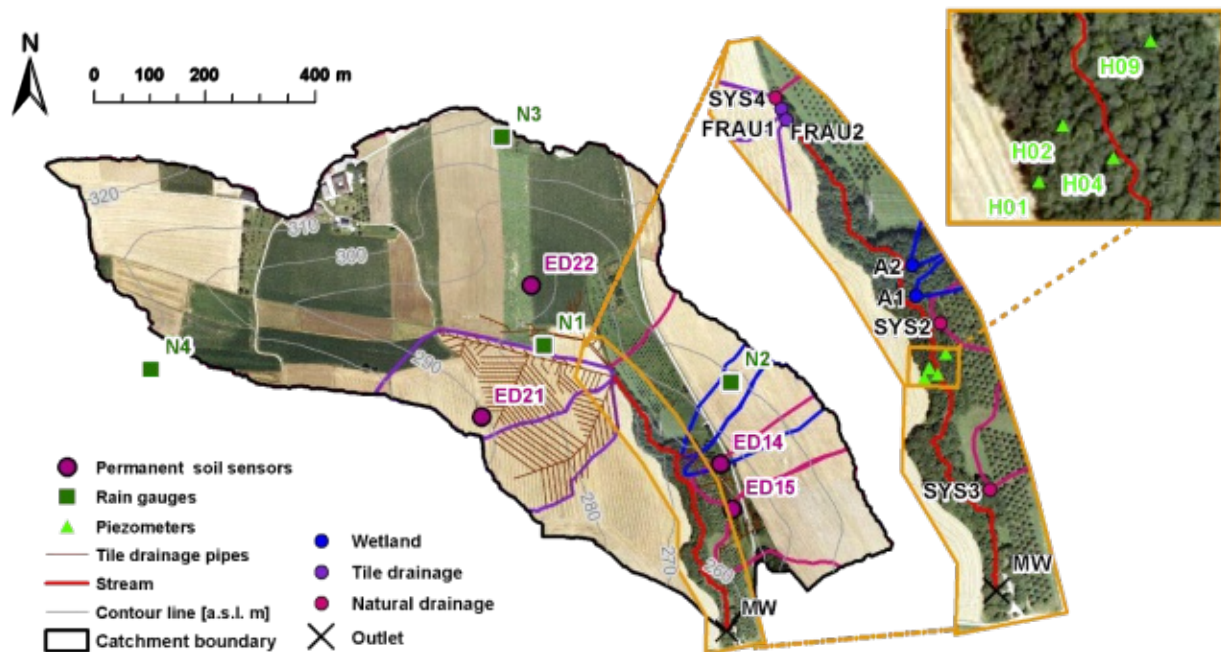


Figure 10. HOAL catchment and its subcatchments. Locations of stream gauges, soil moisture sensors and piezometers used in the analyses.

Controls on event runoff coefficients and recession time constants for different runoff generation mechanisms identified by three regression methods

Additionally, data from four rain gauges (N1-N4), four soil moisture sensors (ED14, ED15, ED21 and ED22) at 5, 10 and 20 cm depth and four groundwater piezometers (H01, H02, H04 and H09) are used (see (Blöschl *et al.*, 2016) for details). Soil moisture data are averaged over depth for extracting soil moisture related variables. Precipitation measurements are averaged by using Thiessen polygon method, and the catchment averages range from 0 to 21.5 mm/hrs (average: 0.09 mm/hrs). The higher and smaller precipitation intensities are observed in summer and in winter periods, respectively (Figure 11 (a)). The mean annual precipitation in the study period is decreasing from 937 mm in 2013 to 573 mm in 2015. Comparison of the frequency of daily maximum precipitation from the period 1946 to 2018 indicates that selected study period represents well the frequency of precipitation intensities larger than 30 mm/d or 50 mm/d. Observed air temperature ranges from -15.2 to 36.3°C during the period from 2013 to 2015 and seasonal dynamics of potential evapotranspiration corresponds to the seasonal dynamics of air temperature (Figure 11 (b)). The effect of increased air temperature and potential evaporation in summer is reflected by decreasing soil moisture and groundwater levels (Figure 11 (c)). The seasonal dynamics of event runoff coefficient (R_c) and recession time constant (T_c) (Figure 11 (d,e)) indicates smaller values of R_c and T_c in summer and their gradual increase towards winter season.

Controls on event runoff coefficients and recession time constants for different runoff generation mechanisms identified by three regression methods

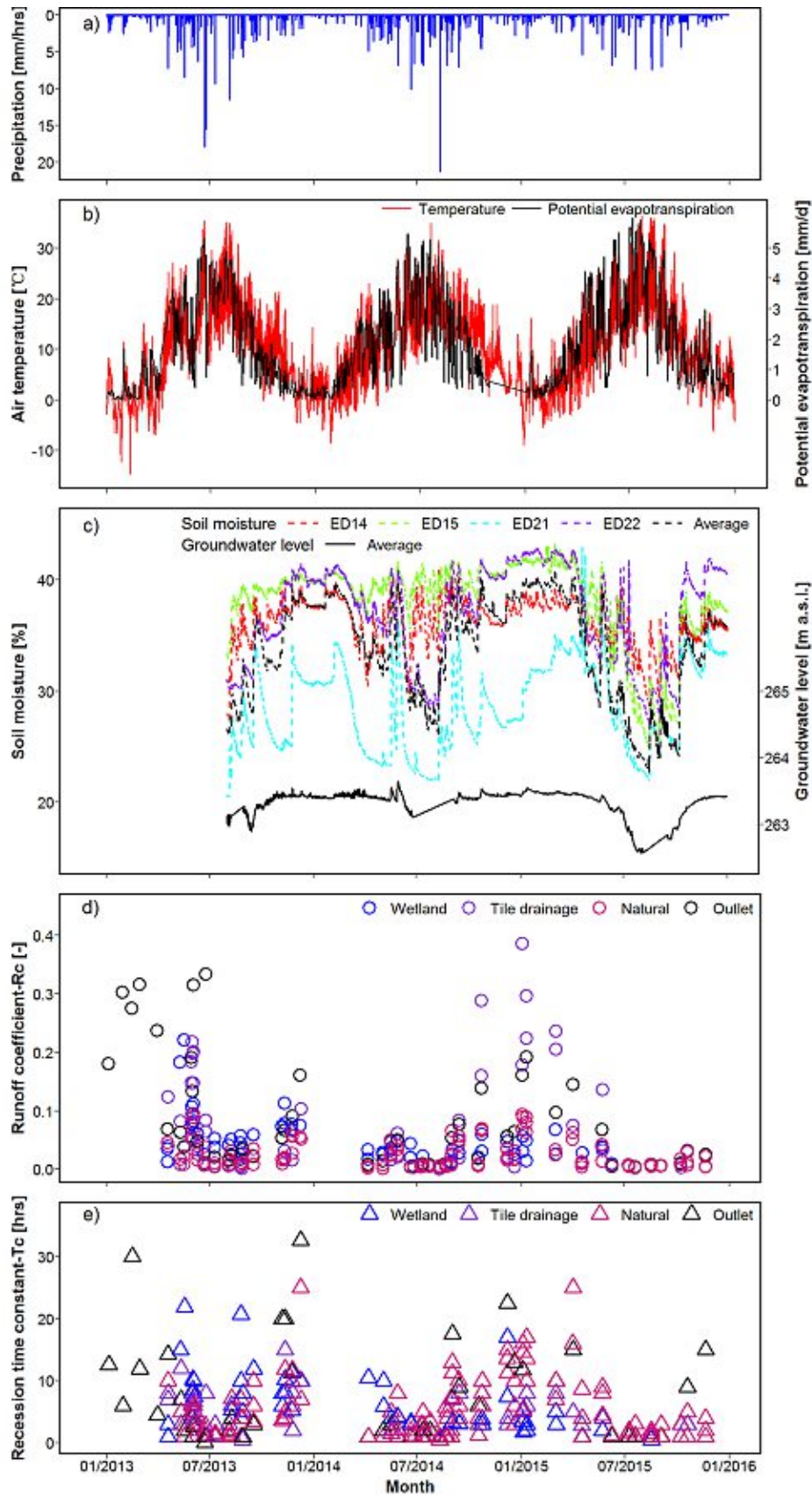


Figure 11. Temporal variability of precipitation (panel a), air temperature and potential evapotranspiration (panel b), soil moisture and groundwater level (panel c), event runoff coefficient (panel d) and recession time constant (panel e) in HOAL in the period 2013 to 2015.

3.6. Methodology

3.6.1. Estimation of event runoff coefficients and recession time constants

The event runoff coefficients and recession time constants are estimated for each of the eight stream gauges separately using the method of *Merz et al.* (2006). The analysis is based on an hourly time step and consists of four steps:

- (1) Catchment rainfall estimation: For each of the eight stream gauges, catchment average rainfall is estimated at an hourly time step by spatially interpolating the measurements of four rain gauges using the Thiessen polygon method.
- (2) Baseflow separation: Baseflow is estimated for each stream gauge using the *Chapman and Maxwell* (1996) filter. More details about the filter are given in *Merz et al.* (2006).
- (3) Identification of runoff events: An event peak is identified, if the direct flow is more than double of the baseflow at a certain time step and larger runoff is not observed 5 hours before and after the peak. Around these peaks, the beginning and end times are estimated. An example of an identified event in May of 2014 is shown in Figure 12 (a). This event is driven by a late spring precipitation event with a peak of 7.0 mm/hrs, which is larger than 80% of identified events. The event runoff coefficient in a tile drain system Frau2 is about 0.06 higher than at the main catchment outlet MW. Figure 12 (b) shows the dynamics of the ratio of cumulative direct runoff to cumulative precipitation as a function of time during an event for different gauges. The ratio gradually increases and approaches a stable value at the end of the event, which is the R_c of that event. There is a large difference between Frau1 and Frau2 due to differences in the controls. A total of 57 event periods are identified at MW outlet. At the tributaries slightly fewer are identified, as they do not always respond to rainfall. The number of identified events in individual subcatchments and main outlet are 30 (A1), 38 (A2), 21 (Frau1), 30 (Frau2), 32 (Sys2), 39 (Sys3), 51 (Sys4) and 57 (MW outlet), respectively. This results in a total of 298 event hydrographs from 2013 to 2015 to be further analysed.
- (4) Fitting a linear reservoir model: In order to reduce the effect of the selection of the end time of the runoff events, a linear reservoir model is fitted to the direct flow by minimizing the root mean square difference between observed and simulated runoff for each event and stream gauge separately. The event runoff coefficient R_c (-) and the recession time constant T_c (hrs) are the optimised model parameters.

Controls on event runoff coefficients and recession time constants for different runoff generation mechanisms identified by three regression methods

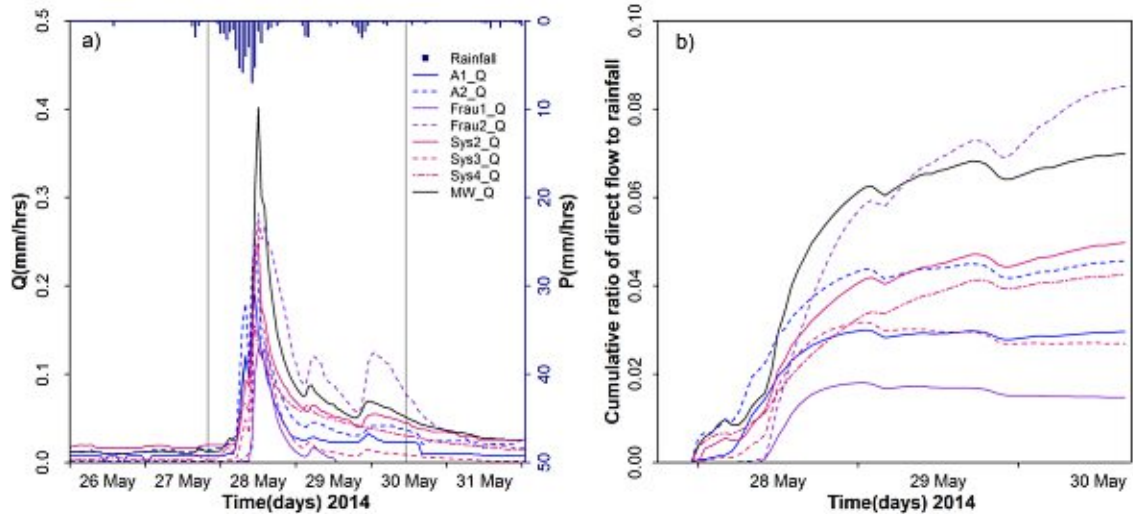


Figure 12. Example event in May 2014. Line colours according to runoff generation mechanisms (wetland runoff is blue; tile drainage is purple; natural discharge is dark pink and outlet flow is black). (a) Hydrographs. Vertical lines indicate start and end of the event. (b) Ratio of cumulative direct flow to cumulative precipitation during the event.

3.6.2. Ensemble learning techniques for regression

For the purpose of the study, three learning techniques are used to build regression models. Ensemble learning techniques have been proved in the past to describe and learn various nonlinear relationships (Dietterich, 1997). The main advantage of ensemble learning approaches is that they learn in a hierarchical fashion by repeatedly splitting input dataset into separate branches that maximize the information gain of each split. The challenge with their application is, however, that for the selection of an optimal approach, evaluation of performance of different algorithms is recommended (Shen, 2018). Random forests, gradient boost decision trees and support vector machines are chosen in this chapter. As the most popular algorithms, both random forests and gradient boost decision trees are easier to explain and have lower training times compared to support vector machines, while support vector machines are more efficient both for high-dimensional spaces and small samples. Thus the aim of our study is to test these three different approaches individually in four different settings represented by four runoff generation systems (wetland, tile drainage, natural and outlet) which are termed as Classified regression model in our study, and in an aggregated system that combines all runoff generation systems termed here as Unclassified regression model.

3.6.2.1. Random Forests (RF)

Random forests consist of a number of tree predictors. As the number of trees increases, the mean squared error of out of bag data (OOBError) in prediction decreases until it reaches a constant, low level (Ho, 1995). There are two main steps:

(a) Random sampling from the entire database to train a decision tree. The input subsets are different from each other to avoid over-fitting. Out of bag data (OOB) is the remaining subset,

Controls on event runoff coefficients and recession time constants for different runoff generation mechanisms identified by three regression methods

which is not used in building a tree. At each node of the trees, the feature that produces the best split in sub-sampling from all features is used for splitting.

(b) Splitting at each node: Each decision tree is completely split until all samples belong to one class or the leaf node can not be further divided. The feature importance outputs of the RF model with good predictions are used to evaluate the influence of the variables on Rc and Tc.

3.6.2.2. Gradient Boost Decision Trees (GBDT)

A Gradient Boost Decision Tree GBDT regression model is established by integrating multiple decision trees (DTs) in an iterative process (Friedman, 2001; 2002). In every iteration (adding a new tree to the model), model losses are reduced. A Gaussian distribution is chosen as a loss function L for minimizing the squared error,

$$L(y, f(x)) = \frac{1}{\sum_i \omega_i} \sum \omega_i (y_i - f(x_i))^2 \quad (1)$$

where ω_i is the weight of sample i , y_i are the objectives and $f(x_i)$ are the predictions.

3.6.2.3. Support Vector Machines (SVM)

For a support vector machine (SVM) regression to represent non-linear problems, a proper kernel function needs to be chosen by projecting the data to a high-dimensional space where one can use a linear decision boundary to separate classes (Osuna, 1998). A radial basis function, K, is used here which can be expressed for an infinite dimensional space (Horn and Johnson, 1985) as Function (2)

$$K(u, v) = e^{-\gamma \|u-v\|^2} \quad (2)$$

where u and v are two vectors, $\|u-v\|^2$ is the squared Euclidean distance of these two vectors, and γ influences the number of support vectors. Larger γ results in fewer support vectors.

The ε regression option is adopted here for better controlling model error. Errors beyond the specified ε are penalized in proportion to C, which is the regularization parameter. The ε insensitive loss function L_ε proposed by Chapelle and Vapnik (2000) is used according to Function (3)

$$L_\varepsilon = \begin{cases} 0 & \text{if } |y - f(x)| < \varepsilon \\ |y - f(x)| - \varepsilon & \text{otherwise} \end{cases} \quad (3)$$

For brevity, only the variable importance of the SVM model, $I_{i,SVM}$ which can reflect the level of variable influences to model objectives (Rc and Tc in this study), are presented in the study. In order to quantify such importance of variables, we take advantage of the Average Absolute Deviation (AAD) from the median in the theory of 1-D sensitivity analysis (Cortez and Embrechts, 2013). $I_{i,SVM}$ is estimated according to the following function

$$I_{i,SVM} = \sum_{j=1}^L \frac{|y_j - \tilde{y}|}{L} \quad (4)$$

where \tilde{y} is the baseline of the objectives (median) and y_j is the prediction related to the j^{th} level of input (totally $L=7$ levels).

Controls on event runoff coefficients and recession time constants for different runoff generation mechanisms identified by three regression methods

The detailed procedures of building the SVM regression models are introduced by *Cortes and Vapnik (1995)*.

3.6.3. Calibration and validation performance of the non-linear regression models

In order to compare the performance of the three machine learning methods, two types of validations are performed. The first is the temporal validation using approximately 20% of total events which is not included in calibration to avoid overfitting. Performance is evaluated by the coefficients of determination (R^2)

$$R^2 = 1 - \frac{\sum_i (y_i - f(x_i))^2}{\sum_i (y_i - \bar{y})^2} \quad (5)$$

where $f(x_i)$ is the prediction of Rc or Tc for event i , y_i is the observed value, and \bar{y} is the mean of the observed values over all events of a particular runoff generation type. R^2 is regarded as 0 when it is negative.

The second type is the validation in space by using leave-one-out cross-validation. Here, the regressions fitted separately to one of the subcatchments representing wetland (A2 station), tile drainage (Frau2 station) and natural drainage (Sys3 and Sys4 stations) are validated in the other stations representing the same runoff generation type, i.e. A1 (wetland), Frau1 (tile drainage), Sys2 (natural drainage). The performance is evaluated by R^2 , similarly to Function (5).

3.7. Results

3.7.1. Evaluation of the runoff event characteristics and their potential controls

In order to analyse the potential controls on Rc and Tc, 22 hydrological variables are considered for each stream gauge (Table 5). Event precipitation (VolP), precipitation peak during the event (PeakP) and precipitation duration during the event (DurP) are estimated from the catchment precipitation time series with hourly temporal resolution. Antecedent soil moisture (PreSM), average soil moisture during the event (AverSM), soil moisture at the end of the event (EndSM), soil moisture at the time of peak rainfall (PeakPSM) and soil moisture peak during the event (PeakSM) are estimated from the soil moisture data. Depending on the stream gauge, different soil moisture sensors are used (ED15 for Sys2 and Sys3; ED22 for Sys4; ED21 for Frau1 and Frau2; ED14 for A1 and A2; and the average of all sensors for MW). Soil moisture peak delay to precipitation (DelaySM) is estimated as the time difference between the precipitation peak and the soil moisture peak. Pre-event groundwater level (PreWL), average groundwater level during the event (AverWL), groundwater level at the end of the event (EndWL), groundwater level at the time of peak precipitation (PeakPWL) and peak groundwater level (PeakWL) are estimated from the average groundwater level of all four piezometers, as no separate piezometer data are available for the individual catchments. Groundwater level peak delay to precipitation (DelayWL) is estimated as the time difference between the precipitation peak and the groundwater peak. Potential evapotranspiration (EP) on the day of the event is estimated by the Penman-Monteith equation. Additionally, the month of the event occurred (Month), the Normalized Difference Vegetation Index (NDVI) and the runoff generation type (Type: 1-wetland; 2-tile drainage; 3-outlet; 4-natural drainage) are considered as variables. NDVI represents the mean catchment or subcatchment value and it is estimated by linear interpolation between 57 Landsat 7 and 8 scenes

Controls on event runoff coefficients and recession time constants for different runoff generation mechanisms identified by three regression methods

available in the period 2013-2015. Finally, drainage area (Area), percentage of piped area (AreaPipes) and forest cover (AreaForest) are also used. 22 hydrological variables and R_c and T_c are normalised to the range between 0 and 1 for all runoff generation systems together.

Table 5. Event based hydrological variables examined as potential controls on R_c and T_c . While the variables differ between stream gauges, the combined statistics of all stream gauges are shown here.

Variables	Explanation	Min	25%	50%	75%	Max
VolP	Volume of precipitation during event (mm)	3.5	12.7	17.5	27.5	99.3
PeakP	Precipitation peak during event (mm/hrs)	0.2	2.8	3.7	6.7	21.5
DurP	Precipitation duration during event (hrs)	2.0	9.0	17.0	29.8	102.0
PreSM	Antecedent soil moisture (%)	20.5	30.2	35.5	38.6	42.4
PeakSM	Peak of soil moisture during event (%)	24.9	34.2	38.2	40.0	43.2
PeakPSM	Soil moisture at the time of peak precipitation (%)	20.5	30.2	36.9	39.3	43.0
AverSM	Average soil moisture during event (%)	22.6	31.7	37.0	39.2	42.6
EndSM	Soil moisture at the end of event (%)	23.6	33.6	37.9	39.4	42.6
DelaySM	Soil moisture peak delay to precipitation (hrs) (positive value indicates earlier flow peak than soil moisture)	-13.0	2.0	7.0	11.0	63.0
PreWL	Pre-event groundwater level (m)	262.6	263.3	263.4	263.5	264.7
PeakWL	Peak groundwater level (m)	262.7	263.3	263.5	263.5	264.9
PeakPWL	Groundwater level at the time of peak precipitation (m)	262.7	263.3	263.4	263.5	264.7
AverWL	Average groundwater level during event (m)	262.7	263.3	263.5	263.5	264.7
EndWL	Groundwater level at the end of event (m)	262.7	263.3	263.5	263.5	264.8
DelayWL	Groundwater level peak delay to precipitation (hrs) (positive value indicates earlier flow peak than groundwater level)	-12.0	13.0	18.0	27.0	103.0
EP	Potential evapotranspiration during the day of event (mm/d)	0.0	0.9	1.7	2.7	5.1
Month	Month when event occurred (month)	1	5	7	9	12
NDVI	Normalized Difference Vegetation Index	0.1	0.2	0.3	0.3	0.5
AreaPipes	Piped area relative to drainage area (%)	4.3	6.5	10.7	12.9	96.6
AreaForest	Forest covered area percentage to drainage area (%)	0.0	4.6	9.6	14.2	18.8
Area	Drainage area of subcatchment (ha)	1.1	2.4	4.3	37.4	65.8
Type	Runoff generation type (1-wetland; 2-tile drainage; 3-outlet; 4-natural drainage)	1	2	3	4	4

The statistics and cumulative distributions of the resulting coefficients are respectively showed in Table 6 and Figure 13. R_c varies from 0.0003 to 0.4. The tile drainage catchment Frau 2 has the highest median (0.054), the natural subsurface drainage Sys4 the lowest (0.012). The tile

Controls on event runoff coefficients and recession time constants for different runoff generation mechanisms identified by three regression methods

drainage catchment Frau 2 has the highest median of Tc (5.5 hrs), the outlet MW the lowest (3.0 hrs) but the 75% quantile is larger than that of the subcatchments (10 hrs). The correlation coefficient of Rc and Tc over all 298 hydrographs is about 0.38. High Rc is usually associated with high antecedent flows which may result in slower runoff recession (Patnaik *et al.*, 2015) because of large groundwater contributions (Exner-Kittridge *et al.*, 2016).

Table 6. Statistics of the event runoff coefficients Rc and recession time constants Tc, including minimum, quartiles and maximum, for the eight stream gauges based on 40 events which can be observed at least at 5 stations.

Gauge	Runoff generation mechanism	Rc (-)					Tc (hrs)				
		Min	25%	50%	75%	Max	Min	25%	50%	75%	Max
A1	Wetland	0.010	0.026	0.033	0.049	0.082	1.00	3.00	4.00	8.00	16.98
A2	Wetland	0.006	0.028	0.048	0.068	0.222	0.50	2.00	3.89	7.57	21.90
Frau1	Tile drain	0.001	0.016	0.033	0.181	0.297	0.50	3.00	4.00	6.00	10.00
Frau2	Tile drain	0.0003	0.026	0.054	0.139	0.386	1.00	3.00	5.50	8.00	15.00
Sys2	Natural drainage	0.006	0.010	0.034	0.058	0.089	1.00	4.00	5.00	7.00	17.00
Sys3	Natural drainage	0.001	0.005	0.018	0.026	0.094	0.50	1.63	4.20	7.60	14.67
Sys4	Natural drainage	0.004	0.008	0.012	0.037	0.096	1.00	1.04	3.36	8.00	25.00
MW	Outlet	0.004	0.014	0.048	0.071	0.316	0.10	1.00	3.00	10.00	32.56
All gauges		0.0003	0.012	0.032	0.063	0.386	0.10	2.00	4.00	8.00	32.56

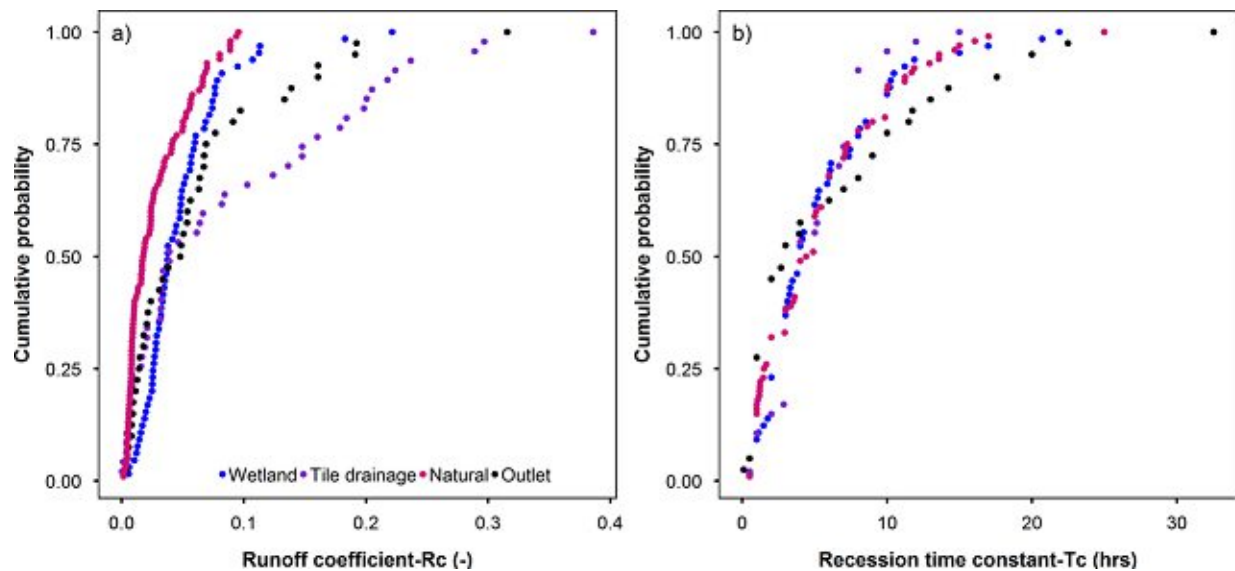


Figure 13. Cumulative distribution of (a) event runoff coefficients and (b) recession time constants for the four types of runoff generation mechanisms.

Controls on event runoff coefficients and recession time constants for different runoff generation mechanisms identified by three regression methods

3.7.2. Parameter sensitivities of the three non-linear regression models

The parameter sensitivities of the unclassified regression models are explored based on 252 event hydrographs, when events are observed at a minimum of 5 stations (Figure 14, 15&16) including all runoff generation types. Additionally 46 event hydrographs are used for validation (Table 7).

Table 7. Number of event hydrographs and number of event periods (in brackets) used for the calibration and validation for the Rc and Tc regressions. The models are fitted for the four runoff generation types (wetland, tile drainage, natural and outlet) termed as Classified regression model, and all together (Unclassified regression model).

	Number of events for Classified regression model				Number of events for Unclassified regression model
	Wetland (A1, A2)	Tile drainage (Frau1, Frau2)	Natural drainage (Sys2, Sys3, Sys4)	Outlet (MW)	All
Calibration	54	40	97	45	252 (40 event periods)
Validation	14	11	25	12	46 (17 event periods)
Total	68	51	122	57	298 (57 event periods)

3.7.2.1. RF model (*ntree* and *mtry*)

The number of trees in the model, *ntree*, has a controlling function in the model performance (Figure 14 (a,c)). As *ntree* increases, *OOBError*, i.e. the mean squared error (MSE) based on out of bag data (OOB data), decreases up to a threshold. *OOBError* is calculated according to Function (6)

$$\text{OOBError} = \frac{\sum_i^M (y'_i - y_i)^2}{M} \quad (6)$$

where M is the number of out of bag data, y_i is *i*th observation value of OOB and y'_i is the model prediction of OOB based on trees that are not trained by the *i*th sample.

OOBError stabilises at around 0.009 and 0.013 for Rc and Tc, respectively. The model performance would be improved by diversifying regression trees, however, it is difficult to build a new diverse tree if the ensemble size is large. Therefore, *OOBError* tends to approach a constant level (*Friedman, 2001*).

If the number of variables *mtry* randomly sampled as candidates at each split is close to the total number of variables, regression trees are more likely to be similar, which will reduce the predictive ability. In our case of only 22 variables, the results do not change much by *mtry* (Figure 14 (b,d), as suggested by (*Liaw and Wiener, 2002*).

Finally, for the unclassified models, *ntree* is set to 63 and 68 for the Rc and Tc regressions, respectively, by minimizing MSE of all 298 events, while *mtry* is automatically optimized. The parameters of the classified models are calibrated in the same way. The final values of *ntree* and *mtry* are listed in Table 8.

Controls on event runoff coefficients and recession time constants for different runoff generation mechanisms identified by three regression methods

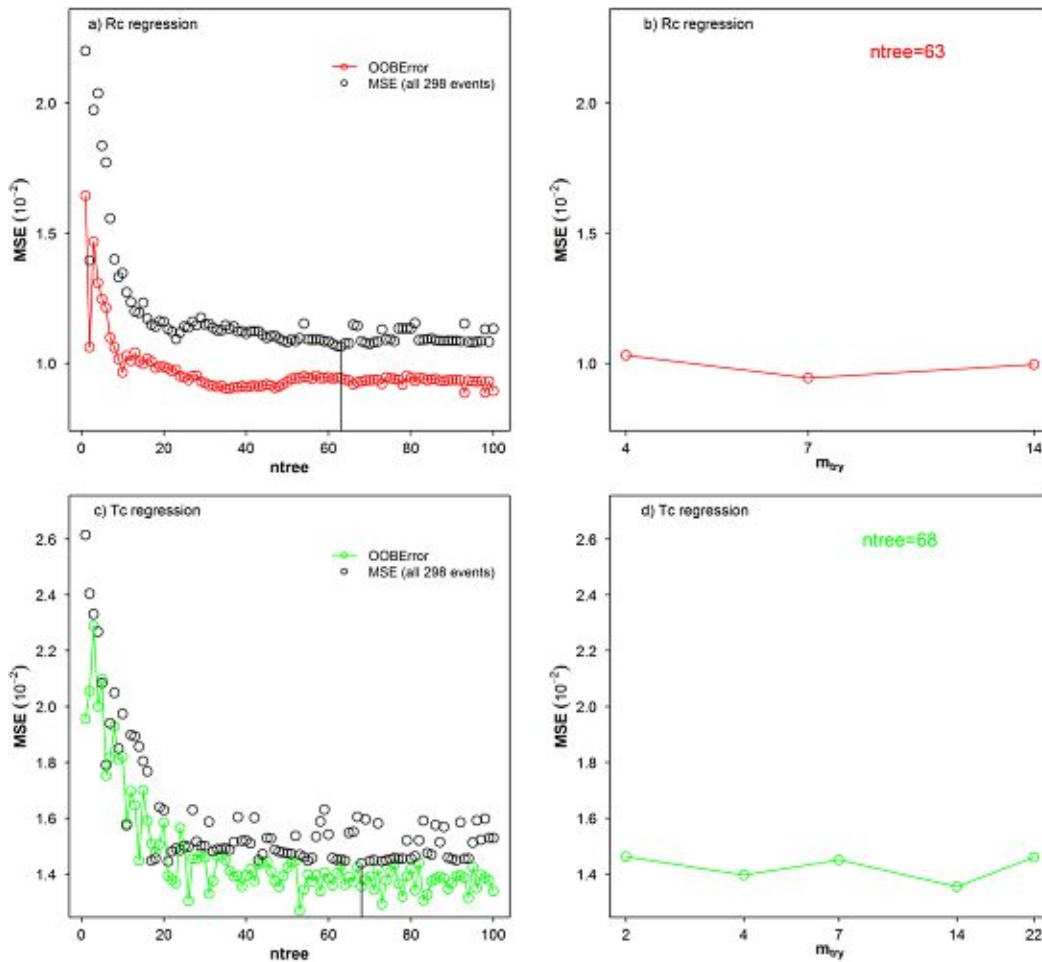


Figure 14. Sensitivity of the model error, MSE, to n_{tree} and m_{try} in the RF models for Rc and Tc regressions based on unclassified events (Table 7). The vertical black line indicates the n_{tree} chosen, 63 for the Rc regression and 68 for the Tc regression.

Table 8. Parameters of n_{tree} and m_{try} of the RF models stratified by runoff generation type. The models are fitted for the four runoff generation types (wetland, tile drainage, natural and outlet) termed as Classified regression model, and all together (Unclassified regression model).

Parameters of Random Forest model	Rc					Tc				
	Classified regression model				Unclassified regression model	Classified regression model				Unclassified regression model
	Wetland (A1, A2)	Tile drainage (Frau1, Frau2)	Natural (Sys2, Sys3, Sys4)	Outlet (MW)	All	Wetland (A1, A2)	Tile drainage (Frau1, Frau2)	Natural (Sys2, Sys3, Sys4)	Outlet (MW)	All
N_{tree}	94	52	28	83	63	86	100	60	58	68
m_{try}	7	22	4	3	7	4	4	2	4	14

Controls on event runoff coefficients and recession time constants for different runoff generation mechanisms identified by three regression methods

3.7.2.2. GBDT model (n.trees)

There are four main parameters needed for the GBDT model, shrinkage, n.minobsinnode, interaction.depth and n.trees. Reducing shrinkage, the learning rate, improves the performance while increasing the computational cost, so shrinkage is set to a low value of 0.001 (Friedman, 2001; 2002). n.minobsinnode is the minimum number of observations in a tree's terminal node, and interaction.depth represents the number of splits performed on a tree. Model performance is not sensitive to these parameters, so they were set to 10 and 6, respectively, by minimizing the cross validation errors. n.trees is the number of iterations, i.e., the number of trees in the GBDT model. Its sensitivity is analysed in Figure 15. The squared error loss of CV is calculated by averaging MSE of $k=5$ across folders

$$\text{Squared error loss of CV} = \frac{1}{k} \sum_{i=1}^k \frac{\sum_{j=1}^n (y'_{i,j} - y_{i,j})^2}{n} \quad (7)$$

where n is the number of samples in the i th folder (a total of $k=5$ folders), $y'_{i,j}$ and $y_{i,j}$ are respectively the model prediction and the objective value of sample j in folder i .

The squared error loss of CV in the Rc regression is slightly lower than that in the Tc regression (Figure 15). Increasing n.trees provides a greater improvement of performance when n.trees is small. The optimum n.trees values for the Rc and Tc regressions based on all unclassified events are manually set to n.trees=750 and 125 respectively by minimizing the squared error loss of CV in calibration and by controlling the MSE reduction (e.g. 0.015) between calibration and validation to avoid overfitting. The values of n.trees are listed in Table 9.

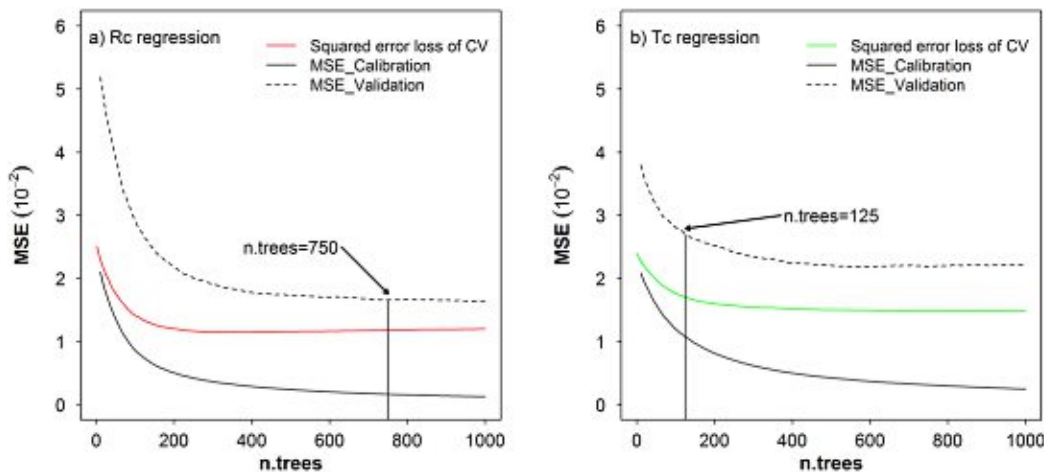


Figure 15. Sensitivity of the model error, MSE, to n.trees in the GBDT regression models for Rc and Tc regressions based on unclassified events (Table 7). Vertical black line indicates n.trees chosen: 750 for the Rc regression and 125 for the Tc regression.

Controls on event runoff coefficients and recession time constants for different runoff generation mechanisms identified by three regression methods

Table 9. Parameter of n.trees of the GBDT models stratified by runoff generation type. The models are fitted for the four runoff generation types (wetland, tile drainage, natural and outlet) termed as Classified regression model, and all together (Unclassified regression model).

Parameters of GBDT model	Rc					Tc				
	Classified regression model				Unclassified regression model	Classified regression model				Unclassified regression model
	Wetland (A1, A2)	Tile drainage (Frau1, Frau2)	Natural (Sys2, Sys3, Sys4)	Outlet (MW)	All	Wetland (A1, A2)	Tile drainage (Frau1, Frau2)	Natural (Sys2, Sys3, Sys4)	Outlet (MW)	All
<i>n.trees</i>	20	665	180	100	750	20	45	35	80	125
<i>interaction.depth=6 n.minobsinnode = 10 shrinkage = 0.001 seed=537</i>										

3.7.2.3. SVM model (γ , ϵ and C)

When calibrating the Radial Basis Function (RBF) kernel of the SVM models, three parameters are needed, γ , ϵ and C. γ is the kernel coefficient of the RBF and reducing γ will increase the performance and reduce the bias, as the number of support vectors increases. ϵ is a parameter in the insensitive-loss function (Eq. 4). Reducing ϵ increases the number of support vectors. C is the cost of violating the constraints of the regularization term in the Lagrange formulation. Large C aims at a smaller margin with better prediction but may lead to overfitting.

The squared error loss of 10 fold cross validation (Equation 8 in which k is set to 10) and the MSE reduction between calibration and validation is used for optimizing the parameters, thus preventing overfitting. A "grid-search" on γ , ϵ and C is performed using the R tune.svm function. Various triples of values are tried and the one with the best cross-validation accuracy is selected. The test sequences of the parameters are $\gamma=2^{(-7:2)}$, $\epsilon=(0.003, 0.01, 0.03, 0.1, 0.3, 1.3)$ and $C=2^{(0:6)}$ (Hsu et al., 2003). 3D sensitivity plots of the three parameters are shown in Figure 16. Table 10 gives the optimised parameter value for the classified regression models. There are many good combinations of three parameters resulting in the lowest squared error loss of 10 fold cross validation (Figure 16). The final parameter combinations are chosen by both minimizing the squared error loss of CV in the calibration and controlling the MSE reduction.

Controls on event runoff coefficients and recession time constants for different runoff generation mechanisms identified by three regression methods

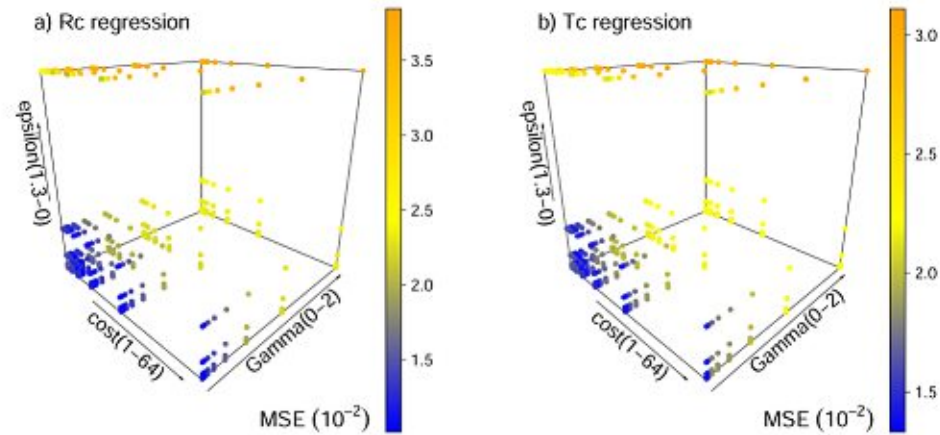


Figure 16. Sensitivity of the model error, MSE, to different combinations of γ , ϵ and C for the SVM models based on unclassified events (Table 7). MSE is the squared error loss of 10 fold cross validation.

Table 10. Parameters of the SVM models stratified by runoff generation type. The models are fitted for the four runoff generation types (wetland, tile drainage, natural and outlet) termed as Classified regression model, and all together (Unclassified regression model).

Parameters of SVM model	Rc					Tc				
	Classified regression model				Unclassified regression model	Classified regression model				Unclassified regression model
	Wetland (A1, A2)	Tile drainage (Frau1, Frau2)	Natural (Sys2, Sys3, Sys4)	Outlet (MW)	All	Wetland (A1, A2)	Tile drainage (Frau1, Frau2)	Natural (Sys2, Sys3, Sys4)	Outlet (MW)	All
γ	2^{-7}	2^{-5}	2^{-7}	2^{-6}	2^{-7}	2^{-6}	2^{-6}	2^{-7}	2^{-5}	2^{-5}
ϵ	1.3	0.1	0.1	0.03	0.01	1.3	0.1	0.3	0.1	0.03
C	2	2	2^5	2^6	2^6	1	1	1	1	2^3

3.7.3. Temporal calibration and validation performance of regression models

Figure 17 shows the estimates of R_c and T_c for the RF, GBDT and SVM models based on unclassified events as in the last column in Table 7. The performances of the R_c regressions based on the GBDT and SVM algorithms are better than that of the RF model with R^2 of 0.71 and 0.67 in validation, respectively. The performances of the T_c regressions based on the RF and SVM algorithms are better than that of the GBDT model with R^2 of 0.44 and 0.45 in validation, respectively.

Controls on event runoff coefficients and recession time constants for different runoff generation mechanisms identified by three regression methods

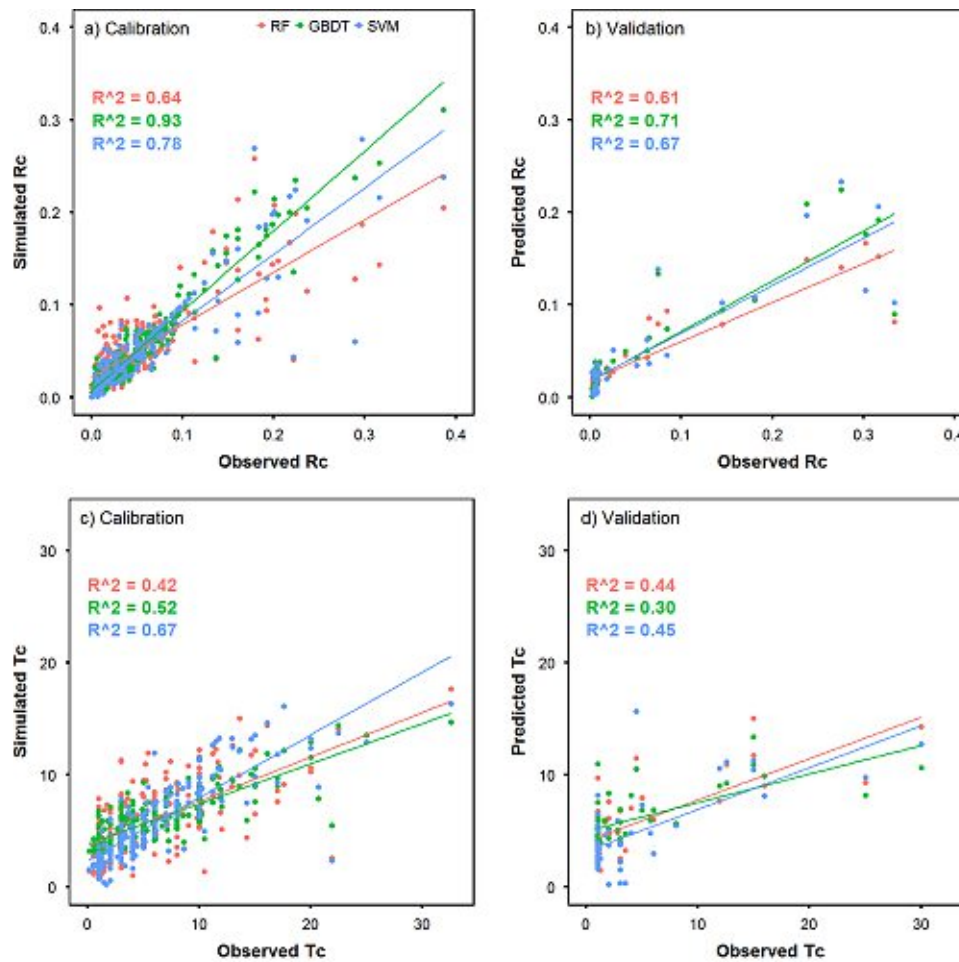


Figure 17. Estimates of the RF, GBDT and SVM regression models plotted against the observations of Rc and Tc. Estimation is based on unclassified events (252 are used for calibration and 46 for validation). Colours indicate the regression models. Lines represent linear relation between estimation and observation. Panels a) and c): calibration. Panels b) and d): validation.

Figure 18 compares the calibration and validation performance of the regressions (as in Table 7). The performance of the SVM model is generally higher than that of the others, which may be due to the higher dimensional space of the SVM regression (Asefa *et al.*, 2006). The performance of the Tc regression models is generally low for all methods. This may be due to the lack of subcatchment groundwater data that might improve the performance, particularly for wetlands and natural drainage runoff generation systems which are in HOAL closely related to groundwater level dynamics. On the other hand, the Rc and Tc regressions of the natural drainage subcatchment and the unclassified events have a somewhat higher performance than the other systems, probably because of the larger number of events that are available. The models highlighted by boxes in the left panel have higher values of R^2 than 0.6, both in calibration and validation.

Controls on event runoff coefficients and recession time constants for different runoff generation mechanisms identified by three regression methods

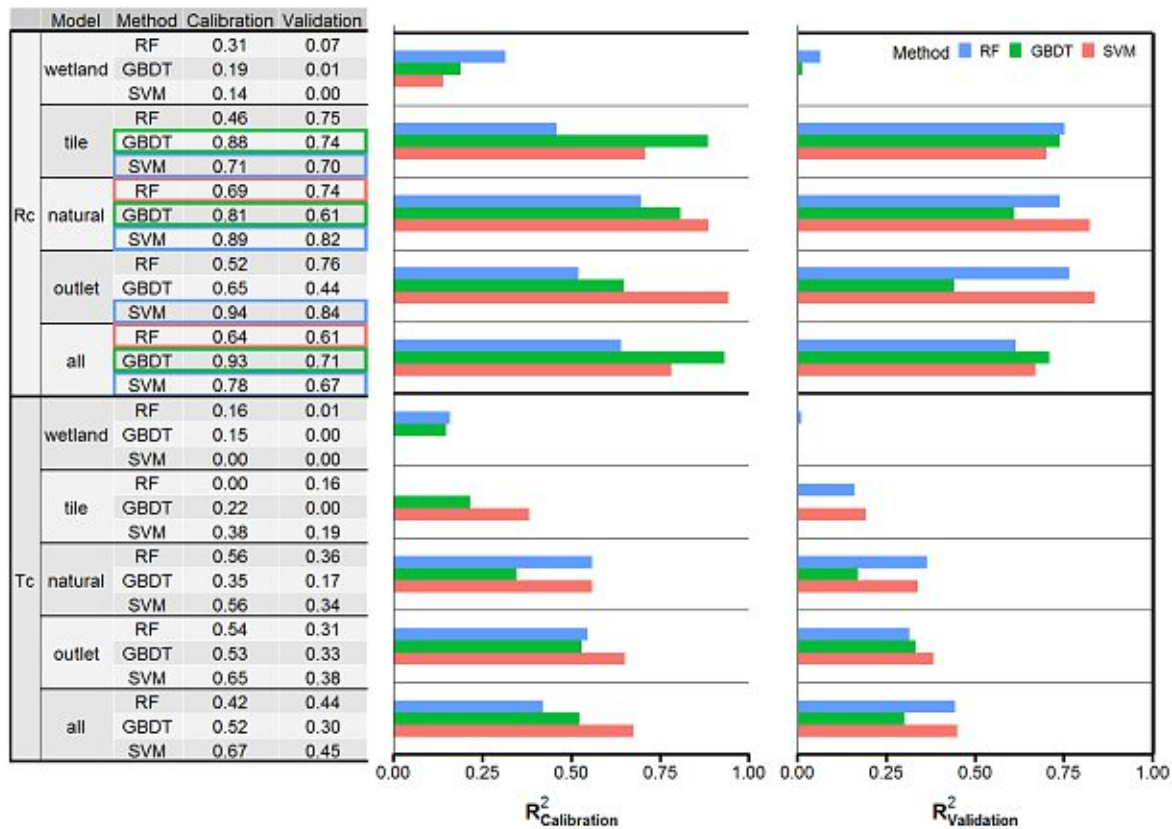


Figure 18. Comparison of R^2 (coefficients of determination) of temporal calibration and validation between different regression methods (colours) used to estimate R_c and T_c stratified by runoff generation type. Models with $R^2 > 0.6$ both in calibration and validation are highlighted by boxes at the left.

3.7.4. Spatial calibration and validation performance of regression models

Table 11 lists the number of events used for calibration and validation in a spatial leave one out mode. The classified regressions of R_c and T_c including wetland, tile drainage and natural subsurface flow, are spatially validated. For the wetland regressions, 38 events from station A2 are used for calibration and 30 events from station A1 for validation; for the tile drainage regressions, 30 events from Frau2 are used for calibration and 21 events from Frau1 for validation; for natural subsurface flow, 90 events in Sys3 and Sys4 are used for calibration and 32 events in Sys2 for validation. Additionally, a total of 252 hydrographs during 40 events that are observed in at least 5 stations, are used for building 8 Leave_one_out models in which the events of one of the subcatchments are used for validation and the rest for calibration. The SVM regression models generally have a better performance (measured by R^2) than the other models, which is similar to the temporal validation (Figure 19).

Controls on event runoff coefficients and recession time constants for different runoff generation mechanisms identified by three regression methods

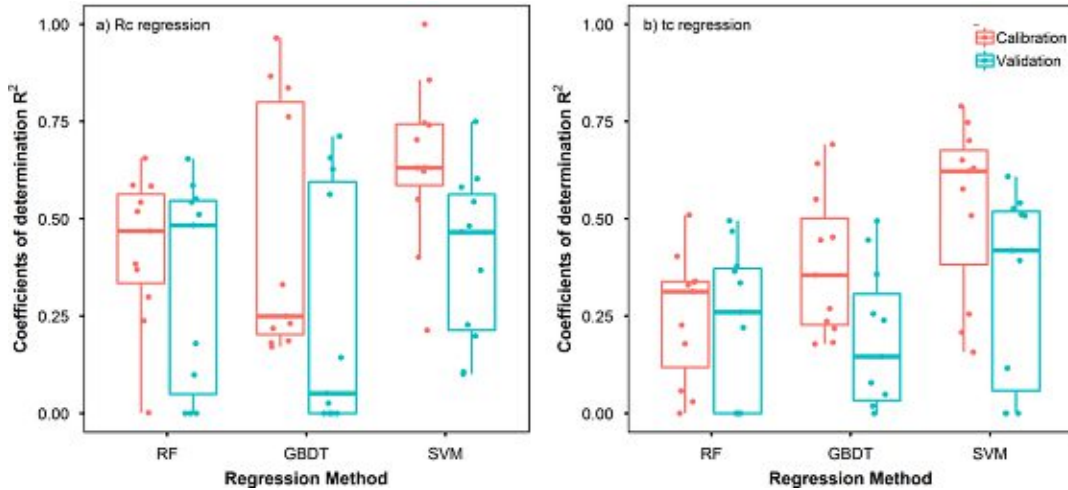


Figure 19. Performance, R^2 (coefficients of determination), of the Rc/Tc regression methods (RF, GBDT and SVM) with spatial calibration and validation as in Table 11.

Table 11. Number of events used for spatial calibration and validation of the Rc/Tc regressions by runoff generation type. The models are fitted for the four runoff generation types (wetland, tile drainage, natural and outlet) termed as Classified regression model, and all together (Unclassified regression model).

Number of events	Rc/Tc regression										
	Classified regression model			Unclassified regression model							
	Wetland	Tile drainage	Natural	Leave_A1_out	Leave_A2_out	Leave_Frau1_out	Leave_Frau2_out	Leave_Sys2_out	Leave_Sys3_out	Leave_Sys4_out	Leave_MW_out
Calibration	38 (A2)	30 (Frau2)	90 (Sys3, Sys4)	223	216	233	224	223	220	213	212
Validation	30 (A1)	21 (Frau1)	32 (Sys2)	29 (A1)	36 (A2)	19 (Frau1)	28 (Frau2)	29 (Sys2)	32 (Sys3)	39 (Sys4)	40 (MW)
Total	68	51	122	252	252	252	252	252	252	252	252

3.7.5. Linear correlations of Rc and Tc with the explanatory variables

Pearson's correlation coefficient (r) of Rc and Tc with the explanatory variables of Table 5 is evaluated for the entire set of 298 events, i.e. for all stream gauges together (Table 12). Rc is positively correlated with DurP, VolP, AreaPipes and groundwater related variables (PreWL, PeakWL, PeakPWL, AverWL, EndWL and DelayWL). The highest r are obtained for EndWL and DurP ($r = 0.5$), suggesting that groundwater and precipitation are the two factors that are most strongly connected to Rc. It is also interesting that the rainfall duration (DurP) affects r more strongly than event precipitation volume (VolP). It seems that higher groundwater levels lead to more direct flow generated during an event. The groundwater level data reflect the catchment storage conditions, particularly those close to the stream, as most piezometers are close to the stream. The peak rainfall intensity (PeakP) is negatively correlated with Rc (but DurP positively), suggesting that saturation excess runoff tends to be more important than infiltration excess runoff.

A clearly positive effect on T_c can be found of the variables $DurP$, $DelayWL$ and the soil moisture related variables ($PreSM$, $PeakSM$, $PeakPSM$, $AverSM$ and $EndSM$). The largest absolute r occurs for the precipitation variables ($PeakP$ and $DurP$). Longer $DurP$ and lower $PeakP$ generally result in slower recessions. Higher rainfall intensities lead to higher peak flows and thinner shapes of the hydrographs with faster recessions. The influence of soil moisture and groundwater on T_c is somewhat lower than that of precipitation. In summer, higher precipitation intensity together with low soil moisture and groundwater levels generally come out with quick streamflow recessions with low T_c , while in winter lower precipitation intensity and wetter conditions usually with higher T_c .

Table 12. Correlation coefficient (r) of R_c and T_c with the explanatory variables according to Table 6.

r	VolP	PeakP	DurP	Pre SM	Peak SM	PeakP SM	Aver SM	End SM	Delay SM	Pre WL	Peak WL
R_c	0.15	-0.29	0.50	-0.04	-0.02	-0.01	-0.01	-0.03	0.02	0.43	0.48
T_c	-0.04	-0.40	0.38	0.30	0.29	0.32	0.31	0.28	-0.01	0.19	0.14
r	PeakP WL	Aver WL	End WL	Delay WL	EP	Month	NDVI	Area Pipes	Area Forest	Area	Type
R_c	0.47	0.47	0.50	0.30	-0.26	-0.32	-0.21	0.28	-0.17	0.08	-0.19
T_c	0.16	0.15	0.14	0.33	-0.33	0.05	-0.22	-0.04	0.05	0.06	-0.002

3.7.6. Importance of explanatory variables for R_c and T_c

The importance of the explanatory variables for estimating R_c and T_c from the non-linear regression models was evaluated on the basis of $I_{i,SVM}$ (section 3.6). The heatmap (Figure 20) shows the relative importance of the explanatory variables, where each column represents one model and the colour indicates the importance of the explanatory variables. The temporal non-linear regression models are used for this analysis because of the larger database (Table 7).

For evaluating the effects of multicollinearity to variable importance of regression model, the variance inflation factor (VIF) has been calculated for each variable. VIF of most variables are smaller than 5 apart from soil moisture ($PreSM$, $EndSM$, $AverSM$, $PeakSM$ and $PeakPSM$) and groundwater related variables ($PreWL$, $EndWL$, $AverWL$, $PeakWL$ and $PeakPWL$). Therefore the difference from five soil moisture/groundwater variables is difficult to be explained from $I_{i,SVM}$. Figure 20 suggests that both antecedent soil moisture ($PreSM$) and groundwater related variables ($PreWL$ and $AverWL$) have a relative high importance for the R_c regression of natural subsurface flow. This is in line with Tarasova et al. (2018a; b) who found that catchment storage plays a considerable role in the prediction of event runoff response. In the wetland drainage area soil moisture is always high, in the tile drainage area soil moisture varies moderately, and in the natural drainage area the seasonal variability of soil moisture is largest, which is reflected in a larger effect on R_c . Precipitation duration ($DurP$) always shows a large influence on R_c in the tile drainage system and at the catchment outlet. Potential evaporation (EP) is another important variable for the R_c regression in the tile drainage systems. This suggests that R_c in the tile drainage systems is more affected by the weather conditions than the subsurface dynamics. Groundwater related variables are more important in the natural system and for the entire catchment. For the unclassified data set, two soil moisture related variables ($PeakSM$ and

Controls on event runoff coefficients and recession time constants for different runoff generation mechanisms identified by three regression methods

EndSM) generally play an important role, which means that soil moisture is a good indicator of catchment storage affecting drainage condition during the events.

The performance of the Tc regressions is not as good as that of the Rc regressions ($R^2 < 0.5$ in validation mode). The precipitation variables (DurP and PeakP) and groundwater peak delay to precipitation (DelayWL) are more important than other variables. Exner-Kittridge et al. (2016) has suggested that most of the HOAL baseflow stems from groundwater, so the time when groundwater starts to contribute to the recession compared to the precipitation peak (DelayWL) may have a controlling function on the discharge recession rate.

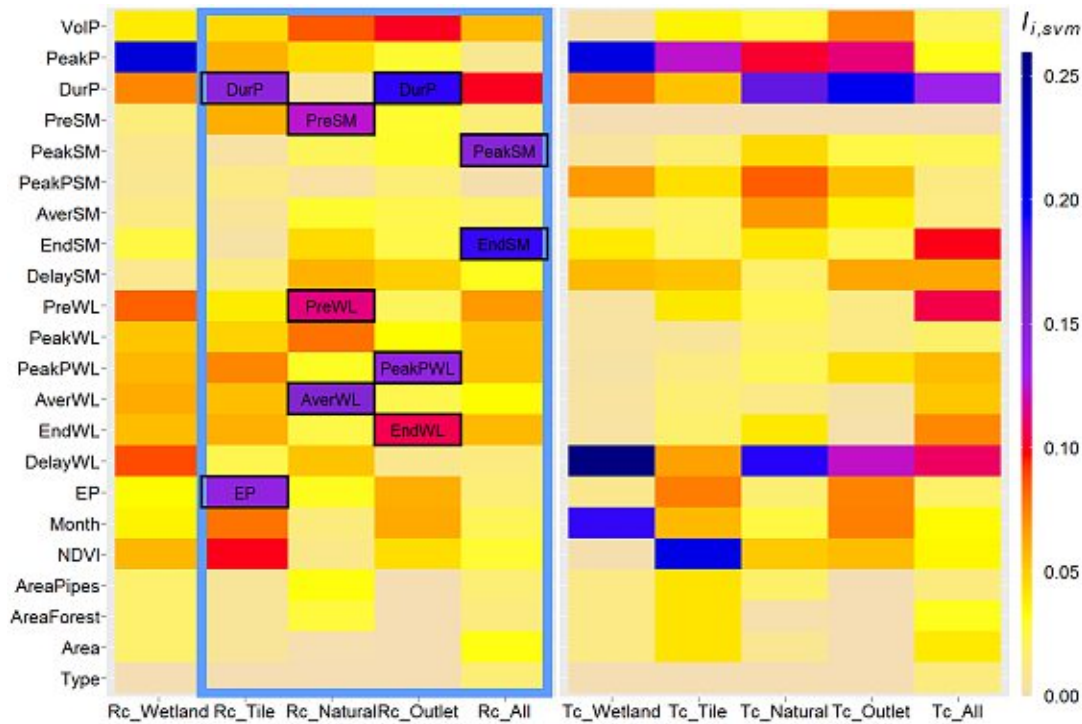


Figure 20. Heatmap of the variable importance $I_{i,SVM}$ for the classified and unclassified models using the SVM regression method. The Y-axis represents 22 variables, the X-axis the models based on different subcatchment types. Left: Rc. Right: Tc. Models with $R^2 > 0.6$ both in calibration and validation (Figure 18) are highlighted by a blue box, and the variables with the best $I_{i,SVM}$ performance are highlighted by black rectangles. Database as in Table 7.

3.8. Discussion

This study addresses two main research questions. The first is the relative performance of three machine learning methods in estimating event runoff coefficients, Rc, and recession time constants, Tc. We use 22 event based explanatory variables in these methods representing precipitation, soil moisture, groundwater level and season. The regressions are performed for four, classified subcatchment groups (wetland, tile drainage, natural, outlet runoff) and for unclassified regressions using all event hydrographs from all subcatchments. Model performances, measured by the coefficient of determination, shows that the SVM algorithm generally gives more accurate Rc and Tc predictions than the other two methods (RF and GBDT). This is due to the fact that the SVM algorithm can transform the 22 dimensional variables to a

higher dimensional space and it generally performs better for small sample sizes. The Rc regressions using SVM for tile drainage, natural, outlet and unclassified events show good performances with R^2 greater than 0.6, but the regression for the wetlands perform less well. The latter is presumably related to the lack of infiltration information in the wetland areas. The best Tc estimates are obtained by the SVM model for unclassified events with $R^2= 0.45$ in calibration mode. Overall, the Tc regressions perform less well than those of Rc which is likely related to the more complex nature of subsurface and surface routing as compared to runoff generation. New geophysical observations about the structure and connectivity of different groundwater storages and understanding of the connections between shallow and deep aquifers will allow to improve model performance in the future.

The second research question relates to the most relevant variables for the Rc and Tc regression based on the models described above by different categories of runoff systems. The relative importance of the variables of the SVM model is assessed by a heatmap. It suggests that precipitation duration plays an important role in predicting Rc for the tile drainage and outlet systems. This is in line with *Merz et al. (2006)* who concluded that the spatial patterns of median event runoff coefficients are highly correlated with the spatial patterns of mean annual precipitation in this climatic region. Antecedent soil moisture only affects Rc for the natural system, but not for the tile drainage and wetland systems. Potential evapotranspiration (EP) is an important factor in the tile drainage systems. It can therefore be concluded that event based Rc of the tile drainage systems is more controlled by weather conditions than by the catchment state, while the opposite is true of the natural drainage systems. This behaviour of the natural drainage systems of the HOAL is similar to the results of *Tarasova et al. (2018a; b)*, who found that the response of lowland catchments with substantial storage is driven by pre-event saturation instead of rainfall properties.

Overall, the chapter shows that both the performance of estimating Rc and Tc and the relative importance of explanatory variables depends strongly on the types of the hydrological systems, i.e. the runoff generation mechanism. The chapter proposes three machine learning techniques as tools for predicting event based Rc and Tc on the basis of weather and land surface characteristics.

3.9. Conclusions

This study quantified the importance of 22 explanatory variables influencing the runoff response for different runoff generation mechanisms in a small agricultural catchment through regressions of event runoff coefficient (Rc) and recession time constant (Tc) based on three machine learning algorithms (Random forest (RF), Gradient Boost Decision Tree (GBDT) and Support vector machine (SVM)). Our results showed that:

- Regressions of Rc and Tc based on the SVM algorithm generally have more accurate predictions than those based on RF and GBDT. Using SVM, the performance (R^2) of Rc regressions is larger than 0.6 for the tile drainage, natural, outlet and unclassified events. The best performance (R^2) of Tc regression is 0.45 for unclassified events in calibration mode. Therefore, Tc is related to more complex subsurface processes, and more geophysical observations could improve the predictions of Tc.
- The controls of event based Rc and Tc heavily depend on the runoff generation mechanisms. Precipitation duration and potential evapotranspiration are very

Controls on event runoff coefficients and recession time constants for different runoff generation mechanisms identified by three regression methods

important in the R_c regression for the tile drainages. Similar to the results of Chapter 2, antecedent soil moisture has only a significant influence on R_c for the natural systems. Therefore it can be concluded that R_c of tile drainage events is more controlled by the weather conditions, while R_c of natural drainages is more influenced by the subsurface state.

4. Impact of climate and geology on runoff event characteristics at the regional scale

4.1. General

The goal of this chapter was to link geology, climate and runoff response in order to understanding the variability of runoff event responses.

This chapter compares runoff responses between various climates and geological settings in four medium sized Austria catchments. It analyses various variables (e.g. antecedent precipitation, maximum precipitation intensity, initial flow, event duration etc.) of runoff event characteristics for different geological settings.

The present chapter is based on the following scientific publication:

Chen, X., Parajka, J., Széles, B., Valent, P., Viglione, A. & Blöschl, G. (2020). Impact of climate and geology on event runoff characteristics at the regional scale. *Water*, 12(12), 3457. doi: 10.3390/w12123457

4.2. Key points

1. The mean event runoff coefficient is positively related to climate humidity, and is the largest in Dornbirnerach which is the wettest catchment with steep slopes.
2. The mean runoff event recession time constant is controlled by the catchment state and the geological classes. It is the largest in Wimitzbach with possesses long flow paths and a large area of deep flow.
3. Runoff coefficient and recession time constant depend on event type, i.e. they are the smallest for short rain events, and larger for long rain events and snowmelt events.

4.3. Abstract

The dynamics of runoff event characteristics, such as runoff coefficient and recession time constant, are different for different catchments due to the differences in climate, geology, runoff generation mechanisms, etc. For understanding the differences in runoff event characteristics for different catchments, this study examines event runoff coefficient (R_c), recession time constant (T_c) and flow peaks (Q_p) in four Austrian catchments, where maps of hydro-geologic runoff process (surface flow, shallow/deep interflow and groundwater flow) are available. 982 events, including 123 in Wimitzbach, 250 in Perschling, 191 in Gail and 418 in Dornbirnerach, are identified during 11 years from 2002 to 2013. For each event, R_c , T_c and Q_p are estimated from hourly discharge and precipitation data. The results show that R_c and Q_p of Dornbirnerach are the largest with mean of 0.43 and 1.57 mm/hrs, respectively, due to the large amount of annual rainfall throughout the year (mean of 1982 mm/yr). The highest mean value of T_c is found in Wimitzbach with a mean value of 18.1 hrs which is caused by long flowpaths and large proportions (37.6%) of deep interflow (29% weathered upper plane parts of the catchment, and 8.6% in the lower parts of the catchment). For runoff events with event precipitation less than 50 mm, both runoff coefficient and recession time constant are negatively related to maximum precipitation intensity. While runoff coefficient is positively related to initial flow, recession time constant is positively related to event duration. All in all, it should link geology, climate and runoff response together to understanding the variability of runoff event responses.

4.4. Introduction

Runoff event characteristics are an essential input for hydrologic design as well as a diagnostic parameter in the hydrological analysis of runoff generation processes and catchment response to rainfall. The event runoff coefficient determines the proportion of rainfall that contributes to direct runoff during a runoff event. It reflects the hydrological state of the catchment, but also the physiographic catchment characteristics, which are combining into runoff response. The runoff recession time constant describes the interaction between groundwater and river flow (Merz *et al.*, 2006), and it indicates the time until streams return to their base flow conditions after a rainfall event (Czikowsky and Fitzjarrald, 2004). Together with the magnitude of event peak flows, the understanding of runoff event characteristics is thus critical for many water-related tasks, including water supply, irrigation, water quality, erosion and flood risk assessment (García-Ruiz *et al.*, 2008; Alberto Viglione *et al.*, 2018).

Previous studies found that factors controlling event runoff characteristics were different in different spatial scales (Chen *et al.*, 2020a; b). Plot and hillslope experiments demonstrated that runoff response at hillslope scale was controlled by the interactions between infiltration rates, change in soil water storage and drainage, and connectivity of the soil water (Liu *et al.*, 2019; Ruggenthaler *et al.*, 2015; Scherrer *et al.*, 2007). Variability and differences in runoff response from plot to small catchment scale were controlled by the connectivity between the ‘infiltrating’ and ‘runoff producing’ areas (Cerdan *et al.*, 2004; Joel *et al.*, 2002). At this scale, the event runoff coefficients tended to decrease with increasing catchment area and the recession time constants and runoff peaks were controlled mainly by the land use (Burns *et al.*, 2005; Cerdan *et al.*, 2004; García-Ruiz *et al.*, 2008). At the catchment scale, the factors controlling runoff formation are less understood, mainly due to the variability in the connectivity of flow paths and larger spatial variability of catchment physiographic characteristics (Cerdan *et al.*, 2004; Silasari *et al.*, 2017; Western *et al.*, 1998). At the regional scale, the main controlling factors were attributed to mean annual precipitation and the runoff regime (Merz *et al.*, 2006), physiographic catchment characteristics (Gottschalk and Weingartner, 1998), and antecedent soil moisture (Norbiato *et al.*, 2009; Penna *et al.*, 2011).

The role of the subsurface characteristics on runoff response is still not well understood. Some studies considered soil-bedrock interface as an impermeable boundary and hypothesized that subsurface storm flow occurred only in the soil layer (Brammer and McDonnell, 1996). In the contrary, some other studies demonstrated that flow through bedrock might play an essential role in rainfall-runoff response (Onda *et al.*, 2001; Vannier *et al.*, 2016), and that the soil-bedrock interface could control the magnitude and timing of rainfall-runoff response or recession time constants during low flow conditions (Dung *et al.*, 2012; Krakauer and Temimi, 2011; Tague and Grant, 2004; Weiler and McDonnell, 2007). At the catchment scale, geology and groundwater flow paths control the transit time distribution of water within catchments (Rinaldo *et al.*, 2011). In a comparative hydrology study, Gaál *et al.* (2012) showed that geology was, together with climate, an even stronger control in determining event runoff characteristics than the catchment area. Although geology was often cited as an important factor driving hydrological response at the catchment scale (Rogger *et al.*, 2012a; Tetzlaff *et al.*, 2007; Vannier *et al.*, 2016; Alberto Viglione *et al.*, 2018), the challenge in attributing subsurface and geological conditions to runoff response is a lack of detailed geological field observations.

The main objective of this study is to examine the variability of selected event runoff characteristics and to relate it to climatic and geological characteristics available at the regional scale. We focus on the seasonal differences of event runoff coefficients, recession time constants and event peaks in four small Austrian catchments with available detailed geological characteristics estimated by field mapping according to *Alberto Viglione et al. (2018)*. The aim is to examine the role of climate (i.e. event precipitation volume, precipitation intensity and antecedent precipitation) and runoff regime (i.e. initial flow before runoff event and event duration) characteristics on the seasonal dynamics of runoff response in different geological settings.

4.5. Study area and data

4.5.1. Study areas

This study is conducted in four Austrian catchments: Wimitzbach, Perschling, Gail and Dornbirnerach. These catchments represent four hot spot regions identified by *Gaál et al. (2012)* which are unique in terms of climate, geology, soils and landform types. These four catchments represent high alpine region (Gail), alpine/midland setting (Dornbirnerach and Wimitzbach), and lowland areas (Perschling). Geological classes and location of these catchments in Austria is presented in Figure 21. The overview of the main climate and physiographic characteristics of the catchments is listed in Table 13.

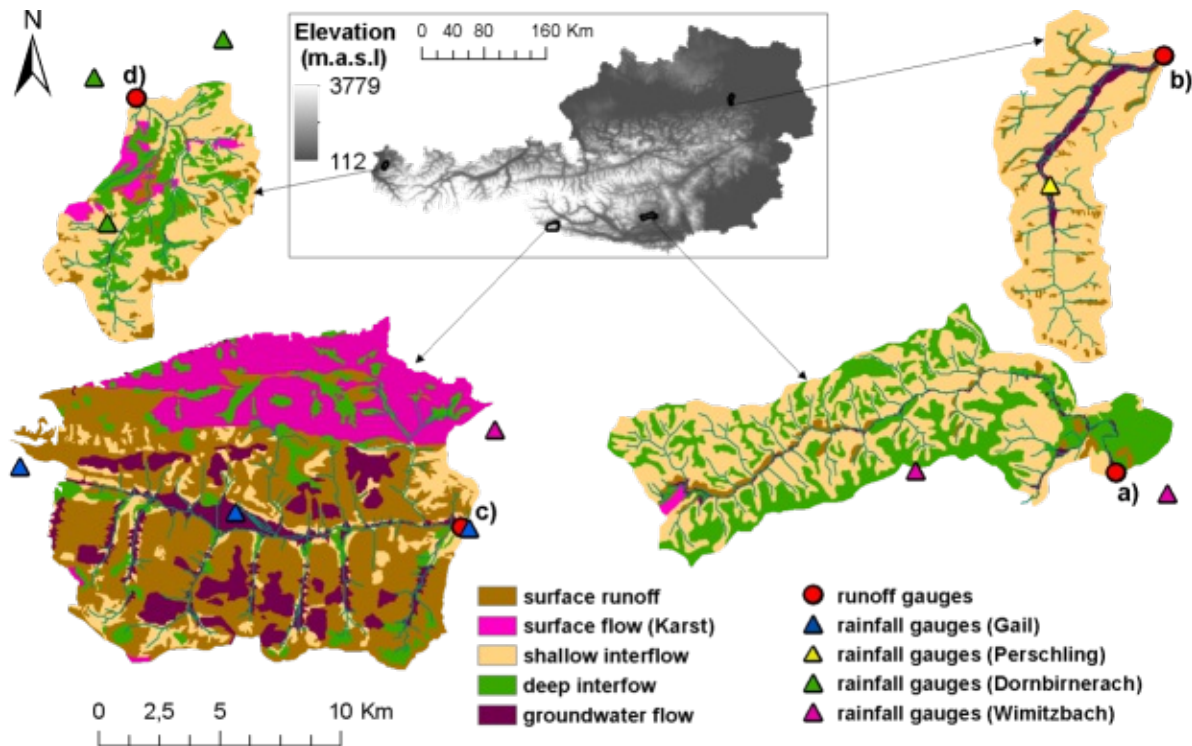


Figure 21. Locations and geological classes of the four catchments presented in this study: a) Wimitzbach, b) Perschling, c) Gail and d) Dornbirnerach (*Alberto Viglione et al., 2018*). Streamflow lines are presented as green lines in each catchment. The runoff gauges are shown with circle points, while the rainfall gauges with triangle points.

Table 13. Catchment overview. Temporal means of catchment attributes are lumped basin averages from 2002–2013. The hydro-geologic information describes proportion (area percentage) of the geological classes.

Attribute	Wimitzbach	Perschling	Gail	Dornbirnerach
Hotspot region (<i>Gaál et al.</i> , 2012)	Gurktal (Gurk)	Flysch (Flysch)	Gail (Gail)	Bregenzwald (BreWa)
Area (km ²)	106.5	55.3	146.1	51.1
Mean slope (%)	39.4	14.3	53.4	45.0
Min-max elevation (m)	529-1309	230-640	1094-2622	485-1804
Mean elevation (m)	900	379	1793	1118
Maximum flow length (km)	30.8	18.6	23.3	13.9
Mean annual runoff (mm/yr)	273	301	869	1793
Mean annual precipitation (mm/yr)	744	876	1081	1982
Mean annual runoff coefficient (-)	0.37	0.34	0.80	0.90
Proportion of surface runoff area (%)	4.0	0	7.7	9.5
Proportion of area with Karst (%)	0.5	0	51.0	6.0
Proportion of area with shallow interflow (%)	55.4	93.5	14.0	60.0
Proportion of area with deep interflow (%)	37.6	0	7.3	24.0
Proportion of area with groundwater flow (%)	2.5	6.5	20.0	0.5

The Dornbirnerach is an alpine catchment (51 km²) located in the western part of Austria. The elevation ranges from 485 m a.s.l. to 1804 m a.s.l., and it is characterised by very steep slopes (mean slope is 45%). The catchment is mainly forested, grassland and pastures are sparsely located in the higher elevations. The catchment is characterised by shallow soils and a large amount of annual precipitation (over 1900 mm/y) which results in highly saturated soils and hence high mean annual runoff coefficient.

The Gail is the highest, steepest and largest catchment in this study with a total area of 146 km² and the maximum flow length of 23.3 km. It is located in the Eastern Tyrol, and its elevations range from 1094 to 2622 m.a.s.l. The land cover is dominated by forest and grassland on hillslopes and arable land and pastures in the valley bottom.

The Wimitzbach is a midland catchment in Carinthia. It is mainly covered by forest, with small parts of arable land in the middle and lower parts of the catchment. Mean annual precipitation of Wimitzbach is the lowest (less than 750 mm/yr) among the study catchments.

The lowlands are represented by the Perschling catchment, which is located in Lower Austria. The elevation ranges from 230 m to 640 m a.s.l. The catchment is dominated by forest in the

southern part and agricultural areas in the northern part and has the lowest annual runoff coefficient.

For the four study sites, the description of the dominant runoff processes based on hydro-geologic information was prepared by a geologist (Pirkl, 2009; 2012). The report includes information about different hydro-geologic response units. In each catchment, areas dominated by different flow paths, i.e. interflow, deep groundwater flow or surface runoff processes were mapped. More information about the implementation of the geological mapping method are given by Rogger *et al.* (2012a; b) and Alberto Viglione *et al.* (2018). The geologic conditions and proportion of different units describing the hydro-geologic runoff processes in the four study sites are presented in Figure 21 and listed in Table 13. The Dornbirnerach is part of the Helvetic zone, which is dominated by limestone, sandstone and marl with a small amount of flysch in the northern area. The largest part of the catchment (60%) is characterised by shallow interflow flow paths. The scree areas in the lower parts of the hillslopes have rather large depth and are dominated by deeper interflow processes which may buffer some of the fast surface runoff generated in the upper parts (Alberto Viglione *et al.*, 2018). The Gail is part of the Karnic Alps, the Gail crystalline and the Lienzer dolomites. More than 51% runoff process in the Gail catchment are characterised as near-surface and surface runoff from karst area. The central valley is east-west orientated with rather steep valleys discharging into the Gail from north and shallower valleys from the south. Runoff retention and deep groundwater flow occur on the large alluvial cone in the valley bottom. During very wet conditions, however, the valley bottom can get saturated so that tributaries can bypass it (Alberto Viglione *et al.*, 2018). The Wimitzbach is characterised by mica schist, phyllites, amphibolites and marble. The hillslopes are plane in the upper parts and steeper in the lower parts. The Wimitzbach was not glaciated during the last ice age, so the upper parts of the hillslopes are strongly weathered and characterised by deep interflow flow paths (37.6%). The lower parts of the hillslopes are steeper and are characterised by the faster storage due to shallow interflow or surface runoff flow paths. The Perschling catchment is located in the flysch/molasse zone of Austria. The whole catchment is characterised by interflow processes in the weathering zone that has a depth from 2 to 5 m. Sandy gravel in the valley bottom influences the groundwater flow paths. On the upper parts of the hillslopes, water infiltrates into the shallow subsurface while at the slope toes, some saturation and surface runoff may occur (Alberto Viglione *et al.*, 2018).

4.5.2. Meteorological and hydrological data

The event runoff characteristics are estimated from hourly runoff and rainfall data observed in the period 2002-2013. The measurements of runoff are carried out at 15-minute temporal resolution and aggregated to hourly values. The mean catchment hourly rainfall is interpolated from hourly observations by using the Thiessen polygon method. The location of the rainfall gauges is shown in Figure 21. The aggregated annual rainfall and runoff values are presented in Figure 22. The evaluation of mean annual runoff and precipitation indicates that the largest annual precipitation, runoff and their inter-annual variability is observed in Dornbirnerach, followed by the Gail catchment. The annual precipitation in Wimitzbach and Perschling catchment is slightly lower than in Gail. Still, the mean annual runoff is significantly smaller, indicating the role of vegetation and evapotranspiration processes on the water balance.

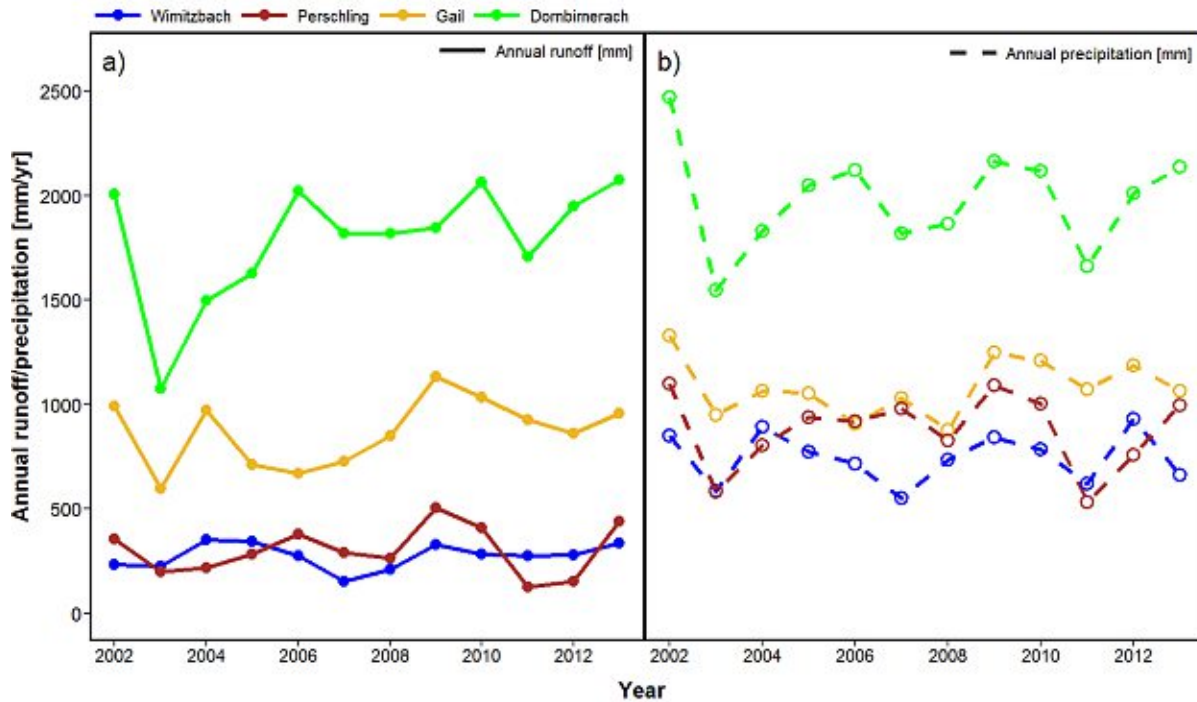


Figure 22. Inter-annual dynamics of mean annual precipitation and runoff in four Austrian catchments in the period 2002-2013.

4.6. Methodology

4.6.1. Estimation of event runoff characteristics

The rainfall-runoff events are separated using the methodology presented by *Merz et al.* (2006). The approach consists of the following steps:

1. Determination of direct runoff and baseflow;
2. Identification of the start and end of the runoff events;
3. Calculation of the selected event runoff characteristics, i.e. peak discharge, runoff coefficient and recession time constant.

Baseflow is estimated by an automatic digital filter proposed by *Chapman and Maxwell* (1996). The details of the applied digital filter are described in detail in *Merz et al.* (2006). Runoff event peaks are identified, if the ratio of direct runoff and baseflow at time t is larger than a threshold value of parameter $qdrat$ and there was no larger flow in the previous and following $imax$ (hrs) time steps. The parameters $qdrat$ and $imax$ are chosen in this study to be 2 and 12 hrs respectively, based on sensitivity analyses (*Chen et al.*, 2020a; *Merz et al.*, 2006). Storage parameter $k2$ (hrs) used for determination of runoff recession is chosen to be 5 hrs for Dornbirnerach and 7 hrs for Wimitzbach, Perschling and Gail. These values are determined by visual inspection of the hourly runoff data time series for each catchment.

The start of an event is determined by searching backwards from a peak to find the time when the direct runoff is less than 1% of the direct runoff at peak time. The number of time steps in the

backward search (size of the time window) depends on the characteristic time scale of an event *Merz et al.* (2006). If no such point in the predefined time window is found, a higher limit for minimum direct runoff is allowed (stepwise increased from 1% to 40%). The end of an event is found in an analogue way by searching forwards (*Chen et al.*, 2020a).

For each runoff event, we estimate three characteristics: the event runoff coefficient (R_c), the event recession time constant (T_c) and the event peak flow (Q_p). The runoff coefficient R_c and recession time constant T_c are determined by an automatic calibration using the shuffled complex evolution optimization scheme (*Duan et al.*, 1992). The linear reservoir model is fitted to the direct flow (difference between runoff observation and base flow) by minimizing the root mean square difference between observed and simulated runoff. In the next step, final hydrographs are visually checked, and in some cases, T_c is manually adjusted and fixed to match the form one would separate manually. Subsequently, R_c is again automatically optimized until the simulated hydrograph fits the observed one. More details on the method are given by *Merz et al.* (2006).

The impact of solid precipitation and snowmelt on the magnitude of event runoff characteristics is accounted by using a daily snowmelt model. The model used in this study is a semi-distributed conceptual model (TUWmodel) (*Alberto Viglione and Parajka*, 2020), which is calibrated to daily observed discharge time series (*Parajka et al.*, 2007). The snow simulations of the model are disaggregated to hourly values following the approach of *Merz et al.* (2006). We assume a constant ratio of liquid to solid precipitation for each day from which liquid hourly precipitation is estimated. For the temporal pattern of snowmelt during a day, a truncated cosine statistical distribution is applied, where snowmelt starts at 9 a.m., the maximum occurs at 3 p.m. and snowmelt ceases at 9 p.m. (*Chen et al.*, 2020a). Finally, hourly precipitation in different catchments is calculated by removing snow and adding melt to rainfall in each time step.

4.6.2. Potential impact variables of runoff response

For each identified runoff event, seven potential variables are estimated including event volume, event duration, initial flow, event precipitation, antecedent precipitation, maximum precipitation intensity and melt percentage. Event volume is the sum of runoff observation during identified event period in unit of mm. Event duration is length of identified event period in unit of hrs. For understanding catchment water storage before event, initial flow is calculated as the value of runoff at the identified start time in the unit of mm/hrs. Event precipitation is the sum of precipitation during identified event period in unit of mm. Antecedent precipitation is calculated by summing precipitation during 30 days before event in the units of mm, which could reflect soil moisture condition before event in a way. Maximum precipitation intensity is the peak precipitation during one event. Melt percentage is the volume ratio between melt and precipitation during event period. In order to compare distributions of above variables on event runoff and precipitation between different catchments, Gaussian kernel density and empirical cumulative density function are estimated in section 4. Gaussian kernel density is a popular estimator of unknown density function by summing all sample distributions and assuming that each sample are normally distributed.

4.7. Results

4.7.1. Spatial and temporal variability of runoff response

Table 14 shows a summary of the seasonal frequency of the identified runoff characteristics in four selected catchments in the period 2002-2013. All runoff event characteristics of identified events are summarized in the Appendix A3. Based on melt percentage, events are divided into two categories: rainfall and melt events. In the following discussions, runoff events are included into melt events when its melt percentage is larger than 0.1. The largest number of events is identified in Dornbirnerach, which is a catchment with the largest mean annual precipitation. More than 300 events are driven by rainfall, and 55 events are classified as snowmelt events. Much smaller number of events, only 123, is identified in the midland catchment of Wimitzbach, which has the smallest mean annual precipitation among the studied catchments. Seasonally, the largest number of events is observed during summer months (June to August) in all catchments.

Table 14. The seasonal frequency of identified runoff events in Wimitzbach, Perschling, Gail and Dornbirnerach catchments in the period 2002-2013.

Catchments	Runoff event types	Spring (Mar-May)	Summer (Jun-Aug)	Autumn (Sep-Nov)	Winter (Dec-Feb)	Total
Wimitzbach	Rainfall events	23	69	26	2	120
	Melt events	1	0	0	2	3
	Sum	24	69	26	4	123
Perschling	Rainfall events	48	120	46	4	218
	Melt events	7	0	5	20	32
	Sum	55	120	51	24	250
Gail	Rainfall events	12	128	32	3	175
	Melt events	10	2	4	0	16
	Sum	22	130	36	3	191
Dornbirnerach	Rainfall events	63	183	93	24	363
	Melt events	22	0	5	28	55
	Sum	85	183	98	52	418

The statistical evaluation of selected event runoff characteristics is summarized in Table 15. The comparison indicates a distinct difference between the catchments. While the largest R_c and Q_p are observed in Dornbirnerach (mean $R_c=0.43$ and mean $Q_p=1.6$ mm/hrs), the smallest R_c and Q_p are identified in Wimitzbach (mean $R_c=0.05$, mean $Q_p=0.07$ mm/hrs). The Dornbirnerach is the catchment with the wettest climate, as well as with the largest, i.e. 9.5% of the catchment that contributes to surface runoff. 7.7% of the catchment area of Gail contributes to surface runoff and 20% of the catchment area contributes to groundwater flow. The mean R_c is 0.16 in Gail, but it has almost two times larger mean T_c compared to Dornbirnerach (12.5 hrs in Gail compared to 6.4 hrs in Dornbirnerach). The largest mean T_c (18.1 hrs) is found in Wimitzbach which has the largest proportion of area with deep interflow. The Perschling has more than 90% area contributing to shallow interflow processes, which is reflected in the second smallest (fastest) mean T_c (10 hrs). This is an interesting finding because the catchment is situated in lowland and mean annual precipitation is the second lowest (876 mm).

Table 15. Summary of event runoff characteristics in Wimitzbach, Perschling, Gail and Dornbirnerach catchments in the period 2002-2013.

Characteristics of runoff events		Wimitzbach	Perschling	Gail	Dornbirnerach
Runoff coefficient (Rc) [-]	Min	0.01	0.00	0.02	0.03
	Max	0.21	0.52	0.80	1.00
	Mean	0.05	0.09	0.16	0.43
	Median	0.05	0.05	0.11	0.37
Recession time constant (Tc) [hrs]	Min	1.0	1.0	2.0	1.0
	Max	100.0	55.0	65.0	45.0
	Mean	18.1	10.3	12.5	6.4
	Median	15.0	7.1	9.0	5.0
Peak flow (Qp) [mm/hrs]	Min	0.02	0.01	0.06	0.05
	Max	0.26	3.49	1.21	16.71
	Mean	0.07	0.23	0.25	1.57
	Median	0.06	0.07	0.18	0.89

The seasonal distribution of event runoff coefficient (Rc), recession time constant (Tc) and event peak (Qp) for the four study catchments is presented in Figure 23. The variability in Rc indicates a clear seasonal pattern with larger Rc in winter and spring and smaller Rc in the summer. The seasonal variability of Rc is the highest in Dornbirnerach and the smallest in Wimitzbach catchment. Interestingly, the seasonal variability of Tc is the smallest in Dornbirnerach. More pronounced seasonal patterns of Tc are observed in Perschling and Gail catchments. The Gail catchment with 51% area generated runoff in Karst has the highest median Tc (40 hrs) in January/February and the lowest (6 hrs) in July/August. Such difference is likely connected to the seasonal catchment storage variation as discussed by *Chen et al. (2020a)* and *Patnaik et al. (2015)*. The largest event peaks are observed in all catchments in the summer months, and the smallest peaks tend to occur in winter. The seasonal variability of Qp is the largest in Dornbirnerach (it ranges from 0.7 to 1.0 mm/hrs) where the most extreme events with Qp larger than 2 mm/hrs, usually occur from May to August.

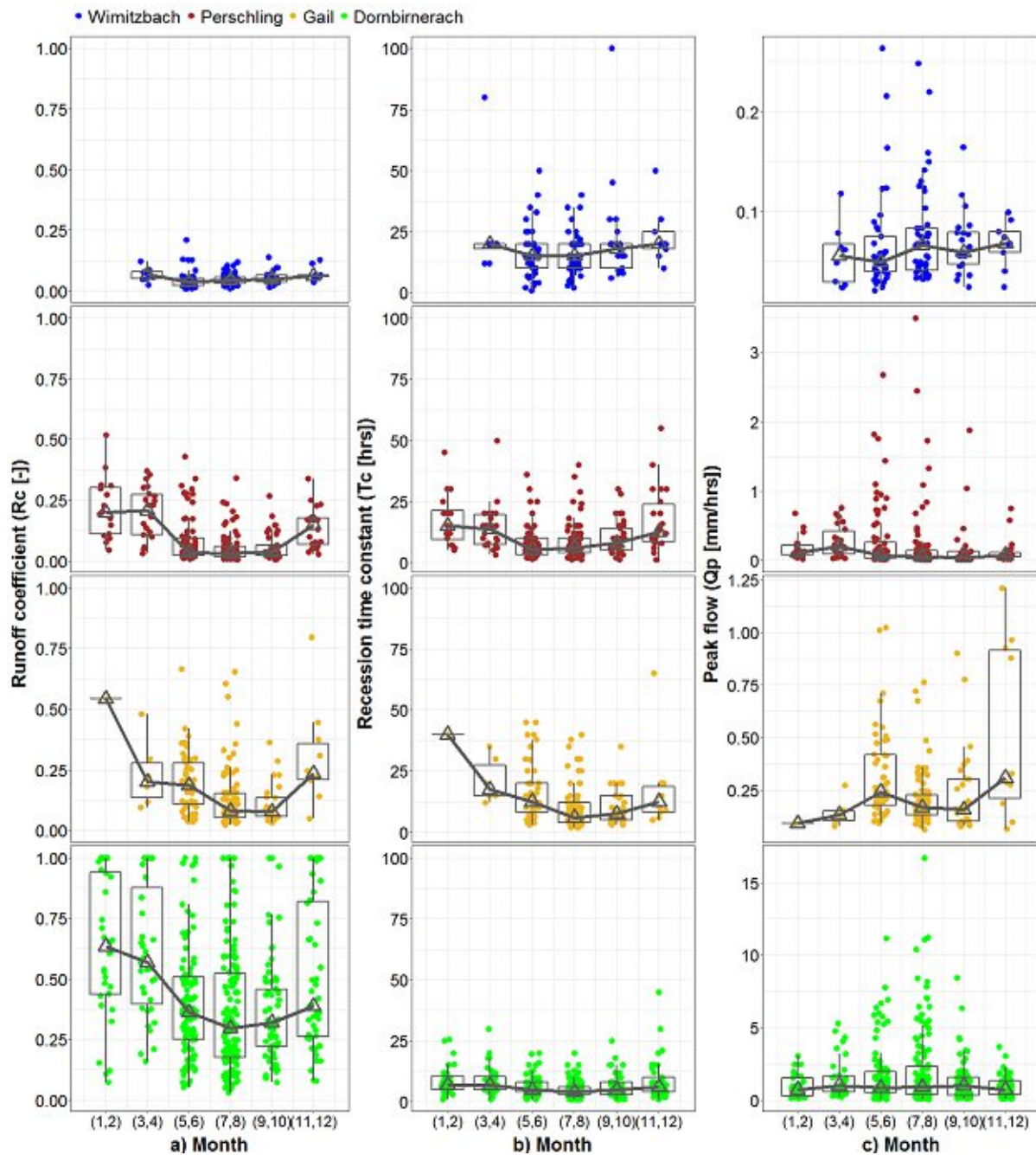


Figure 23. Seasonal dynamics of event runoff characteristics: the runoff coefficient (left panels), recession time constant (middle panels) and peak flow (right panels) in the four study catchments.

4.7.2. Distributions of event and precipitation characteristics

To understand the factors controlling runoff response in the study catchments, Figure 24&25 summarize the differences in the distributions of event flow and precipitation characteristics. Figure 24 demonstrates that the runoff coefficients and recession time constants are linked to the

event flow volume. While the smallest event flow volumes are observed in Wimitzbach, the largest volumes are observed in Dornbirnerach catchment. The small runoff coefficients in Wimitzbach are connected to small event flow volumes and larger event duration, and vice-versa. In contrast, the recession time constants tend to be the smallest in Dornbirnerach, which is characterised by events with large flow volumes, large runoff coefficients and the shortest event duration. Interestingly, the initial flow at the start of runoff events is noticeably larger in Dornbirnerach and Gail (median of initial flow larger than 0.08 mm/hrs) than in Perschling and Wimitzbach (median of initial flow less than 0.03 mm/hrs). The larger initial flow in Dornbirnerach and Gail is likely caused by seasonality of runoff regime, i.e. larger flow in spring due to snowmelt.

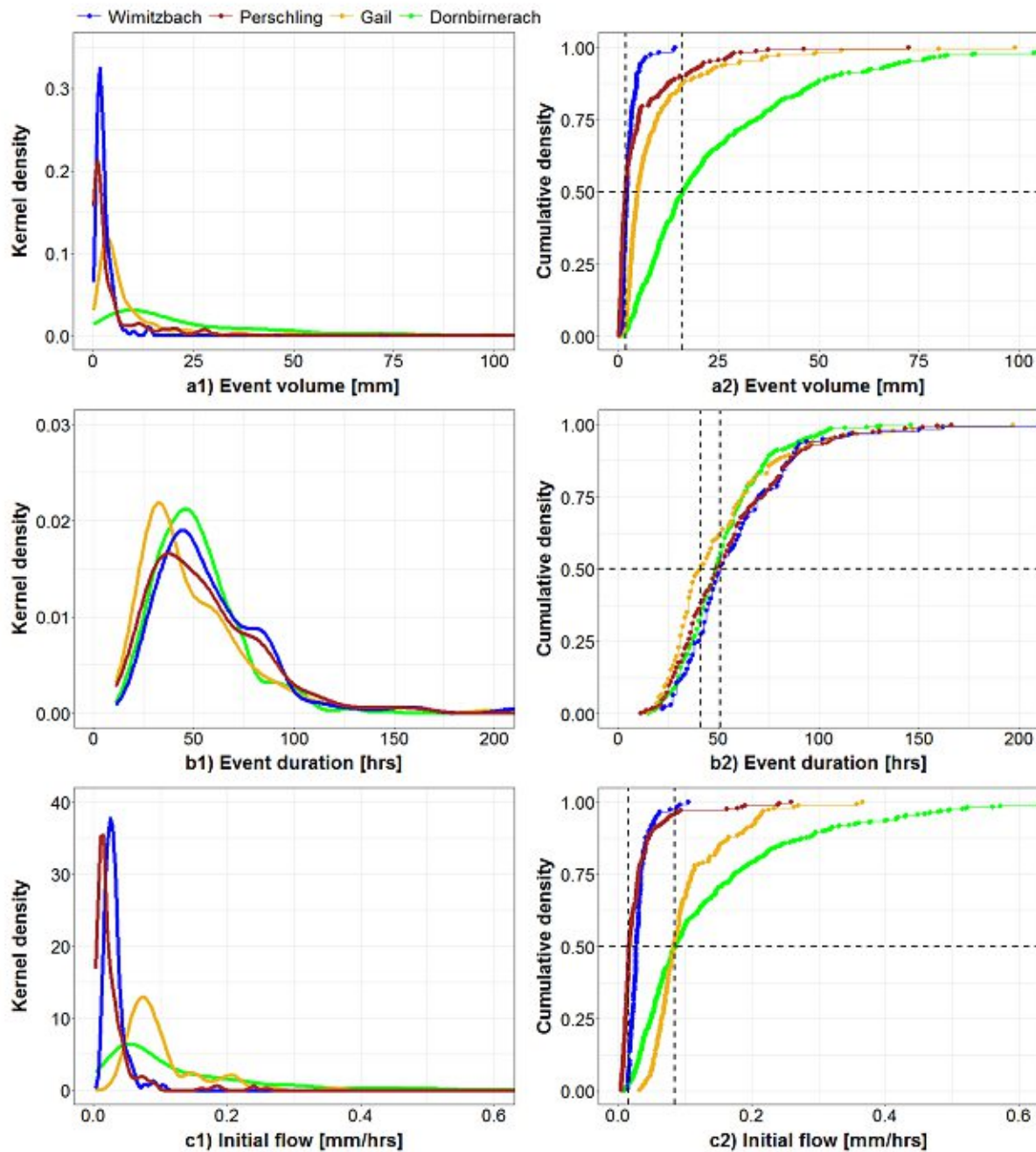


Figure 24. Kernel density (left panels) and cumulative density (right panels) functions of event volume, duration and initial flow (prior to the runoff event) in four selected catchments: Wimitzbach, Perschling, Gail and Dornbirnerach.

Precipitation characteristics of the analysed runoff events are evaluated in Figure 25. The statistical evaluation of the distributions of selected event characteristics shows that event precipitation volume and maximum intensities do not differ much between the four analysed catchments. The medians of event precipitation volume of four catchments vary between 19 and 28 mm, and for Dornbirnerach the median is somewhat the largest of 28 mm. The event

precipitation volume follows the seasonality of precipitation and it is larger in May and June and lower in the winter months. An exception is Gail, where the largest precipitation events are observed in November. The maximum precipitation intensity during runoff events is similar in all catchments, while the median varies between 4.9 and 5.8 mm/hrs. The precipitation intensities are larger in the summer months, and the largest intensities (exceeding 10 mm/hrs) are observed in Dornbirnerach in July and August. The most noticeable difference is observed for the antecedent 30-days precipitation. This characteristic is used as an indicator of catchment wetness before the runoff events. The analysis indicates that Dornbirnerach is significantly wetter than the other catchments and the median of antecedent precipitation is about 189 mm, which is more than 100 mm larger than in Perschling or Wimitzbach. The antecedent precipitation is the largest in the summer months and follows the seasonality of precipitation regime in Austria.

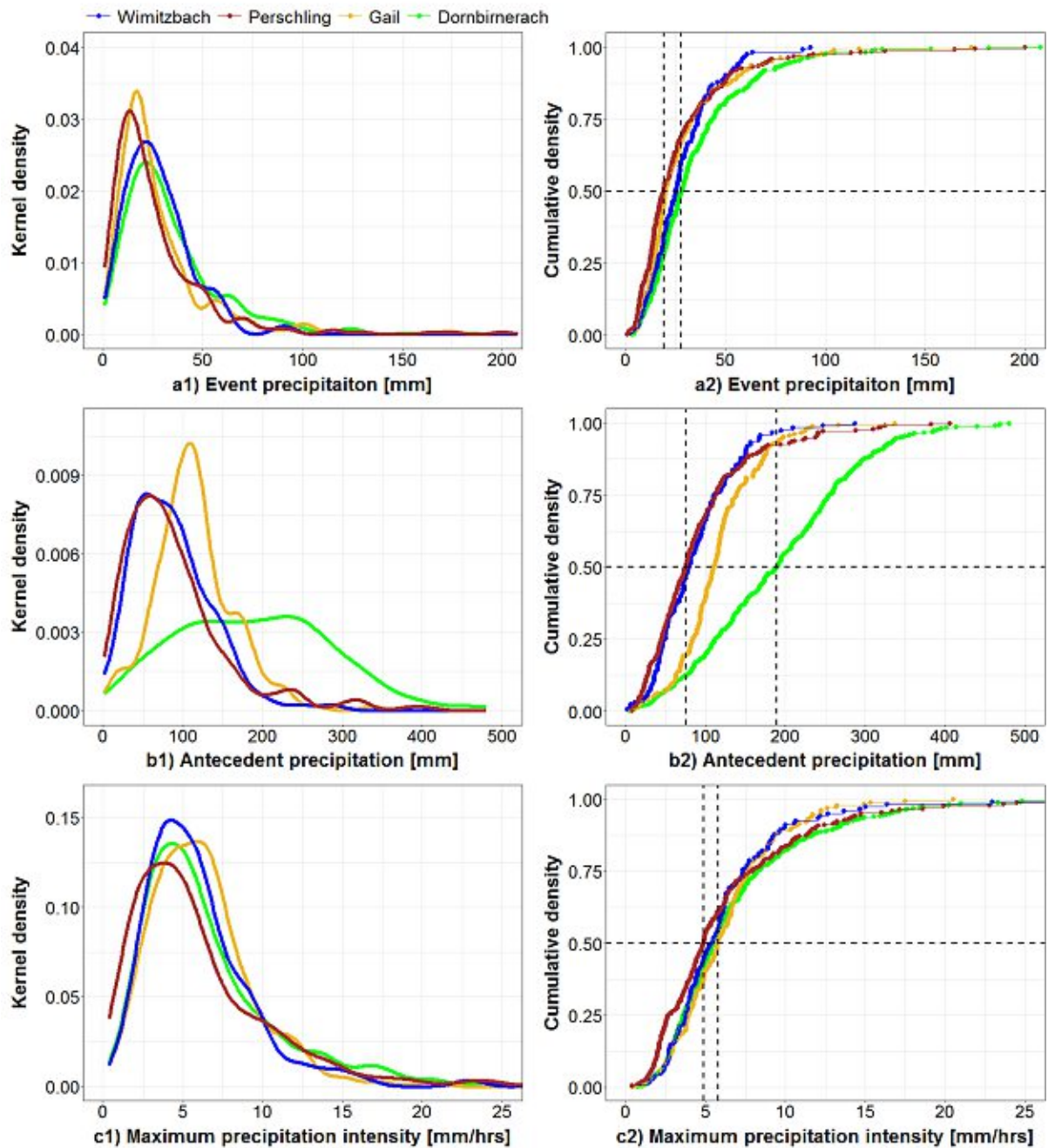


Figure 25. Kernel density (left panels) and cumulative density (right panels) functions of total precipitation volume during runoff event, maximum precipitation intensity and 30-days antecedent precipitation volume (prior to the runoff event) in four selected catchments: Wimnitzbach, Perschling, Gail and Dornbirnerach.

4.7.3. Effects of event and precipitation characteristics on runoff response.

The comparison of event precipitation volume (Figure 25) indicates that the majority (more than 75%) of event precipitation volume is less than 50 mm in all catchments. To explore the

differences in runoff response for similar precipitation events in all catchments (i.e. events precipitation less than 50 mm), Figure 26, 27&28 show the change of runoff characteristics with changing antecedent precipitation, maximum precipitation intensity, initial flow and event duration. The results in Figure 26 indicate that the antecedent precipitation is a poor indicator of the runoff coefficient. An increase of antecedent precipitation is not related to a significant rise in R_c . Interestingly, maximum precipitation is inversely associated to runoff coefficients. The R_c tends to be larger for events with smaller maximum precipitation intensity and vice versa. The most explanatory characteristic is the initial flow before the runoff event. The larger the initial flow is, the larger runoff coefficient is observed in all catchments. In Karstic (Gail) and Flysch (Perschling) catchments, the R_c tends to increase with increasing duration of runoff events.

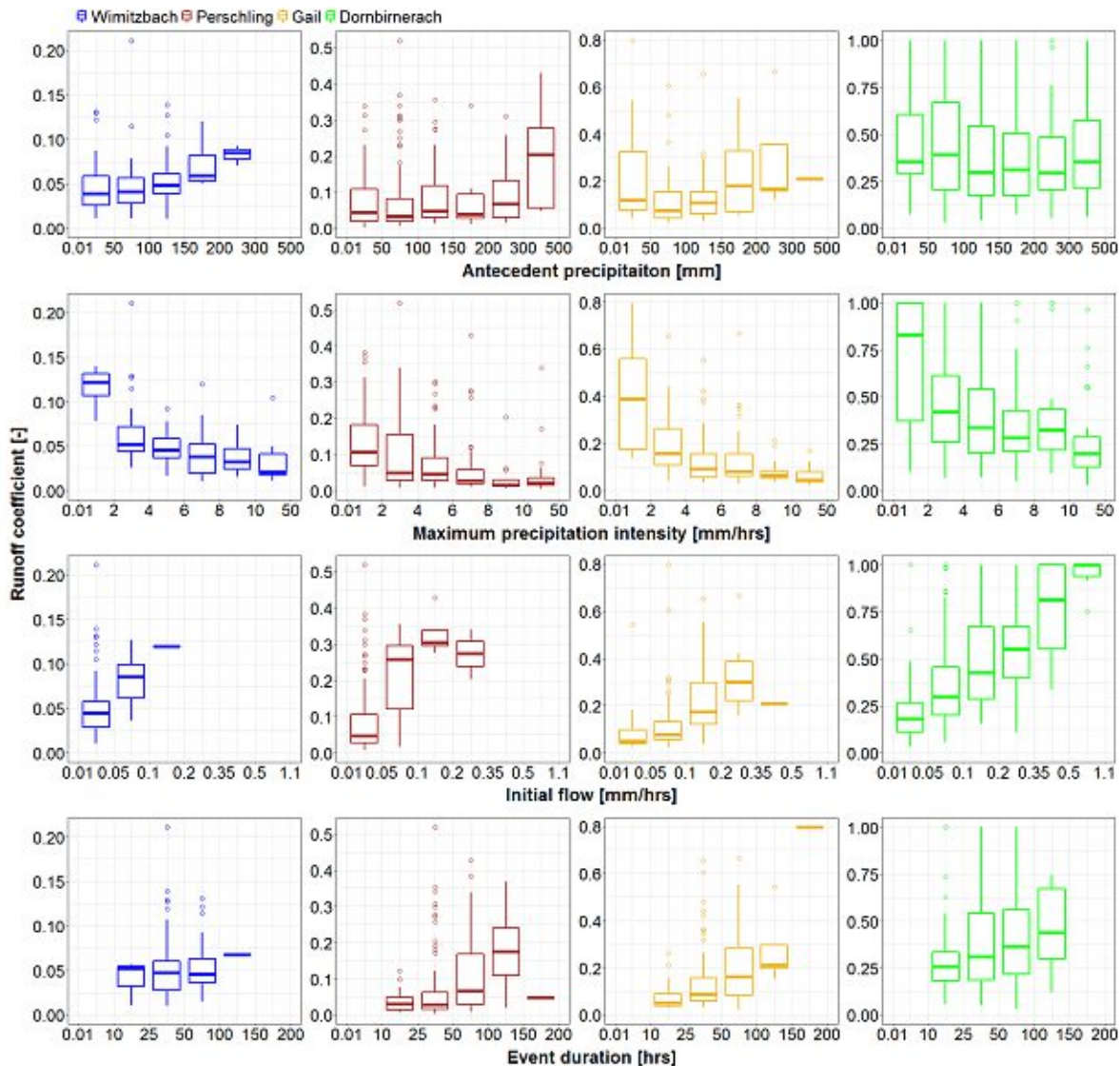


Figure 26. Variability of runoff coefficient (R_c) for different classes of antecedent precipitation, maximum precipitation intensity, initial flow prior to the event and event duration in four selected catchments: Dornbirnerach, Gail, Wimitzbach and Perschling. The changes are evaluated for events with precipitation volumes less than 50 mm.

Runoff peaks are somewhat related to antecedent precipitation (Figure 27). An increase of event peaks with increasing antecedent precipitation is observed mainly in catchments with lower annual precipitation (Wimitzbach, Perschling and Gail). An increase of Q_p with increasing maximum precipitation intensity is found only for Dornbirnerach catchment, which has a large proportion of area with shallow interflow processes. Similarly, as for R_c , Q_p rises in all catchments with the increasing initial flow and is not related to the duration of a runoff event.

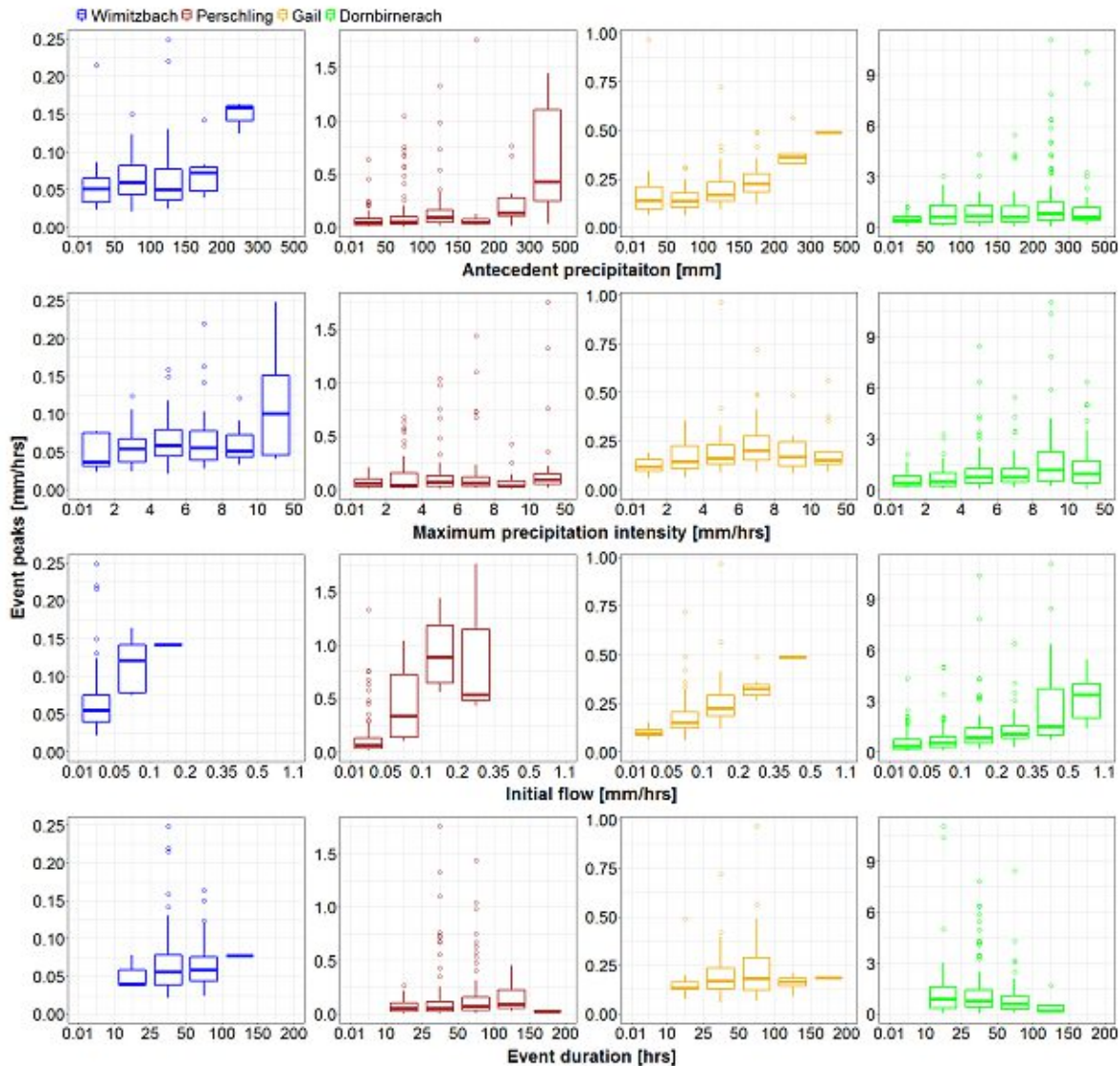


Figure 27. Variability of event peaks (Q_p) for different classes of antecedent precipitation, maximum precipitation intensity, initial flow prior to the event and event duration in four selected catchments: Dornbirnerach, Gail, Wimitzbach and Perschling. The changes are evaluated for events with precipitation volumes less than 50 mm.

The variability of recession time constant is presented in Figure 28. T_c is not related to antecedent precipitation, but it decreases with increasing precipitation intensity. An exception is Wimitzbach, which has a large proportion of deep interflow processes. In Wimitzbach, the T_c is

not heavily related to the change of maximum precipitation intensity. The initial flow is not associated with the variability of T_c in most of the catchments. Only in Karstic (Gail) catchment, T_c tends to increase with increasing initial flow before the event. The most apparent pattern is found for the event duration, where for increasing event duration also T_c tends to increase.

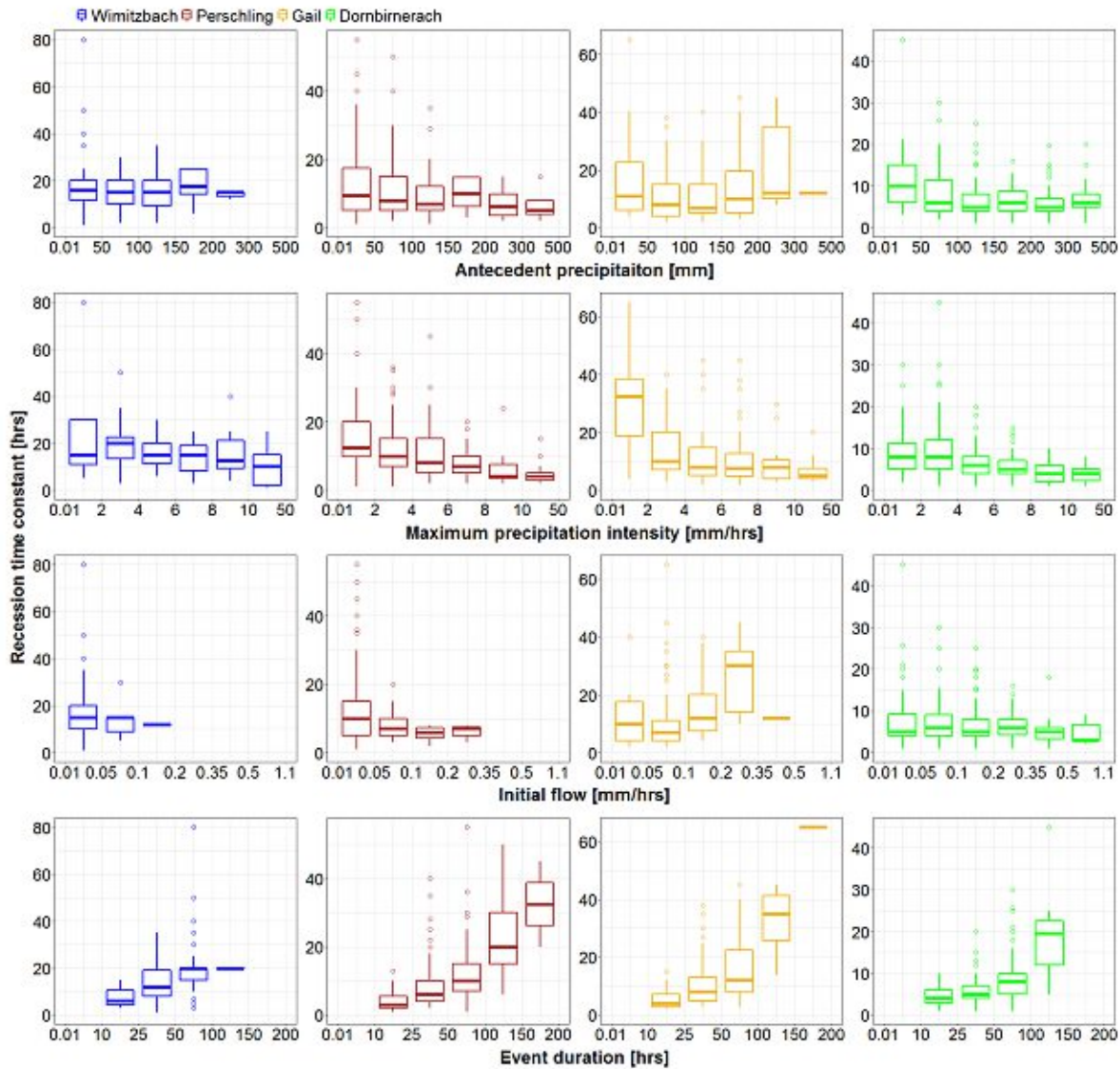


Figure 28. Variability of recession time constant (T_c) for different classes of antecedent precipitation, maximum precipitation intensity, initial flow prior to the event and event duration in four selected catchments: Dornbirnerach, Gail, Wimitzbach and Perschling. The changes are evaluated for events with precipitation volumes less than 50 mm.

The analysis of events caused by precipitation volumes less than 50 mm (Figs. 6, 7, and 8) has shown that the duration of runoff events can have a noticeable effect on the variability of event runoff characteristics. The variability of R_c , Q_p and T_c for short, medium, long and snowmelt events is presented in Figure 29 and summarized in Table 16. The results show that the largest R_c are, in all catchments, attributed to runoff events impacted by snowmelt. While T_c of melt

events are generally in the same high level as long duration events. Interestingly, antecedent precipitation for melt events is the smallest (except for Gail, where it is slightly higher than rainfall events, Table 16). In general, R_c and T_c tend to increase with increasing duration of events. An exception is Wimitzbach, where the difference in R_c between short and long events is minimal. The patterns found for R_c and T_c are, however, not observed for runoff peaks Q_p . In Dornbirnerach and Wimitzbach, Q_p has the same variability for all event types. In Gail and Perschling, Q_p tends to be the largest for snowmelt peaks.

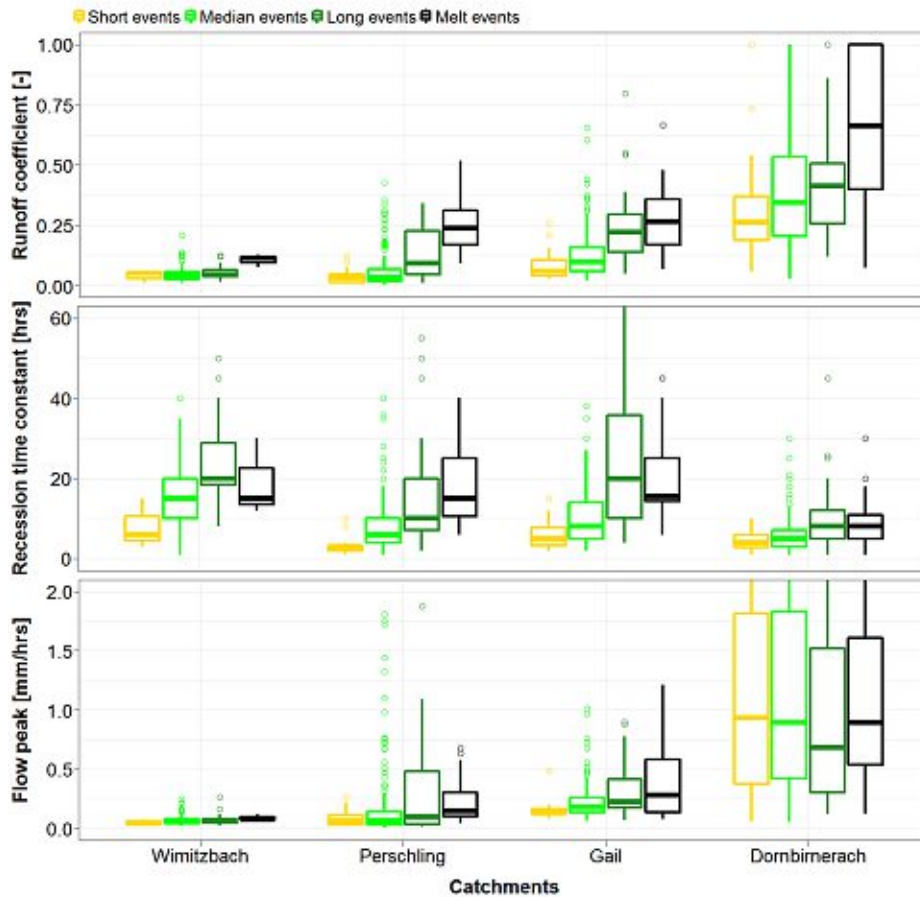


Figure 29. Variability of runoff coefficient, recession time constant and event peaks for four types of runoff events. Type of runoff event is defined by its duration, i.e. short (duration less than 24 hrs), medium (duration between 24 and 72 hrs), long (duration more than 72 hrs). Event with contribution of snowmelt are classified as melt events.

Table 16. Summary of event and median values of their characteristics (median values) grouped according to four event types: short (duration less than 24 hrs), medium (duration between 24 and 72 hrs), long (duration more than 72 hrs) and snowmelt (having contribution from snowmelt).

Catchments	Event type	No. of events	Event prec. (mm)	Max. prec. Intensity (mm/hrs)	Antec. precip (mm)	Initial flow (mm/hrs)	Duration (hrs)
Wimitzbach	Short	3	8.3	6.2	167.5	0.03	22

	Medium	87	22.4	5.2	86.0	0.03	46
	Long	30	40.2	5.8	70.1	0.03	86
	Melt	3	18.5	3.7	53.3	0.05	46
Perschling	Short	14	7.8	4.9	68.1	0.02	21
	Medium	165	17.2	5.6	79.7	0.01	43
	Long	49	29.2	4.4	65.2	0.02	84
	Melt	22	22.6	2.5	50.0	0.03	82
Gail	Short	18	11.3	5.3	101.5	0.08	20
	Medium	133	19.6	5.8	111.2	0.08	38
	Long	24	37.4	5.3	109.0	0.09	94
	Melt	16	27.2	5.6	118.9	0.17	75
Dornbirnerach	Short	24	21.9	8.7	202.3	0.10	21
	Medium	294	28.0	5.7	198.4	0.08	46
	Long	45	43.9	5.4	190.9	0.08	89
	Melt	55	25.6	3.6	111.0	0.17	60

4.8. Discussion

This study aims to examine the role of climate (i.e. event precipitation volume, precipitation intensity and antecedent precipitation) and runoff regime (i.e. initial flow before runoff event and event duration) on the seasonal dynamics of event runoff coefficient, recession time constant and event peak flow in different geological settings represented by four small catchments in Austria. Previous studies have shown that at the regional scale the event runoff coefficients are highly correlated with mean annual precipitation but less related to soil type and land use (*Merz et al.*, 2006; *Norbiato et al.*, 2009). *Merz et al.* (2006) reported that regional differences in runoff coefficient tend to be larger than the variability of runoff coefficient with event rainfall or antecedent precipitation in individual catchments. The results of this study showed a similar pattern of significantly larger event runoff coefficients in the catchments with high mean annual precipitation (Dornbirnerach) than in drier catchments (Wimitzbach, Perschling). This result supports the hypothesis that in wetter climate, precipitation events provide not only sufficient amount of water for producing runoff at the event time scale, but also have an impact on the development of co-evolution feedbacks between geology, stream network and geomorphological structures, soils and vegetation at longer time scales (*Gaál et al.*, 2012; *Sivapalan and Blöschl*, 2015).

In contrast to some previous studies (*Merz et al.*, 2006; *Rodríguez-Blanco et al.*, 2012), however, the results of this study show only poor relation between antecedent precipitation as an index of catchment wetness and event runoff response. We performed a sensitivity analysis (not shown in the results) of testing the different length of periods used for the estimation of antecedent precipitation with very similar results. Still, this finding is in agreement with *Longobardi et al.* (2003) who reported that antecedent precipitation was a generally lower predictor of catchment state than soil moisture or base flow estimates. *Scherrer et al.* (2007) reported that the sensitivity of runoff response on antecedent wetness was related to dominant runoff generation processes and the sensitivity was small in catchments with dominant overland flow, but significantly larger in catchments with subsurface flow generation. The role of initial flow condition and baseflow has been highlighted by *Rodríguez-Blanco et al.* (2012). They showed that baseflow variability appeared to be more influential than rainfall amount in controlling the hydrological response of humid catchments. We found that initial flow was the main factor influencing the magnitude of

runoff coefficient and event peaks in all analysed catchments and geological settings, which indicates the important role of groundwater. The recession time constant tended to be inversely related to the maximum event precipitation intensity, with an exception for one catchment (Wimitzbach) with the largest proportion of deep interflow contribution to runoff.

The role of geology on runoff response at the event time scale was evaluated only in a few studies. *Tarasova et al.* (2018) pointed out that several catchments in Germany showed similar runoff response although with considerably different elevation and precipitation, which was mainly attributed to the similarity in soil and hydrogeological properties. *Norbiato et al.* (2009) analysed the geological maps for selected catchments in the Italian Alps and derived for each catchment a permeability index. They found that the ‘permeability index’ was an essential control of variability of runoff coefficients, particularly for catchments with mean annual precipitation less than 1200 mm. The results of *Norbiato et al.* (2009) showed that the permeability was closely linked with a subsurface water storage capacity index (*Borga et al.*, 2007). This index related 90% daily runoff quantile to the median daily flow (Q90/Q50), and lower values corresponded to lower variance of daily flows, caused by the damping effects of groundwater storages (for example, in extensive karstified or limestone aquifers). We used in this study classification of geological features based on field mapping and hydro-geologic runoff process characterisation. Based on this information, different hydro-geologic response units were defined, and catchment proportion of areas dominated by interflow, deep groundwater flow or surface runoff processes were estimated. We found that the largest runoff coefficients, event peaks and fastest recession were observed in Dornbirnerach catchment. Dornbirnerach is a catchment with very steep hillslopes, and shallow interflow processes characterise large parts of the catchment. Moreover, this catchment is very humid with large and frequent precipitation. The subsurface water storage index of *Norbiato et al.* (2009) was 0.28, which indicated a catchment with low permeability. Low permeability index (0.39) was also found for Perschling catchment, which is located in Flysch zone and has almost the whole catchment in the weathering zone characterised by shallow interflow. This catchment, however, is located in lowlands, has much smaller precipitation and rainfall is dominated in the summer time (*Gaál et al.*, 2012). The recession time constant is short, similarly to Dornbirnerach, but the runoff coefficients are much smaller due to much smaller rainfall. The largest proportion of deep groundwater flow was mapped in Wimitzbach catchment. Wimitzbach is a catchment with the lowest runoff coefficients and event peaks and largest recession time constants. It also has the highest permeability index (0.59) of *Norbiato et al.* (2009). Comparing the results of Perschling and Wimitzbach with those of *Merz et al.* (2006), they had less than half of the median value of runoff coefficient compared to catchments with the same precipitation. The hydro-geological mapping here allowed us to explain and attribute the characteristics of runoff response, which was not possible before. The Gail catchment represents a mixture of different runoff processes. It has only a somewhat lower proportion of surface flow area than Dornbirnerach, but also a large proportion of karst (51%). In combination with mean annual rainfall exceeding 1000 mm, in this catchment, we observed the second-largest runoff coefficients as well as recession time constants.

The analysis of the runoff response by different event types indicated that runoff coefficients and recession time constants increased with event snowmelt. The runoff event peaks tended to be larger for snowmelt events, except for one catchment (Dornbirnerach) which is very wet in all seasons. This finding is in agreement with *Merz et al.* (2006). They found that in a humid climate and at the scale of the small and medium catchments, the main controls of event runoff

coefficients were the climate and the runoff regime through the seasonal catchment water balance and hence antecedent soil moisture. The runoff coefficients tended to increase in a similar order as in our study, i.e. the smallest for short rain events, and larger for long rain events, and snowmelt events.

Overall, this study complements our understanding of the variability of event runoff response characteristics between small catchment and regional scales. While at the small catchment scale, the runoff response is related mainly to the main runoff generation mechanism (*Chen et al.*, 2020a), at the regional scale it is strongly correlated to climate and mean annual precipitation. *Chen et al.* (2020a) demonstrated that in small agricultural catchments, groundwater levels explain the variability of runoff response more than soil moisture or precipitation, suggesting the role of connectivity and flow paths. The use of field mapping of hydro-geological flow paths used in this study has shown the importance and usefulness of such information for interpreting the spatial and temporal variability of event runoff characteristics. This study provides an illustrative example of the link between geology, climate and runoff response. It demonstrates the value of field hydro-geological mapping for understanding the runoff response at the medium catchment scale, which provides a basis toward improving prediction of event runoff characteristics and to transfer the understanding to the regional scale.

4.9. Conclusions

For understanding the controls of runoff response at medium catchment scales, we examined the role of climate, runoff regime and geological classes in producing runoff event characteristic in four small to median catchments in Austria. The study links geology, climate and runoff regime to explain runoff event characteristics, as well as different scales. Our results showed that:

- The spatial patterns of event runoff coefficients and mean annual precipitation tend to be consistent, which supports the hypothesis that higher precipitation could not only provide sufficient water at the event scale, but also recharges the subsurface conditions at longer time scales. The highest runoff coefficients occur in the wettest catchment of Dornbirnerach with the largest area of saturated surface runoff, a low permeability index of 0.28 and steep hillslopes.
- The spatial patterns of the event recession time constants are closely related to geological class and catchment state. Because of the highest permeability index of 0.59 and the largest area proportion of deep groundwater flow occur in the Wimitzbach catchment, the recession time constants are the largest, but runoff coefficients and event peaks are the lowest among the four catchments examined.
- The seasonal variability of runoff coefficients and event peaks is largely related to the initial flow for various geological setting of the four catchments. Only event flow is also related to antecedent precipitation in the drier catchments of Wimitzbach, Perschling and Gail. The recession time constant is inversely related to the maximum event precipitation intensity, except for one catchment (Wimitzbach) that possesses the largest proportion of deep interflow contribution to runoff.

5. Summary and conclusions

It is critical to investigate runoff event characteristics in catchments with various climate, topography and geological characteristics, in order to provide fundamental information to runoff simulation and forecasting, especially in small ungauged basins. The goal of this thesis is to identify variability and controlling factors of event runoff coefficient (R_c), recession time constant (T_c) and peak flow (Q_p) at the small catchment scale. The spatial and temporal dynamics of event runoff characteristics are explained by event precipitation characteristics, subsurface wetness, topography or runoff generation mechanisms. The thesis first discusses runoff response in different runoff generation systems in the Hydrologic Open Air Laboratory (HOAL) (Chapters 2 and 3). Next, the variability of runoff event characteristics is examined and attributed to detailed field observations of hydrogeological process classifications in four Austrian catchments (Chapter 4).

Chapter 2 investigates the spatial and temporal dynamics of runoff event runoff coefficient and recession time constant in the HOAL. Clear relationships between runoff generation mechanisms and the spatial dynamics of runoff event characteristics are observed in the HOAL. While the mean R_c of runoff events is larger for tile drainages, and the main outlet (0.08-0.09), the mean R_c of natural drainage and wetland flow tends to be lower (0.03- 0.04). The variability of T_c and the difference between runoff generation mechanisms in the HOAL is lower. Runoff event recession at the main outlet is generally slower (mean T_c of 6.6 hrs), than in the subcatchments (mean T_c ranges from 4.2 to 5.7 hrs), which indicates shallower flow paths in the sub-catchments.

On the other hand, the seasonal variability of R_c is relatively larger for tile drainages and outlet flow, with the highest value in January and February and the lowest in July and August. This phenomenon is likely caused by higher evapotranspiration and lower soil moisture in July and August. There is a similar seasonal trend for T_c in the natural drainage system and the main outlet, which could be explained by the subsurface storage dynamics. The results indicate that the pre-event groundwater levels explain the variability of R_c and T_c in most of the runoff generation systems except for wetlands. Event precipitation volume controls only the peak flows, but not R_c and T_c .

Chapter 3 compares the performance of three machine learning methods (Random forest, RF; Gradient Boost Decision Tree, GBDT; Support vector machine, SVM) for the estimation of event runoff coefficient and recession time constant from 22 event-based explanatory characteristics. The regression models are developed for individual runoff generation systems as well as for their combination in HOAL. The results show that the SVM algorithm is the most accurate in predicting runoff coefficient and recession time constant, likely because of its flexibility in the transformation of high-dimensional space of characteristics. Coefficient of determinations of R_c regressions using SVM is larger than 0.6 for runoff events in tile drainages, natural drainages, outlet flow and unclassified flow. An exception is models for wetlands where only limited observations of infiltration characteristics exist. Performances of T_c regressions are generally less good than those of R_c which could result from the lack of observations on subsurface storages and their connectivity. The second objective of Chapter 3 is to quantify the relative importance of 22 event-based explanatory variables in R_c and T_c regressions using the SVM algorithm. Results show that R_c of the tile drainage systems is more controlled by weather conditions like precipitation duration and potential evapotranspiration. Still R_c in natural drainages is more influenced by antecedent soil moisture and groundwater levels. These

conclusions explain the role of seasonal dynamics of R_c and T_c in Chapter 2. The controlling factors of runoff event characteristics differ, therefore, for various runoff generation mechanisms.

While Chapters 2 and 3 examine runoff event characteristics in a small agricultural catchment characterized by a rather uniform climate and geological structure, Chapter 4 complements these investigations, exploring the role of climate in catchments with different hydro-geological characteristics. Chapter 4 links climate, geology and runoff regime to understand the dynamics of runoff response at a somewhat larger catchment scale than the HOAL. The results show that the spatial variability of R_c is consistent with the variability of annual precipitation. This finding confirms the assumption that a wetter climate with higher annual precipitation increases the ratio of direct flow and event rainfall, but also suggest an effect of the wetter climate on the subsurface drainage ability in the long term. Compared to the natural drainages on the hillslopes of the HOAL, however, the results show less correlation between subsurface wetness (indexed by antecedent precipitation) and runoff response because of the larger scales and multiple runoff generation mechanisms. Moreover, in all catchments, subsurface storage indexed by initial flow greatly influences the event runoff coefficient and peak flow, which is in accordance with findings in the HOAL. Except for the catchment with the largest area of deep interflow, runoff event recession time is negatively correlated to precipitation intensity, which is the largest in catchment dominated by karst surface flow.

In Chapter 4, field mapping of hydro-geologic runoff generation mechanisms derived from geologic and hydro-geologic information, is taken into consideration for explaining runoff event characteristics in each catchment. The results show that the hydro-geological mapping helps to explain and attribute the characteristics of runoff response. The larger R_c , event peaks and the fastest recessions are observed in the catchment with the largest precipitation, lowest permeability, steepest hillslopes and with a large proportion of areas characterized by shallow interflow processes. In contrast, catchments that are drier and have a significant portion of deep groundwater flow and large permeability exhibit the lowest R_c , lowest event peaks and longest T_c . The evaluation of the role of climate in different hydro-geological settings indicates that the snowmelt driven runoff events tend to have higher runoff coefficients and recession time constants in all studied catchments. The magnitude of runoff coefficient, recession time constant and peak flow tends to differ by runoff event type, and increase from short rain, median rain, long rain and snowmelt events.

Overall, this thesis has expanded the understanding of the spatial and temporal variability of runoff event characteristics at small and medium catchment scales. This variability is explained from a point of view of runoff generation mechanisms combined with an analysis of the subsurface geological structures, which has rarely been discussed before. It is found that the effects of the runoff generation mechanisms on event runoff characteristics are more significant at the small catchment scale, but less significant at regional scale, than climate. By using machine learning algorithms and comparative analyses, this thesis links climate and hydro-geological structure. Such links help to understand the runoff response better, and hence provide an improved knowledge base for runoff simulation and prediction. This thesis also provides new knowledge regarding the transfer of runoff event characteristics from small to regional catchment scales, which is particularly important for improving runoff prediction at ungauged sites where no measurements are available. In other ungauged small catchments such as the HOAL, surveys of the subsurface geological structure would be helpful to improve the runoff prediction. For example, if a small catchment is fully covered by underground tile drainage pipes, its runoff

Summary and conclusions

response should be larger than that of its neighbours but with lower baseflow and stable recession times. In ungauged catchments at the regional scale, on the other hand, climate should be considered with priority when transferring runoff event characteristics from other catchments. These findings of the thesis provide further evidence on the behaviour of runoff response which could be support parameter selection and the improvement of conceptual hydrological models. In the future, runoff generation mechanisms could be classified by combining climate and geology characteristics which are two main controlling elements of runoff response, for better explaining runoff event variability.

References

- Asefa, T., M. Kemblowski, M. McKee, and A. Khalil (2006), Multi-time scale stream flow predictions: The support vector machines approach, *Journal of Hydrology*, 318(1), 7-16, doi:10.1016/j.jhydrol.2005.06.001.
- Basak, D., S. Pal, and D. C. Patranabis (2007), Support vector regression, *Neural Information Processing-Letters and Reviews*, 11(10), 203-224.
- Baudron, P., F. Alonso-Sarría, J. L. García-Aróstegui, F. Cánovas-García, D. Martínez-Vicente, and J. Moreno-Brotóns (2013), Identifying the origin of groundwater samples in a multi-layer aquifer system with Random Forest classification, *Journal of Hydrology*, 499, 303-315, doi:10.1016/j.jhydrol.2013.07.009.
- Ben-Hur, A., and J. Weston (2010), A user's guide to support vector machines, in *Data mining techniques for the life sciences*, edited, pp. 223-239, Springer.
- Biswal, B., and D. Nagesh Kumar (2014a), Study of dynamic behaviour of recession curves, *Hydrological Processes*, 28(3), 784-792, doi:10.1002/hyp.9604.
- Biswal, B., and D. Nagesh Kumar (2014b), What mainly controls recession flows in river basins?, *Advances in Water Resources*, 65, 25-33, doi:10.1016/j.advwatres.2014.01.001.
- Blöschl, G., T. Nester, J. Komma, J. Parajka, and R. A. P. Perdigão (2013), The June 2013 flood in the Upper Danube Basin, and comparisons with the 2002, 1954 and 1899 floods, *Hydrology and Earth System Sciences*, 17(12), 5197-5212, doi:10.5194/hess-17-5197-2013.
- Blöschl, G., et al. (2016), The Hydrological Open Air Laboratory (HOAL) in Petzenkirchen: a hypothesis-driven observatory, *Hydrology and Earth System Sciences*, 20(1), 227-255, doi:10.5194/hess-20-227-2016.
- Blume, T., E. Zehe, and A. Bronstert (2007), Rainfall—runoff response, event-based runoff coefficients and hydrograph separation, *Hydrological Sciences Journal*, 52(5), 843-862, doi:10.1623/hysj.52.5.843.
- Borga, M., P. Boscolo, F. Zanone, and M. Sangati (2007), Hydrometeorological Analysis of the 29 August 2003 Flash Flood in the Eastern Italian Alps, *Journal of Hydrometeorology*, 8(5), 1049-1067, doi:10.1175/jhm593.1.
- Brammer, D. D., and J. J. McDonnell (1996), An evolving perceptual model of hillslope flow at the Maimai catchment, *Advances in hillslope processes*, 1, 35-60.
- Brutsaert, W., and J. L. Nieber (1977), Regionalized drought flow hydrographs from a mature glaciated plateau, *Water Resources Research*, 13(3), 637-643, doi:10.1029/WR013i003p00637.
- Burns, D., T. Vitvar, J. McDonnell, J. Hassett, J. Duncan, and C. Kendall (2005), Effects of suburban development on runoff generation in the Croton River basin, New York, USA, *Journal of Hydrology*, 311(1), 266-281, doi:10.1016/j.jhydrol.2005.01.022.
- Cánovas-García, F., F. Alonso-Sarría, F. Gomariz-Castillo, and F. Oñate-Valdivieso (2017), Modification of the random forest algorithm to avoid statistical dependence problems when classifying remote sensing imagery, *Computers & Geosciences*, 103, 1-11, doi:10.1016/j.cageo.2017.02.012.
- Cerdan, O., Y. Le Bissonnais, G. Govers, V. Lecomte, K. van Oost, A. Couturier, C. King, and N. Dubreuil (2004), Scale effect on runoff from experimental plots to catchments in agricultural areas in Normandy, *Journal of Hydrology*, 299(1), 4-14, doi:10.1016/j.jhydrol.2004.02.017.

References

- Chapelle, O., and V. Vapnik (2000), Model selection for support vector machines, paper presented at Advances in neural information processing systems.
- Chapman, T., and A. Maxwell (1996), Baseflow separation-comparison of numerical methods with tracer experiments, paper presented at Hydrology and Water Resources Symposium 1996: Water and the Environment; Preprints of Papers, Institution of Engineers, Australia.
- Chen, B., and W. F. Krajewski (2015), Recession analysis across scales: The impact of both random and nonrandom spatial variability on aggregated hydrologic response, *Journal of Hydrology*, 523, 97-106, doi:10.1016/j.jhydrol.2015.01.049.
- Chen, B., W. F. Krajewski, M. J. Helmers, and Z. Zhang (2019), Spatial Variability and Temporal Persistence of Event Runoff Coefficients for Cropland Hillslopes, *Water Resources Research*, 55(2), 1583-1597, doi:10.1029/2018wr023576.
- Chen, X., J. Parajka, B. Széles, P. Strauss, and G. Blöschl (2020a), Spatial and temporal variability of event runoff characteristics in a small agricultural catchment, *Hydrological Sciences Journal*, 65(13), 2185-2195, doi:10.1080/02626667.2020.1798451.
- Chen, X., J. Parajka, B. Széles, P. Strauss, and G. Blöschl (2020b), Controls on event runoff coefficients and recession coefficients for different runoff generation mechanisms identified by three regression methods, *Journal of Hydrology and Hydromechanics*, 68(2), 155-169, doi:10.2478/johh-2020-0008.
- Chiffard, P., J. Kranl, G. zur Strassen, and H. Zepp (2018), The significance of soil moisture in forecasting characteristics of flood events. A statistical analysis in two nested catchments, *Journal of Hydrology and Hydromechanics*, 66(1), 1-11, doi:10.1515/johh-2017-0037.
- Cortes, C., and V. Vapnik (1995), Support-vector networks, *Machine Learning*, 20(3), 273-297, doi:10.1007/BF00994018.
- Cortez, P., and M. J. Embrechts (2013), Using sensitivity analysis and visualization techniques to open black box data mining models, *Information Sciences*, 225, 1-17, doi:10.1016/j.ins.2012.10.039.
- Czikowsky, M. J., and D. R. Fitzjarrald (2004), Evidence of Seasonal Changes in Evapotranspiration in Eastern U.S. Hydrological Records, *Journal of Hydrometeorology*, 5(5), 974-988, doi:10.1175/1525-7541(2004)005<0974:eoscie>2.0.co;2.
- Del Giudice, G., R. Padulano, and G. Rasulo (2012), Factors affecting the runoff coefficient, *Hydrology and Earth System Sciences*, 9, 4919-4941, doi:10.5194/hessd-9-4919-2012.
- Dewandel, B., P. Lachassagne, M. Bakalowicz, P. Weng, and A. Al-Malki (2003), Evaluation of aquifer thickness by analysing recession hydrographs. Application to the Oman ophiolite hard-rock aquifer, *Journal of Hydrology*, 274(1), 248-269, doi:10.1016/S0022-1694(02)00418-3.
- Dietterich, T. G. (1997), Machine-Learning Research, *AI Magazine*, 18(4), doi:10.1609/aimag.v18i4.1324.
- Duan, Q., S. Sorooshian, and V. Gupta (1992), Effective and efficient global optimization for conceptual rainfall-runoff models, *Water Resources Research*, 28(4), 1015-1031, doi:10.1029/91wr02985.
- Dung, B. X., T. Gomi, S. Miyata, and R. C. Sidle (2012), Peak flow responses and recession flow characteristics after thinning of Japanese cypress forest in a headwater catchment, *Hydrological Research Letters*, 6, 35-40, doi:10.3178/hrl.6.35.
- Erdal, H. I., and O. Karakurt (2013), Advancing monthly streamflow prediction accuracy of CART models using ensemble learning paradigms, *Journal of Hydrology*, 477, 119-128, doi:10.1016/j.jhydrol.2012.11.015.

References

- Exner-Kittridge, M., P. Strauss, G. Blöschl, A. Eder, E. Saracevic, and M. Zessner (2016), The seasonal dynamics of the stream sources and input flow paths of water and nitrogen of an Austrian headwater agricultural catchment, *Science of the Total Environment*, 542, 935-945, doi: 10.1016/j.scitotenv.2015.10.151.
- Federer, C. A. (1973), Forest transpiration greatly speeds streamflow recession, *Water Resources Research*, 9(6), 1599-1604, doi:10.1029/WR009i006p01599.
- Friedman, J. H. (2001), Greedy Function Approximation: A Gradient Boosting Machine, *The Annals of Statistics*, 29(5), 1189-1232.
- Friedman, J. H. (2002), Stochastic gradient boosting, *Computational Statistics & Data Analysis*, 38(4), 367-378, doi:10.1016/S0167-9473(01)00065-2.
- Gaál, L., J. Szolgay, S. Kohnová, J. Parajka, R. Merz, A. Viglione, and G. Blöschl (2012), Flood timescales: Understanding the interplay of climate and catchment processes through comparative hydrology, *Water Resources Research*, 48(4), W04511, doi:10.1029/2011WR011509.
- García-Ruiz, J. M., D. Regüés, B. Alvera, N. Lana-Renault, P. Serrano-Muela, E. Nadal-Romero, A. Navas, J. Latron, C. Martí-Bono, and J. Arnáez (2008), Flood generation and sediment transport in experimental catchments affected by land use changes in the central Pyrenees, *Journal of Hydrology*, 356(1), 245-260, doi:10.1016/j.jhydrol.2008.04.013.
- Gottschalk, L., and R. Weingartner (1998), Distribution of peak flow derived from a distribution of rainfall volume and runoff coefficient, and a unit hydrograph, *Journal of Hydrology*, 208(3), 148-162, doi:10.1016/S0022-1694(98)00152-8.
- Hayes, D. C., and R. L. Young (2006), Comparison of peak discharge and runoff characteristic estimates from the rational method to field observations for small basins in central Virginia, *Rep. 2328-0328*.
- Hewlett, J. D., and A. R. Hibbert (1967), Factors affecting the response of small watersheds to precipitation in humid areas, *Forest hydrology*, 1, 275-290.
- Ho, T. K. (1995), Random decision forests, paper presented at Proceedings of 3rd international conference on document analysis and recognition, IEEE.
- Horn, R. A., and C. R. Johnson (1985), *Matrix analysis*, Cambridge university press.
- Hsu, C.-W., C.-C. Chang, and C.-J. Lin (2003), A practical guide to support vector classification.
- Hwang, S. H., D. H. Ham, and J. H. Kim (2012), Forecasting performance of LS-SVM for nonlinear hydrological time series, *KSCE Journal of Civil Engineering*, 16(5), 870-882, doi:10.1007/s12205-012-1519-3.
- James, A. L., and N. T. Roulet (2007), Investigating hydrologic connectivity and its association with threshold change in runoff response in a temperate forested watershed, *Hydrological Processes*, 21(25), 3391-3408, doi:10.1002/hyp.6554.
- Joel, A., I. Messing, O. Seguel, and M. Casanova (2002), Measurement of surface water runoff from plots of two different sizes, *Hydrological Processes*, 16(7), 1467-1478, doi:10.1002/hyp.356.
- Kostka, Z., and L. Holko (2003), Analysis of rainfall-runoff events in a mountain catchment, *Interdisciplinary approaches in small catchment hydrology: Monitoring and research*, 67, 19-25.
- Krakauer, N. Y., and M. Temimi (2011), Stream recession curves and storage variability in small watersheds, *Hydrology and Earth System Sciences*, 15(7), 2377-2389, doi:10.5194/hess-15-2377-2011.

References

- La Torre Torres, I. B., D. M. Amatya, G. Sun, and T. J. Callahan (2011), Seasonal rainfall–runoff relationships in a lowland forested watershed in the southeastern USA, *Hydrological Processes*, 25(13), 2032-2045, doi:10.1002/hyp.7955.
- Liaw, A., and M. Wiener (2002), Classification and regression by randomForest, *R news*, 2(3), 18-22.
- Liu, J., B. A. Engel, Y. Wang, Y. Wu, Z. Zhang, and M. Zhang (2019), Runoff Response to Soil Moisture and Micro-topographic Structure on the Plot Scale, *Scientific Reports*, 9(1), 2532, doi:10.1038/s41598-019-39409-6.
- Longobardi, A., P. Villani, R. Grayson, and A. Western (2003), On the relationship between runoff coefficient and catchment initial conditions, paper presented at Proceedings of MODSIM, 2003.
- Merz, R., and G. Blöschl (2009), A regional analysis of event runoff coefficients with respect to climate and catchment characteristics in Austria, *Water Resources Research*, 45(1), W01405, doi:10.1029/2008WR007163.
- Merz, R., G. Blöschl, and J. Parajka (2006), Spatio-temporal variability of event runoff coefficients, *Journal of Hydrology*, 331(3), 591-604, doi:10.1016/j.jhydrol.2006.06.008.
- Naghibi, S. A., H. R. Pourghasemi, and B. Dixon (2015), GIS-based groundwater potential mapping using boosted regression tree, classification and regression tree, and random forest machine learning models in Iran, *Environmental Monitoring and Assessment*, 188(1), 44, doi:10.1007/s10661-015-5049-6.
- Naghibi, S. A., K. Ahmadi, and A. Daneshi (2017), Application of Support Vector Machine, Random Forest, and Genetic Algorithm Optimized Random Forest Models in Groundwater Potential Mapping, *Water Resources Management*, 31(9), 2761-2775, doi:10.1007/s11269-017-1660-3.
- Norbiato, D., M. Borga, R. Merz, G. Blöschl, and A. Carton (2009), Controls on event runoff coefficients in the eastern Italian Alps, *Journal of Hydrology*, 375(3), 312-325, doi:10.1016/j.jhydrol.2009.06.044.
- Onda, Y., Y. Komatsu, M. Tsujimura, and J.-i. Fujihara (2001), The role of subsurface runoff through bedrock on storm flow generation, *Hydrological Processes*, 15(10), 1693-1706, doi:10.1002/hyp.234.
- Osuna, E. E. (1998), Support vector machines: Training and applications, Massachusetts Institute of Technology.
- Palleiro, L., M. L. Rodríguez-Blanco, M. M. Taboada-Castro, and M. T. Taboada-Castro (2014), Hydrological response of a humid agroforestry catchment at different time scales, *Hydrological Processes*, 28(4), 1677-1688, doi:10.1002/hyp.9714.
- Parajka, J., R. Merz, and G. Blöschl (2007), Uncertainty and multiple objective calibration in regional water balance modelling: case study in 320 Austrian catchments, *Hydrological Processes*, 21(4), 435-446, doi:10.1002/hyp.6253.
- Patnaik, S., B. Biswal, D. Nagesh Kumar, and B. Sivakumar (2015), Effect of catchment characteristics on the relationship between past discharge and the power law recession coefficient, *Journal of Hydrology*, 528, 321-328, doi:10.1016/j.jhydrol.2015.06.032.
- Penna, D., H. Tromp-van Meerveld, A. Gobbi, M. Borga, and G. Dalla Fontana (2011), The influence of soil moisture on threshold runoff generation processes in an alpine headwater catchment, *Hydrology and Earth System Sciences*, 15(3), 689-702, doi:10.5194/hess-15-689-2011.

References

- Pirkl, H. (2009), Hydrogeologische und geohydrologische Grundlagen für die ausgewählten Leiteinzugsgebiete - Unveröffentl. Bericht im Rahmen Projekt Hochwasser Tirol (HOWATI).
- Pirkl, H. (2012), Untergrundabhängige Abflussprozesse. Kartierung und Quantifizierung für das Bundesland Tirol. Flächendeckende Aufnahme Osttirols.
- Raghavendra, N. S., and P. C. Deka (2014), Support vector machine applications in the field of hydrology: A review, *Applied Soft Computing*, 19, 372-386, doi:10.1016/j.asoc.2014.02.002.
- Rajib, M., B. P. P., and B. Ashish (2010), Potential of support vector regression for prediction of monthly streamflow using endogenous property, *Hydrological Processes*, 24(7), 917-923, doi:10.1002/hyp.7535.
- Rinaldo, A., K. J. Beven, E. Bertuzzo, L. Nicotina, J. Davies, A. Fiori, D. Russo, and G. Botter (2011), Catchment travel time distributions and water flow in soils, *Water Resources Research*, 47(7), W07537, doi:10.1029/2011wr010478.
- Rodríguez-Blanco, M. L., M. M. Taboada-Castro, and M. T. Taboada-Castro (2012), Rainfall-runoff response and event-based runoff coefficients in a humid area (northwest Spain), *Hydrological Sciences Journal*, 57(3), 445-459, doi:10.1080/02626667.2012.666351.
- Rogger, M., H. Pirkl, A. Viglione, J. Komma, B. Kohl, R. Kirnbauer, R. Merz, and G. Blöschl (2012a), Step changes in the flood frequency curve: Process controls, *Water Resources Research*, 48(5), W05544, doi:10.1029/2011wr011187.
- Rogger, M., B. Kohl, H. Pirkl, A. Viglione, J. Komma, R. Kirnbauer, R. Merz, and G. Blöschl (2012b), Runoff models and flood frequency statistics for design flood estimation in Austria – Do they tell a consistent story?, *Journal of Hydrology*, 456-457, 30-43, doi:10.1016/j.jhydrol.2012.05.068.
- Rugenthaler, R., F. Schöberl, G. Markart, K. Klebinder, A. Hammerle, and G. Leitinger (2015), Quantification of Soil Moisture Effects on Runoff Formation at the Hillslope Scale, *Journal of Irrigation and Drainage Engineering*, 141(9), 05015001, doi:10.1061/(ASCE)IR.1943-4774.0000880.
- Sachdeva, S., T. Bhatia, and A. K. Verma (2018), GIS-based evolutionary optimized Gradient Boosted Decision Trees for forest fire susceptibility mapping, *Natural Hazards*, 92(3), 1399-1418, doi:10.1007/s11069-018-3256-5.
- Scherrer, S., F. Naef, A. O. Faeh, and I. Cordery (2007), Formation of runoff at the hillslope scale during intense precipitation, *Hydrology and Earth System Sciences Discussions*, 11(2), 907-922.
- Şen, Z., and A. Altunkaynak (2006), A comparative fuzzy logic approach to runoff coefficient and runoff estimation, *Hydrological Processes*, 20(9), 1993-2009, doi:10.1002/hyp.5992.
- Shaw, S. B., T. M. McHardy, and S. J. Riha (2013), Evaluating the influence of watershed moisture storage on variations in base flow recession rates during prolonged rain-free periods in medium-sized catchments in New York and Illinois, USA, *Water Resources Research*, 49(9), 6022-6028, doi:10.1002/wrcr.20507.
- Shen, C. (2018), A Transdisciplinary Review of Deep Learning Research and Its Relevance for Water Resources Scientists, *Water Resources Research*, 54(11), 8558-8593, doi:10.1029/2018WR022643.
- Silasari, R., J. Parajka, C. Ressler, P. Strauss, and G. Blöschl (2017), Potential of time-lapse photography for identifying saturation area dynamics on agricultural hillslopes, *Hydrological Processes*, 31(21), 3610-3627, doi:10.1002/hyp.11272.

References

- Sivapalan, M. (2003), Prediction in ungauged basins: a grand challenge for theoretical hydrology, *Hydrological Processes*, 17(15), 3163-3170, doi:10.1002/hyp.5155.
- Sivapalan, M., and G. Blöschl (2015), Time scale interactions and the coevolution of humans and water, *Water Resources Research*, 51(9), 6988-7022, doi:10.1002/2015wr017896.
- Széles, B., M. Broer, J. Parajka, P. Hogan, A. Eder, P. Strauss, and G. Blöschl (2018), Separation of Scales in Transpiration Effects on Low Flows: A Spatial Analysis in the Hydrological Open Air Laboratory, *Water Resources Research*, 54(9), 6168-6188, doi:10.1029/2017wr022037.
- Tachecí, P., P. Žlábek, T. Kvítek, and J. Peterková (2013), Analysis of rainfall-runoff events in four subcatchments of the Kopaninský potok (Czech Republic), *Bodenkultur*, 64(3-4), 105-111.
- Tague, C., and G. E. Grant (2004), A geological framework for interpreting the low-flow regimes of Cascade streams, Willamette River Basin, Oregon, *Water Resources Research*, 40(4), W04303, doi:10.1029/2003WR002629.
- Tallaksen, L. M. (1995), A review of baseflow recession analysis, *Journal of Hydrology*, 165(1), 349-370, doi:10.1016/0022-1694(94)02540-R.
- Tarasova, L., S. Basso, M. Zink, and R. Merz (2018a), Exploring Controls on Rainfall-Runoff Events: 1. Time Series-Based Event Separation and Temporal Dynamics of Event Runoff Response in Germany, *Water Resources Research*, 54(10), 7711-7732, doi:10.1029/2018wr022587.
- Tarasova, L., S. Basso, C. Poncelet, and R. Merz (2018b), Exploring Controls on Rainfall-Runoff Events: 2. Regional Patterns and Spatial Controls of Event Characteristics in Germany, *Water Resources Research*, 54(10), 7688-7710, doi:10.1029/2018wr022588.
- Tetzlaff, D., C. Soulsby, S. Waldron, I. A. Malcolm, P. J. Bacon, S. M. Dunn, A. Lilly, and A. F. Youngson (2007), Conceptualization of runoff processes using a geographical information system and tracers in a nested mesoscale catchment, *Hydrological Processes*, 21(10), 1289-1307, doi:10.1002/hyp.6309.
- Thomas, B. F., R. M. Vogel, and J. S. Famiglietti (2015), Objective hydrograph baseflow recession analysis, *Journal of Hydrology*, 525, 102-112, doi:10.1016/j.jhydrol.2015.03.028.
- Tian, F., H. Li, and M. Sivapalan (2012), Model diagnostic analysis of seasonal switching of runoff generation mechanisms in the Blue River basin, Oklahoma, *Journal of Hydrology*, 418-419, 136-149, doi:10.1016/j.jhydrol.2010.03.011.
- Vannier, O., S. Anquetin, and I. Braud (2016), Investigating the role of geology in the hydrological response of Mediterranean catchments prone to flash-floods: Regional modelling study and process understanding, *Journal of Hydrology*, 541, 158-172, doi:10.1016/j.jhydrol.2016.04.001.
- Vapnik, V., S. E. Golowich, and A. J. Smola (1997), Support vector method for function approximation, regression estimation and signal processing, paper presented at Advances in neural information processing systems.
- Viglione, A., and J. Parajka (2020), TUWmodel: Lumped/Semi-Distributed Hydrological Model for Education Purposes, edited.
- Viglione, A., R. Merz, and G. Blöschl (2009), On the role of the runoff coefficient in the mapping of rainfall to flood return periods, *Hydrology and Earth System Sciences*, 13(5), 577-593, doi:10.5194/hess-13-577-2009.

References

- Viglione, A., M. Rogger, H. Pirkl, J. Parajka, and G. Blöschl (2018), Conceptual model building inspired by field-mapped runoff generation mechanisms, *Journal of Hydrology and Hydromechanics*, 66(3), 303-315, doi:10.2478/johh-2018-0010.
- Villarini, G., and J. A. Smith (2010), Flood peak distributions for the eastern United States, *Water Resources Research*, 46(6), W06504, doi:10.1029/2009wr008395.
- Vogel, R. M., and C. N. Kroll (1996), Estimation of baseflow recession constants, *Water Resources Management*, 10(4), 303-320, doi:10.1007/BF00508898.
- Wainwright, J., and A. J. Parsons (2002), The effect of temporal variations in rainfall on scale dependency in runoff coefficients, *Water Resources Research*, 38(12), 1271, doi:10.1029/2000WR000188.
- Weiler, M., and J. J. McDonnell (2007), Conceptualizing lateral preferential flow and flow networks and simulating the effects on gauged and ungauged hillslopes, *Water Resources Research*, 43(3), W03403, doi:10.1029/2006wr004867.
- Western, A. W., G. Blöschl, and R. B. Grayson (1998), How well do indicator variograms capture the spatial connectivity of soil moisture?, *Hydrological Processes*, 12(12), 1851-1868, doi:10.1002/(sici)1099-1085(19981015)12:12<1851::aid-hyp670>3.0.co;2-p.
- Zimmermann, B., A. Zimmermann, B. L. Turner, T. Francke, and H. Elsenbeer (2014), Connectivity of overland flow by drainage network expansion in a rain forest catchment, *Water Resources Research*, 50(2), 1457-1473, doi:10.1002/2012WR012660.

Appendix A1

Appendix A1 contains the results of the sensitivity analysis of parameters in automatic runoff event identification in Chapter 2.

Table A1.1. Ranges of model parameters involved in the automatic runoff event identification process and their optimal values for maximizing identified events in outlet gauge (MW). Univariate discriminant approach is used for generating samples of parameter combinations from these ranges.

Parameters	Descriptions	Range of values		Optimal values
		Min.	Max.	
k2	Storage parameter (hours)	2	15	5
kday2	Fast recession time (hours)	0.1	1	1
khours	Smoothing constant (-)	1	5	3
qdrat	The lowest ratio of direct runoff to baseflow at peak time (-)	1	3	2
imax	The lowest peak interval time (hours)	6	18	12

Appendix A2

Appendix A2 shows identified runoff event characteristics in tributaries and outlet of HOAL during 57 event periods. These identified runoff events are mainly applied in Chapter 2&3.

Table A2.1. List of events with runoff coefficient, Rc (-), recession time constant, Tc (h), and peak discharge, Qp (mm/hrs).

NA: missing discharge observation because of equipment failure or regular maintenance.

NI: runoff event that was not identified by the event separation procedure.

Event start Event end (dd/mm/yy hh)	MW	A1	A2	Frau1	Frau2	Sys2	Sys3	Sys4
2013-01-04 16:00:00 2013-01-09 13:00:00	Rc:0.18 Tc:12.54 Qp:0.25	NA	NA	NA	NA	NA	NA	NA
2013-01-29 11:00:00 2013-01-31 15:00:00	Rc:0.3 Tc:6 Qp:0.74	NA	NA	NA	NA	NA	NA	NA
2013-02-14 22:00:00 2013-02-23 14:00:00	Rc:0.28 Tc:30 Qp:0.05	NA	NA	NA	NA	NA	NA	NA
2013-02-28 02:00:00 2013-03-03 23:00:00	Rc:0.32 Tc:11.95 Qp:0.15	NA	NA	NA	NA	NA	NA	NA
2013-03-31 03:00:00 2013-04-05 18:00:00	Rc:0.24 Tc:4.46 Qp:0.13	NA	NA	NA	NA	NA	NA	NA
2013-04-18 18:00:00 2013-04-20 12:00:00	Rc:0.07 Tc:14.24 Qp:0.13	0.03 3 0.12	0.01 1 0.1	0.12 8 0.06	0.04 7 0.1	0.05 10 0.1		NA
2013-05-11 09:00:00 2013-05-12 20:00:00	Rc:0.06 Tc:7 Qp:0.07	NI	0.18 15 0.13	0.01 3 0.01	0.08 12 0.06		NI	0.02 5 0.02

Appendix A2

Event start Event end (dd/mm/yy hh)	MW	A1	A2	Frau1	Frau2	Sys2	Sys3	Sys4
2013-05-17 20:00:00 2013-05-19 07:00:00	Rc:0.04 Tc:2 Qp:0.15	0.04 3 0.11	0.22 21.9 0.14			0.02 3 0.09		0.01 1.07 0.05
2013-05-30 17:00:00 2013-06-01 08:00:00	Rc:0.19 Tc:3.94 Qp:0.46	0.06 5 0.14	0.11 6.12 0.15	0.18 3 0.45	0.15 8 0.28	0.08 6 0.15		0.05 5 0.11
2013-06-01 18:00:00 2013-06-03 03:00:00	Rc:0.13 Tc:1 Qp:0.43	0.08 8.51 0.12	0.09 10.25 0.14	0.22 4 0.37	0.2 8 0.27	0.07 7 0.13		0.05 3 0.1
2013-06-03 13:00:00 2013-06-05 14:00:00	Rc:0.32 Tc:2.66 Qp:1.3	0.08 7.36 0.17	0.11 10 0.23	0.2 6 0.39	0.15 6.68 0.3	0.09 6 0.21		0.1 5.09 0.27
2013-06-10 10:00:00 2013-06-12 07:00:00	Rc:0.05 Tc:2 Qp:0.21	0.05 4 0.12	0.06 4 0.19	0.03 4 0.1	0.04 4 0.13		0.03 3 0.08	0.02 2 0.06
2013-06-22 08:00:00 2013-06-23 02:00:00	Rc:0.01 Tc:0.1 Qp:0.51	0.02 2 0.22			0.01 1 0.1	0.01 2 0.11		0.01 1.21 0.1
2013-06-24 16:00:00 2013-06-25 22:00:00	Rc:0.33 Tc:1 Qp:3.04			0.06 1 0.44	0.08 8 0.26			0.04 2.77 0.28
2013-07-10 17:00:00 2013-07-11 11:00:00	Rc:0.02 Tc:1 Qp:0.23	0.04 1.46 0.22	0.05 1.13 0.34		0.01 3 0.05		0.004 1 0.04	0.01 1.45 0.07
2013-08-04 10:00:00 2013-08-05 13:00:00	Rc:0.01 Tc:2 Qp:0.09	0.02 2 0.1	0.04 3 0.17		0.01 3 0.03		0.02 1.67 0.13	0.01 1 0.07
2013-08-08 19:00:00 2013-08-10 14:00:00	Rc:0.02 Tc:4 Qp:0.06	0.03 5.28 0.06	0.05 6.09 0.1		0.01 6 0.02		0.03 7.13 0.07	0.01 1.2 0.04
2013-08-24 21:00:00 2013-08-26 12:00:00	Rc:0.02 Tc:1 Qp:0.1	0.04 10 0.06	0.06 20.7 0.04		0.004 1 0.03	0.01 7 0.06	0.02 4 0.06	0.01 1 0.03
2013-08-28 08:00:00 2013-08-29 09:00:00	Rc:0.03 Tc:1 Qp:0.17	0.03 5 0.07	0.04 8 0.05	0.001 0.5 0.02		0.01 4 0.07		0.01 4 0.03
2013-09-16 13:00:00 2013-09-17 16:00:00	Rc:0.02 Tc:3 Qp:0.07	0.06 11.89 0.1				0.03 6 0.11	0.02 10 0.03	0.01 3.36 0.02
2013-11-05 22:00:00 2013-11-08 21:00:00	Rc:0.05 Tc:20 Qp:0.04	0.07 8 0.07	0.07 6 0.08				0.02 3.61 0.02	0.01 3.54 0.02
2013-11-10 17:00:00 2013-11-12 22:00:00	Rc:0.07 Tc:20 Qp:0.04	0.08 8.11 0.09	0.11 10.18 0.11		0.03 15 0.02	0.02 4 0.09	0.02 4.9 0.03	0.02 11.88 0.02
2013-11-23 19:00:00 2013-11-26 03:00:00	Rc:0.09 Tc:11.5 Qp:0.15	0.08 11.22 0.12	0.07 5.21 0.14	0.02 2 0.06	0.07 8 0.1	0.06 6 0.13	0.06 9.84 0.1	0.03 11.68 0.04
2013-12-08 03:00:00 2013-12-11 11:00:00	Rc:0.16 Tc:32.56 Qp:0.05		0.07 10 0.05		0.1 10 0.06		0.05 7 0.04	0.06 25 0.02
2014-04-06 03:00:00 2014-04-07 00:00:00	Rc:0.01 Tc:1 Qp:0.05	0.03 10.46 0.04	0.02 1 0.1				0.002 1 0.01	0.01 1 0.03
2014-05-02 13:00:00 2014-05-04 10:00:00	Rc:0.01 Tc:2 Qp:0.04	0.03 5.87 0.03	0.03 10 0.02				0.001 1 0.004	0.01 1 0.03
2014-05-16 09:00:00 2014-05-19 05:00:00	Rc:0.05 Tc:3 Qp:0.18	0.03 4 0.09	0.04 5 0.09	0.02 2 0.06	0.05 3 0.18	0.05 5 0.14	0.03 1.5 0.14	0.02 5 0.06
2014-05-27 20:00:00 2014-05-30 11:00:00	Rc:0.05 Tc:2 Qp:0.4	0.03 4.14 0.19	0.05 4.23 0.25	0.02 1 0.13	0.06 4 0.28	0.03 2 0.25	0.02 1 0.27	0.04 8 0.15

Appendix A2

Event start Event end (dd/mm/yy hh)	MW	A1	A2	Frau1	Frau2	Sys2	Sys3	Sys4
2014-06-20 00:00:00 2014-06-21 14:00:00	Rc:0.004 Tc:1 Qp:0.05	0.02 3.32 0.06	0.04 3 0.13	NA	NI	NI	0.005 2 0.02	0.005 1.16 0.03
2014-06-25 10:00:00 2014-06-25 22:00:00	Rc:0.004 Tc:1 Qp:0.04	0.003 1 0.02	0.01 1 0.05	NA	NI	NI	NI	0.003 1 0.02
2014-07-08 11:00:00 2014-07-09 08:00:00	Rc:0.01 Tc:1 Qp:0.03	NA	NA	NA	NA	NI	0.004 3 0.01	0.01 1 0.03
2014-07-11 01:00:00 2014-07-12 09:00:00	Rc:0.01 Tc:2 Qp:0.03	NA	0.02 1 0.1	NA	NA	0.01 5 0.02	0.004 2.92 0.01	0.01 1 0.02
2014-07-23 08:00:00 2014-07-23 23:00:00	Rc:0.01 Tc:2 Qp:0.02	NA	NI	NA	NA	NI	0.004 3.5 0.01	0.01 1.04 0.03
2014-08-09 16:00:00 2014-08-10 08:00:00	Rc:0.01 Tc:0.5 Qp:0.22	NA	NA	NA	0.0003 1 0.01	0.01 1 0.13	0.003 0.5 0.11	0.01 1 0.08
2014-08-20 01:00:00 2014-08-21 14:00:00	Rc:0.01 Tc:1 Qp:0.02	NA	NI	NA	NI	NI	0.01 5.71 0.01	0.01 1.06 0.02
2014-08-22 17:00:00 2014-08-24 09:00:00	Rc:0.005 Tc:1 Qp:0.04	NA	0.01 2 0.01	NA	NI	0.01 5 0.03	0.005 4 0.01	0.01 1 0.04
2014-08-30 04:00:00 2014-08-30 20:00:00	Rc:0.01 Tc:2 Qp:0.03	NA	0.01 2 0.03	NA	NA	0.01 2 0.03	0.01 7.26 0.01	0.01 1 0.03
2014-08-31 19:00:00 2014-09-05 10:00:00	Rc:0.05 Tc:17.58 Qp:0.06	NA	0.03 3.28 0.08	NI	0.03 7 0.05	0.07 12.94 0.08	0.03 7.13 0.04	0.02 11.23 0.03
2014-09-13 00:00:00 2014-09-16 11:00:00	Rc:0.08 Tc:9 Qp:0.11	0.03 3.05 0.07	0.05 3.12 0.13	0.02 6 0.03	0.08 8 0.1	0.06 4 0.16	0.05 6 0.09	0.04 10.06 0.06
2014-10-17 03:00:00 2014-10-18 14:00:00	Rc:0.02 Tc:6 Qp:0.03	NA	0.02 3 0.04	NA	NI	0.01 3 0.03	0.01 4 0.01	0.01 1.24 0.02
2014-10-22 14:00:00 2014-10-25 16:00:00	Rc:0.14 Tc:6 Qp:0.27	0.03 3 0.07	0.06 3.79 0.13	0.16 6 0.25	0.29 8 0.34	0.07 6 0.11	0.07 10 0.06	0.07 8 0.08
2014-12-06 20:00:00 2014-12-08 23:00:00	Rc:0.06 Tc:22.48 Qp:0.03	0.02 16.98 0.02	0.05 7.43 0.05	0.02 4 0.01	0.03 3 0.05	0.04 15 0.04	0.02 11.22 0.02	0.02 13.61 0.01
2014-12-19 11:00:00 2014-12-21 10:00:00	Rc:0.06 Tc:13 Qp:0.04	NI	0.03 3 0.04	0.004 3 0.004	0.06 3 0.12	0.03 10 0.04	0.02 6 0.02	0.02 3 0.03
2015-01-02 16:00:00 2015-01-06 17:00:00	Rc:0.16 Tc:11.76 Qp:0.1	0.03 3.45 0.03	0.06 1.74 0.07	0.18 5.17 0.12	0.39 5 0.27	0.09 5.43 0.06	0.09 14.67 0.05	0.07 16.07 0.04
2015-01-09 12:00:00 2015-01-12 20:00:00	Rc:0.19 Tc:10 Qp:0.19	0.01 2 0.03	0.05 3 0.09	0.3 8 0.26	0.22 6 0.25	0.09 17 0.07	0.06 10 0.05	0.08 13.57 0.06
2015-03-01 23:00:00 2015-03-05 18:00:00	Rc:0.1 Tc:10 Qp:0.08	0.03 3 0.03	0.07 5 0.08	0.24 10 0.11	0.2 8 0.15	NI	0.02 10 0.02	0.03 7 0.03
2015-04-01 02:00:00 2015-04-04 23:00:00	Rc:0.14 Tc:15 Qp:0.07	NA	NI	0.07 5 0.08	NI	NI	0.06 25 0.02	0.05 15.97 0.03
2015-04-16 23:00:00 2015-04-18 13:00:00	Rc:0.01 Tc:1 Qp:0.07	0.01 1 0.05	0.03 1 0.12	NA	0.004 2.85 0.01	0.01 4 0.05	0.01 8.62 0.03	0.004 1 0.02
2015-05-22 17:00:00 2015-05-25 04:00:00	Rc:0.07 Tc:8 Qp:0.17	0.04 4 0.12	0.04 2 0.15	0.03 4 0.03	0.14 4 0.13	0.04 9 0.1	0.01 4.4 0.04	0.04 8 0.11

Appendix A3

Event start Event end (dd/mm/yy hh)	MW	A1	A2	Frau1	Frau2	Sys2	Sys3	Sys4
2015-06-08 12:00:00 2015-06-08 20:00:00	Rc:0.005 Tc:1 Qp:0.04	NA	0.01 1 0.06	NA	NI	NI	NA	0.01 1.26 0.03
2015-07-08 13:00:00 2015-07-09 22:00:00	Rc:0.01 Tc:1 Qp:0.02	NA	NA	NA	NI	NI	0.005 2 0.01	0.01 1.66 0.01
2015-07-19 13:00:00 2015-07-20 12:00:00	Rc:0.004 Tc:1 Qp:0.03	NA	NA	NA	NI	NI	0.002 3.04 0.01	0.003 1.13 0.01
2015-08-16 18:00:00 2015-08-18 10:00:00	Rc:0.01 Tc:1 Qp:0.06	NA	0.01 0.5 0.06	NA	NI	0.01 2 0.05	0.004 1.5 0.03	0.01 1 0.05
2015-09-03 13:00:00 2015-09-04 12:00:00	Rc:0.01 Tc:1 Qp:0.04	NA	NA	NA	NA	0.01 3 0.03	NA	0.01 1 0.04
2015-10-07 20:00:00 2015-10-09 18:00:00	Rc:0.01 Tc:1 Qp:0.04	NA	NI	NA	0.003 3 0.003	0.02 3 0.05	NI	0.01 1 0.03
2015-10-19 08:00:00 2015-10-22 17:00:00	Rc:0.03 Tc:9 Qp:0.04	NA	NA	0.01 3 0.01	0.03 3 0.08	0.03 5 0.05	0.01 1 0.02	0.01 5 0.02
2015-11-20 07:00:00 2015-11-22 10:00:00	Rc:0.03 Tc:15 Qp:0.02	NA	NA	NA	NI	0.02 4 0.03	0.004 2 0.01	0.005 1 0.01

Appendix A3

Appendix A3 shows identified runoff event characteristics in catchments of HOAL, Wimitzbach, Perschling, Gail and Dornbirnerach during event periods from 2002 to 2013. These identified events are mainly applied in Chapter 4.

Table A3.1. List of events with runoff coefficient, Rc (-), recession time constant, Tc (h), and peak discharge, Qp (mm/hrs) in catchments of HOAL, Wimitzbach, Perschling, Gail and Dornbirnerach.

LRC: Rc is greatly larger than 1 may be caused by incorrect rainfall or flow data.

NDF: direct flow are too small to be identified even though precipitation event occurred, mostly because of precipitation is too small.

NP: there are almost no precipitation event happened.

MP: missing precipitation data.

strange flow: flow hydrograph is too strange to identify an event.

MQ: missing discharge data.

BP: direct flow before precipitation.

melt wave: melt wave.

Event start Event end (yyyy-mm-dd hh)	HOAL	Wimitzbach	Perschling	Gail	Dornbirnerach
2002-01-20 18:00:00 2002-01-24 05:00:00	Rc:0.28 Tc:20 Qp:0.06	NDF	0.38 30 0.1	NDF	NDF
2002-01-27 07:00:00 2002-01-30 01:00:00	Rc:0.16 Tc:13 Qp:0.04	NDF	NP	NDF	0.86 5 1.96
2002-02-08 05:00:00 2002-02-11 05:00:00	Rc:NDF Tc:NDF Qp:NDF	NP	NDF	NDF	1 12 0.57

Appendix A3

Event start Event end (yyyy-mm-dd hh)	HOAL	Wimitzbach	Perschling	Gail	Dornbirnerach
2002-02-13 05:00:00 2002-02-16 10:00:00	Rc:0.08 Tc:15 Qp:0.06	NP	0.08 20 0.07	NDF	NDF
2002-02-25 05:00:00 2002-03-01 16:00:00	Rc:0.14 Tc:20 Qp:0.07	NDF	NDF	NDF	1 10 1.07
2002-03-19 02:00:00 2002-03-23 18:00:00	Rc:0.14 Tc:1 Qp:1.79	NP	0.25 7 0.76	0.18 15 0.1	1 4 4.32
2002-03-22 18:00:00 2002-03-23 15:00:00	Rc:NDF Tc:NDF Qp:NDF	NP	NDF	NDF	0.54 6 1.2
2002-04-13 08:00:00 2002-04-17 02:00:00	Rc:NDF Tc:NDF Qp:NDF	NDF	NDF	0.12 20 0.08	0.19 20 0.28
2002-04-23 20:00:00 2002-04-30 17:00:00	Rc:NDF Tc:NDF Qp:NDF	0.05 20 0.03	0.05 20 0.03	NDF	0.65 5 3.21
2002-05-03 05:00:00 2002-05-07 04:00:00	Rc:NDF Tc:NDF Qp:NDF	NDF	NDF	0.26 15 0.71	0.52 8 0.96
2002-05-11 06:00:00 2002-05-16 18:00:00	Rc:NDF Tc:NDF Qp:NDF	0.02 15 0.03	NP	NDF	0.18 4 0.74
2002-05-18 11:00:00 2002-05-20 23:00:00	Rc:NDF Tc:NDF Qp:NDF	NDF	NDF	NDF	0.34 6 1.2
2002-05-23 12:00:00 2002-05-25 03:00:00	Rc:NP Tc:NP Qp:NP	NP	NP	0.18 13 0.24	0.25 4 0.83
2002-05-25 12:00:00 2002-05-29 17:00:00	Rc:0.01 Tc:2 Qp:0.02	0.01 6 0.06	0.02 25 0.01	0.39 35 0.31	0.5 5 1.46
2002-06-05 22:00:00 2002-06-09 04:00:00	Rc:0.07 Tc:1 Qp:1.71	0.02 15 0.03	0.04 5 0.2	0.2 8 1.01	0.78 2 5.99
2002-06-09 13:00:00 2002-06-11 09:00:00	Rc:0.01 Tc:3 Qp:0.02	NP	0.08 5 0.35	NP	0.97 2 5.88
2002-06-19 14:00:00 2002-06-20 12:00:00	Rc:NP Tc:NP Qp:NP	NP	NP	NP	0.07 4 0.28
2002-06-20 11:00:00 2002-06-21 12:00:00	Rc:NP Tc:NP Qp:NP	NP	NP	NP	0.35 4 0.46
2002-06-23 13:00:00 2002-06-26 10:00:00	Rc:0.01 Tc:1 Qp:0.03	NDF	NDF	0.32 5 0.49	0.11 10 0.13
2002-06-27 10:00:00 2002-06-30 17:00:00	Rc:0.01 Tc:2 Qp:0.02	NDF	strange flow	0.12 6 0.24	0.21 2 2
2002-07-03 17:00:00 2002-07-05 11:00:00	Rc:0.01 Tc:1 Qp:0.03	0.01 8 0.04	NDF	0.06 5 0.18	0.32 1 2.44
2002-07-05 23:00:00 2002-07-08 15:00:00	Rc:0.01 Tc:3 Qp:0.01	NP	0.01 5 0.04	NP	0.23 6 0.31

Appendix A3

Event start Event end (yyyy-mm-dd hh)	HOAL	Wimitzbach	Perschling	Gail	Dornbirnerach
2002-07-12 17:00:00 2002-07-15 02:00:00	Rc:0.01 Tc:1 Qp:0.03	NDF	NDF	NDF	0.1 12 0.15
2002-07-15 17:00:00 2002-07-18 19:00:00	Rc:0.03 Tc:1 Qp:0.2	0.02 2 0.13	0.02 4 0.07	0.16 8 0.16	0.63 2 5.48
2002-07-20 22:00:00 2002-07-22 17:00:00	Rc:0.01 Tc:1 Qp:0.05	NDF	NDF	0.11 6 0.15	NDF
2002-07-23 21:00:00 2002-07-27 16:00:00	Rc:0.01 Tc:1 Qp:0.02	NDF	0.03 28.92 0.02	NDF	0.11 6 0.18
2002-08-01 18:00:00 2002-08-02 11:00:00	Rc:0.01 Tc:1 Qp:0.03	NDF	NDF	NDF	NDF
2002-08-05 21:00:00 2002-08-09 16:00:00	Rc:0.13 Tc:1 Qp:2.07	0.09 30 0.08	0.07 2 1.09	0.25 20 0.18	0.31 6 0.92
2002-08-10 14:00:00 2002-08-14 21:00:00	Rc:0.27 Tc:1 Qp:1.96	0.04 12 0.13	0.34 3 2.45	0.3 30 0.32	0.86 1 11.22
2002-08-20 17:00:00 2002-08-23 10:00:00	Rc:0.02 Tc:2 Qp:0.03	0.05 10 0.07	NDF	0.06 5 0.23	0.06 6 0.18
2002-08-31 13:00:00 2002-09-05 03:00:00	Rc:MQ Tc:MQ Qp:MQ	NDF	0.05 15 0.03	0.08 7 0.11	0.22 5 1.18
2002-09-15 04:00:00 2002-09-16 00:00:00	Rc:0.02 Tc:2 Qp:0.02	NDF	NDF	NP	NDF
2002-09-19 07:00:00 2002-09-21 22:00:00	Rc:0.08 Tc:1 Qp:0.78	0.04 10 0.08	NDF	NP	0.38 5 1.53
2002-09-21 11:00:00 2002-09-23 06:00:00	Rc:0.01 Tc:2 Qp:0.04	0.04 15 0.06	0.04 20 0.03	NDF	0.63 6 1.38
2002-09-22 21:00:00 2002-09-29 18:00:00	Rc:0.04 Tc:2 Qp:0.12	0.1 45 0.08	0.06 30 0.06	strange flow	0.41 8 1.34
2002-10-04 13:00:00 2002-10-05 21:00:00	Rc:0.03 Tc:1 Qp:0.16	NP	0.03 10 0.04	NP	NDF
2002-10-05 17:00:00 2002-10-08 19:00:00	Rc:0.02 Tc:1 Qp:0.03	NP	NP	NP	0.53 5 1.52
2002-10-10 15:00:00 2002-10-17 01:00:00	Rc:0.1 Tc:2 Qp:0.36	0.03 10 0.07	0.12 5 0.3	0.23 35 0.14	0.37 7 0.56
2002-10-16 22:00:00 2002-10-21 05:00:00	Rc:0.07 Tc:2 Qp:0.15	0.04 15 0.08	strange flow	0.15 14 0.16	0.51 4 1.72
2002-10-23 05:00:00 2002-10-25 05:00:00	Rc:0.05 Tc:3 Qp:0.11	NDF	NDF	NDF	0.09 15 0.12
2002-10-30 09:00:00 2002-11-01 12:00:00	Rc:0.09 Tc:3 Qp:0.11	NP	NDF	NP	NP

Appendix A3

Event start Event end (yyyy-mm-dd hh)	HOAL	Wimitzbach	Perschling	Gail	Dornbirnerach
2002-11-02 07:00:00 2002-11-07 04:00:00	Rc:0.16 Tc:1 Qp:0.78	NDF	0.17 25 0.07	0.22 15 0.1	0.42 4 1.92
2002-11-08 20:00:00 2002-11-10 09:00:00	Rc:0.09 Tc:10 Qp:0.06	NP	NDF	NP	0.73 3 1.6
2002-11-10 14:00:00 2002-11-14 01:00:00	Rc:0.26 Tc:1 Qp:1.14	NP	0.25 20 0.17	NP	0.34 1 1.64
2002-11-16 06:00:00 2002-11-21 12:00:00	Rc:0.07 Tc:8 Qp:0.06	0.06 20 0.07	NDF	0.21 8 0.88	0.16 4 0.55
2002-11-21 20:00:00 2002-11-25 05:00:00	Rc:0.05 Tc:1 Qp:0.18	0.07 20 0.08	0.13 30 0.05	NDF	0.27 15 0.24
2002-11-24 08:00:00 2002-12-02 12:00:00	Rc:0.08 Tc:4 Qp:0.05	NDF	NDF	0.45 20 1.21	0.27 8 0.44
2002-12-05 03:00:00 2002-12-09 10:00:00	Rc:NDF Tc:NDF Qp:NDF	NDF	0.18 40 0.06	NDF	NP
2002-12-16 12:00:00 2002-12-19 03:00:00	Rc:NDF Tc:NDF Qp:NDF	NP	NDF	NP	0.21 2 0.74
2002-12-21 00:00:00 2002-12-24 22:00:00	Rc:0.3 Tc:1 Qp:0.58	NDF	0.23 12 0.23	NDF	1 8 1.31
2002-12-28 09:00:00 2003-01-01 17:00:00	Rc:0.32 Tc:1 Qp:0.41	NDF	0.17 30 0.1	NDF	0.21 6 0.57
2003-01-02 01:00:00 2003-01-04 11:00:00	Rc:0.26 Tc:1 Qp:1.11	NP	0.3 25 0.09	NP	0.53 5 1.27
2003-01-26 21:00:00 2003-01-30 08:00:00	Rc:0.24 Tc:1 Qp:0.37	NDF	0.31 7 0.41	NP	1 4 0.79
2003-03-01 18:00:00 2003-03-05 22:00:00	Rc:0.06 Tc:2 Qp:0.07	NDF	0.34 9 0.63	NP	0.41 10 0.31
2003-03-06 10:00:00 2003-03-08 19:00:00	Rc:NDF Tc:NDF Qp:NDF	NDF	NDF	NP	0.29 6 0.93
2003-04-21 11:00:00 2003-04-23 10:00:00	Rc:NP Tc:NP Qp:NP	NDF	NP	NDF	0.5 8 0.43
2003-04-26 09:00:00 2003-04-28 11:00:00	Rc:NDF Tc:NDF Qp:NDF	NDF	NDF	NDF	0.44 12 0.45
2003-04-30 15:00:00 2003-05-02 09:00:00	Rc:NP Tc:NP Qp:NP	NP	NDF	NDF	0.31 6 0.57
2003-05-02 17:00:00 2003-05-04 11:00:00	Rc:0.02 Tc:1 Qp:0.03	NP	NDF	NDF	0.37 8 0.59
2003-05-13 07:00:00 2003-05-17 12:00:00	Rc:0.01 Tc:1 Qp:0.05	NDF	0.03 20 0.03	NDF	0.4 2 1.29

Appendix A3

Event start Event end (yyyy-mm-dd hh)	HOAL	Wimitzbach	Perschling	Gail	Dornbirnerach
2003-05-19 10:00:00 2003-05-24 02:00:00	Rc:0.01 Tc:1 Qp:0.03	0.04 8 0.05	NDF	0.21 45 0.21	0.42 6 1.38
2003-05-22 11:00:00 2003-05-24 01:00:00	Rc:NP Tc:NP Qp:NP	NP	NP	NP	0.68 8.01 1.38
2003-05-27 12:00:00 2003-05-28 10:00:00	Rc:0.04 Tc:1 Qp:0.58	0.01 3 0.04	NP	NDF	NDF
2003-05-28 12:00:00 2003-05-31 11:00:00	Rc:NP Tc:NP Qp:NP	NDF	NP	NDF	0.49 10 0.41
2003-05-31 09:00:00 2003-06-01 22:00:00	Rc:0.01 Tc:2 Qp:0.02	0.21 4 0.12	NDF	NDF	0.14 8 0.13
2003-06-08 07:00:00 2003-06-12 14:00:00	Rc:0.01 Tc:1 Qp:0.03	NDF	NDF	NDF	0.12 6 0.12
2003-06-14 15:00:00 2003-06-17 07:00:00	Rc:0.01 Tc:1 Qp:0.03	0.06 20 0.04	0.08 5 0.02	0.16 20 0.15	NDF
2003-06-17 13:00:00 2003-06-19 17:00:00	Rc:NDF Tc:NDF Qp:NDF	NDF	NDF	NDF	0.14 5 0.29
2003-07-01 15:00:00 2003-07-06 05:00:00	Rc:NDF Tc:NDF Qp:NDF	0.04 25 0.05	NDF	0.05 8 0.15	0.14 4 0.44
2003-07-09 10:00:00 2003-07-10 10:00:00	Rc:0.02 Tc:1 Qp:0.04	NP	NDF	NP	NP
2003-07-16 17:00:00 2003-07-19 16:00:00	Rc:0.01 Tc:1 Qp:0.03	NP	0.01 8 0.02	0.02 3 0.12	0.03 6 0.09
2003-07-21 07:00:00 2003-07-22 12:00:00	Rc:NP Tc:NP Qp:NP	NP	0 4 0.02	0.05 5 0.14	NDF
2003-07-22 14:00:00 2003-07-26 04:00:00	Rc:0.01 Tc:0.5 Qp:0.06	NP	0.01 10 0.01	0.1 10 0.17	0.21 3 1
2003-07-27 12:00:00 2003-07-31 01:00:00	Rc:0.01 Tc:1 Qp:0.03	NDF	0.03 40 0.01	0.05 10 0.12	0.12 3 0.44
2003-07-31 10:00:00 2003-08-02 22:00:00	Rc:0.01 Tc:1 Qp:0.08	NP	0.01 8 0.03	NP	NP
2003-08-14 04:00:00 2003-08-17 01:00:00	Rc:NP Tc:NP Qp:NP	NP	NP	NP	0.04 6 0.07
2003-08-18 12:00:00 2003-08-19 10:00:00	Rc:0.01 Tc:1 Qp:0.05	NP	NP	NP	NP
2003-08-29 10:00:00 2003-08-30 11:00:00	Rc:0.01 Tc:1 Qp:0.03	strange flow	NP	0.04 3 0.09	0.1 10 0.1
2003-08-30 09:00:00 2003-09-02 04:00:00	Rc:0.01 Tc:1 Qp:0.02	0.04 7 0.15	MP	0.04 5 0.24	0.2 7 0.48

Appendix A3

Event start Event end (yyyy-mm-dd hh)	HOAL	Wimitzbach	Perschling	Gail	Dornbirnerach
2003-09-01 16:00:00 2003-09-04 00:00:00	Rc:0.01 Tc:1 Qp:0.01	NP	NP	NP	0.1 6 0.13
2003-09-09 22:00:00 2003-09-12 17:00:00	Rc:0.01 Tc:3 Qp:0.01	MP	NDF	NDF	0.24 1 1.72
2003-09-12 19:00:00 2003-09-14 13:00:00	Rc:0.01 Tc:4 Qp:0.02	NP	0.02 5 0.08	NP	NDF
2003-09-23 06:00:00 2003-09-25 12:00:00	Rc:0.01 Tc:1 Qp:0.04	0.05 20 0.02	BP	NDF	0.21 4 0.89
2003-09-28 15:00:00 2003-09-30 18:00:00	Rc:0.01 Tc:3 Qp:0.01	NDF	NDF	NDF	0.15 5 0.47
2003-10-04 19:00:00 2003-10-06 06:00:00	Rc:0.01 Tc:2 Qp:0.04	MP	NDF	MP	strange flow
2003-10-08 17:00:00 2003-10-11 18:00:00	Rc:NDF Tc:NDF Qp:NDF	NP	NDF	NDF	1 1 8.45
2003-10-31 14:00:00 2003-11-05 10:00:00	Rc:0.01 Tc:3 Qp:0.03	0.06 20 0.09	0.03 20 0.02	0.23 20 0.46	0.43 7 1
2003-11-12 22:00:00 2003-11-14 23:00:00	Rc:NP Tc:NP Qp:NP	NP	NP	NP	0.39 6 1.2
2003-11-17 01:00:00 2003-11-19 13:00:00	Rc:NP Tc:NP Qp:NP	NDF	NP	NP	0.26 7 0.73
2003-11-28 16:00:00 2003-11-30 16:00:00	Rc:0.01 Tc:3 Qp:0.01	0.06 10 0.09	NDF	NDF	NDF
2003-12-06 13:00:00 2003-12-07 14:00:00	Rc:0.01 Tc:3 Qp:0.01	NP	NDF	NDF	NDF
2004-01-11 15:00:00 2004-01-16 02:00:00	Rc:0.1 Tc:3 Qp:0.15	NDF	0.11 12 0.1	NP	0.94 6 2.5
2004-02-02 09:00:00 2004-02-06 09:00:00	Rc:0.05 Tc:4 Qp:0.12	NDF	0.15 15 0.14	NDF	NDF
2004-02-07 01:00:00 2004-02-08 11:00:00	Rc:NP Tc:NP Qp:NP	NP	NP	NP	0.62 4 0.95
2004-03-23 08:00:00 2004-03-29 06:00:00	Rc:0.08 Tc:1 Qp:0.28	NDF	0.25 25 0.31	NP	NDF
2004-04-04 11:00:00 2004-04-06 09:00:00	Rc:MP Tc:MP Qp:MP	NDF	NDF	NDF	0.38 8 0.82
2004-04-23 09:00:00 2004-04-25 14:00:00	Rc:MP Tc:MP Qp:MP	NDF	strange flow	NDF	0.57 14 1.13
2004-05-01 13:00:00 2004-05-03 04:00:00	Rc:MP Tc:MP Qp:MP	NP	NP	NDF	0.24 5 0.52

Appendix A3

Event start Event end (yyyy-mm-dd hh)	HOAL	Wimitzbach	Perschling	Gail	Dornbirnerach
2004-05-05 04:00:00 2004-05-08 04:00:00	Rc:MP Tc:MP Qp:MP	NDF	NP	NDF	0.3 10 0.68
2004-05-08 22:00:00 2004-05-10 14:00:00	Rc:MP Tc:MP Qp:MP	NDF	NP	NDF	0.36 8 0.58
2004-05-15 19:00:00 2004-05-18 12:00:00	Rc:MP Tc:MP Qp:MP	NP	0.04 10 0.05	NDF	NDF
2004-05-21 05:00:00 2004-05-25 07:00:00	Rc:MP Tc:MP Qp:MP	0.03 15 0.06	0.03 36 0.02	NDF	0.32 6 1.37
2004-05-27 10:00:00 2004-05-30 23:00:00	Rc:MP Tc:MP Qp:MP	0.05 20 0.06	0.04 25 0.03	NDF	0.21 9 0.38
2004-06-02 16:00:00 2004-06-06 20:00:00	Rc:MP Tc:MP Qp:MP	NP	0.18 8 0.54	NP	0.63 2 4.84
2004-06-11 00:00:00 2004-06-15 23:00:00	Rc:MP Tc:MP Qp:MP	0.03 11 0.09	NDF	0.23 11 0.55	0.27 6 0.76
2004-06-19 11:00:00 2004-06-23 02:00:00	Rc:MP Tc:MP Qp:MP	0.13 33 0.26	0.06 10 0.16	0.36 38 0.41	0.37 11.55 0.42
2004-06-23 14:00:00 2004-06-29 19:00:00	Rc:MP Tc:MP Qp:MP	0.09 15 0.16	0.06 14 0.08	NDF	0.13 8 0.21
2004-07-02 03:00:00 2004-07-04 09:00:00	Rc:NDF Tc:NDF Qp:NDF	0.09 15 0.12	NDF	0.33 15 0.35	0.1 5 0.12
2004-07-05 20:00:00 2004-07-08 00:00:00	Rc:NDF Tc:NDF Qp:NDF	NDF	NP	NDF	0.33 4 1.2
2004-07-08 13:00:00 2004-07-09 22:00:00	Rc:0.01 Tc:1 Qp:0.03	NP	NP	0.16 10 0.33	0.71 1 5.89
2004-07-10 03:00:00 2004-07-12 12:00:00	Rc:0.01 Tc:1 Qp:0.02	0.07 12 0.16	NP	0.36 35 0.32	NDF
2004-07-15 00:00:00 2004-07-17 16:00:00	Rc:0.01 Tc:2 Qp:0.01	NDF	NDF	NDF	NDF
2004-07-23 20:00:00 2004-07-25 10:00:00	Rc:0.01 Tc:1 Qp:0.09	NDF	NDF	NDF	0.53 2 5.48
2004-08-12 08:00:00 2004-08-14 06:00:00	Rc:NP Tc:NP Qp:NP	NDF	NP	0.06 6 0.12	0.1 8 0.31
2004-08-14 11:00:00 2004-08-16 07:00:00	Rc:NP Tc:NP Qp:NP	NP	NP	NP	0.38 5 0.88
2004-08-19 17:00:00 2004-08-23 07:00:00	Rc:NDF Tc:NDF Qp:NDF	0.07 20 0.07	0.01 5 0.02	0.08 4 0.17	0.18 10 0.28
2004-08-25 23:00:00 2004-08-28 06:00:00	Rc:NDF Tc:NDF Qp:NDF	0.03 5 0.1	NP	0.04 4 0.17	0.44 4 0.9

Appendix A3

Event start Event end (yyyy-mm-dd hh)	HOAL	Wimitzbach	Perschling	Gail	Dornbirnerach
2004-08-29 10:00:00 2004-09-02 15:00:00	Rc:NDF Tc:NDF Qp:NDF	0.05 15 0.09	0.01 3 0.06	0.11 10 0.19	0.28 10 0.3
2004-09-12 01:00:00 2004-09-13 18:00:00	Rc:NP Tc:NP Qp:NP	NDF	NDF	NDF	0.22 5 0.64
2004-09-14 11:00:00 2004-09-18 20:00:00	Rc:NDF Tc:NDF Qp:NDF	0.06 8 0.11	0.01 10 0.01	0.07 10 0.16	0.12 7 0.14
2004-09-23 07:00:00 2004-09-26 11:00:00	Rc:0 Tc:3 Qp:0.01	NDF	0.02 4 0.07	NP	0.49 4 1.99
2004-10-08 19:00:00 2004-10-12 13:00:00	Rc:0.01 Tc:1 Qp:0.05	0.05 20 0.06	0.01 4 0.03	0.04 5 0.08	0.18 5 0.41
2004-11-05 03:00:00 2004-11-06 18:00:00	Rc:NP Tc:NP Qp:NP	NP	NDF	NP	0.08 4 0.15
2004-11-19 07:00:00 2004-11-20 10:00:00	Rc:NDF Tc:NDF Qp:NDF	NDF	0.08 1 0.11	NDF	0.82 20 0.11
2004-11-21 21:00:00 2004-11-27 05:00:00	Rc:0.01 Tc:2 Qp:0.02	NP	0.17 30 0.05	NP	0.99 8 0.45
2004-12-25 20:00:00 2004-12-28 16:00:00	Rc:NDF Tc:NDF Qp:NDF	0.07 20 0.06	0.04 10 0.02	NDF	NDF
2005-01-01 18:00:00 2005-01-05 05:00:00	Rc:0.02 Tc:8 Qp:0.02	NP	NDF	NP	0.47 15.44 0.3
2005-01-05 17:00:00 2005-01-07 19:00:00	Rc:0.01 Tc:2 Qp:0.02	NDF	NDF	NP	strange flow
2005-01-20 11:00:00 2005-01-24 05:00:00	Rc:0.08 Tc:4 Qp:0.2	NP	0.09 20 0.04	NP	0.33 25.7 0.17
2005-01-31 02:00:00 2005-02-02 03:00:00	Rc:0.02 Tc:5 Qp:0.02	NP	NDF	NP	NP
2005-02-11 16:00:00 2005-02-14 10:00:00	Rc:0.35 Tc:3 Qp:0.45	NDF	strange flow	NDF	strange flow
2005-03-18 05:00:00 2005-03-21 07:00:00	Rc:0.07 Tc:7 Qp:0.07	NDF	strange flow	NDF	1 18 1.02
2005-03-29 07:00:00 2005-04-02 06:00:00	Rc:NP Tc:NP Qp:NP	0.09 20 0.06	NP	NDF	0.37 11.59 0.81
2005-04-08 12:00:00 2005-04-11 04:00:00	Rc:0.02 Tc:3 Qp:0.02	0.05 12 0.08	NDF	NDF	NDF
2005-04-18 17:00:00 2005-04-23 12:00:00	Rc:0.05 Tc:6 Qp:0.06	0.08 20 0.05	0.15 20 0.1	NDF	0.38 10.66 0.9
2005-04-23 13:00:00 2005-04-28 23:00:00	Rc:0.02 Tc:2 Qp:0.03	NDF	0.06 15 0.05	NDF	0.54 8 0.81

Appendix A3

Event start Event end (yyyy-mm-dd hh)	HOAL	Wimitzbach	Perschling	Gail	Dornbirnerach
2005-05-03 08:00:00 2005-05-04 10:00:00	Rc:NP Tc:NP Qp:NP	NDF	NDF	NDF	0.27 5 1.04
2005-05-07 15:00:00 2005-05-09 19:00:00	Rc:0.01 Tc:1 Qp:0.03	NDF	0.03 10 0.03	NDF	0.48 5 2.39
2005-05-16 13:00:00 2005-05-21 12:00:00	Rc:0.04 Tc:3 Qp:0.16	0.03 7 0.08	0.09 7 0.33	0.28 40 0.2	0.17 7 0.46
2005-05-23 01:00:00 2005-05-25 05:00:00	Rc:0.06 Tc:3 Qp:0.21	NP	0.01 8 0.04	0.17 10 0.23	0.29 8 0.54
2005-05-30 09:00:00 2005-06-01 09:00:00	Rc:0.01 Tc:2 Qp:0.02	NP	0.02 4 0.07	0.26 20 0.14	0.18 5 0.86
2005-06-03 22:00:00 2005-06-07 21:00:00	Rc:0.01 Tc:1 Qp:0.03	0.04 20 0.04	0.03 10 0.05	0.06 20 0.09	0.14 8 0.29
2005-06-06 15:00:00 2005-06-09 10:00:00	Rc:0.04 Tc:1 Qp:0.14	NP	0.04 15 0.03	NP	0.71 3 4.29
2005-06-25 13:00:00 2005-06-27 07:00:00	Rc:0.01 Tc:1 Qp:0.05	0.01 1 0.22	0.05 3 0.02	NP	0.08 20 0.05
2005-06-29 15:00:00 2005-07-02 20:00:00	Rc:NDF Tc:NDF Qp:NDF	0.04 12 0.05	0.01 2 0.1	0.05 10 0.1	0.16 3 1.03
2005-07-04 14:00:00 2005-07-06 19:00:00	Rc:0.01 Tc:2 Qp:0.02	0.04 15 0.07	0.03 10 0.03	0.05 15 0.09	0.17 6 0.61
2005-07-06 16:00:00 2005-07-09 16:00:00	Rc:0.02 Tc:1 Qp:0.1	0.1 15 0.25	0.05 18 0.06	0.11 12 0.24	0.2 6 0.5
2005-07-09 07:00:00 2005-07-12 20:00:00	Rc:0.13 Tc:2 Qp:0.94	0.12 12 0.14	0.15 4 0.68	NP	0.32 3 1.36
2005-07-18 12:00:00 2005-07-20 02:00:00	Rc:0.02 Tc:1 Qp:0.07	0.11 15 0.08	NDF	0.13 5 0.34	0.21 5 0.77
2005-07-20 23:00:00 2005-07-21 19:00:00	Rc:0.03 Tc:3 Qp:0.03	NP	NP	NP	0.23 5 0.86
2005-07-25 07:00:00 2005-07-27 16:00:00	Rc:NP Tc:NP Qp:NP	0.05 6 0.08	NP	0.07 4 0.18	0.34 10 0.62
2005-08-02 13:00:00 2005-08-05 14:00:00	Rc:0.01 Tc:1 Qp:0.02	0.05 20 0.07	0.04 15 0.02	NDF	0.54 5 1.17
2005-08-14 10:00:00 2005-08-19 01:00:00	Rc:0.03 Tc:3 Qp:0.12	0.04 5 0.12	0.09 6 0.27	0.06 3 0.21	0.7 5 1.66
2005-08-18 15:00:00 2005-08-21 15:00:00	Rc:0.06 Tc:3 Qp:0.38	NP	NP	0.61 38 0.06	1 1 7.84
2005-08-21 02:00:00 2005-08-23 21:00:00	Rc:0.06 Tc:2 Qp:0.14	NDF	0.17 2 1.33	0.14 15 0.25	0.9 1 16.71

Appendix A3

Event start Event end (yyyy-mm-dd hh)	HOAL	Wimitzbach	Perschling	Gail	Dornbirnerach
2005-09-09 00:00:00 2005-09-12 01:00:00	Rc:NP Tc:NP Qp:NP	NP	NP	0.08 7 0.3	0.17 10 0.35
2005-09-16 15:00:00 2005-09-19 06:00:00	Rc:MQ Tc:MQ Qp:MQ	NDF	NDF	0.06 8 0.14	0.23 10 0.36
2005-09-29 03:00:00 2005-10-01 14:00:00	Rc:MQ Tc:MQ Qp:MQ	NDF	0.04 10 0.04	0.14 20 0.1	0.3 10 0.44
2005-10-01 11:00:00 2005-10-08 16:00:00	Rc:MQ Tc:MQ Qp:MQ	0.1 20 0.16	NDF	0.29 10 0.9	0.45 4 1.35
2005-11-16 04:00:00 2005-11-18 06:00:00	Rc:MQ Tc:MQ Qp:MQ	NP	NP	NP	0.08 21 0.08
2005-12-15 23:00:00 2005-12-18 08:00:00	Rc:0.06 Tc:12 Qp:0.07	NP	strange flow	NP	NDF
2006-03-08 14:00:00 2006-03-13 10:00:00	Rc:NDF Tc:NDF Qp:NDF	NP	0.37 20 0.2	NP	1 5 1.73
2006-03-28 09:00:00 2006-04-01 11:00:00	Rc:0 Tc:0.5 Qp:0	0.08 12 0.12	0.3 7 0.67	NDF	1 6 2.12
2006-04-27 10:00:00 2006-04-30 14:00:00	Rc:0.02 Tc:1.5 Qp:0.08	NDF	0.05 10 0.07	NDF	0.97 2 5.32
2006-04-28 16:00:00 2006-05-02 11:00:00	Rc:0.09 Tc:18 Qp:0.07	NDF	0.31 8 0.56	NDF	NDF
2006-05-17 01:00:00 2006-05-23 04:00:00	Rc:0.02 Tc:2 Qp:0.03	0.06 18 0.1	0.02 2 0.09	0.3 25 0.51	0.27 6 0.48
2006-05-26 15:00:00 2006-05-29 06:00:00	Rc:0.02 Tc:2 Qp:0.03	NDF	0.12 1.5 0.27	NP	0.42 7 0.53
2006-05-27 21:00:00 2006-05-31 08:00:00	Rc:0.04 Tc:8 Qp:0.06	0.13 30 0.07	0.1 5 0.09	0.3 30 0.26	1 2 6.37
2006-06-02 13:00:00 2006-06-05 12:00:00	Rc:0.04 Tc:5 Qp:0.11	NDF	0.28 7 0.9	NDF	0.67 7 0.94
2006-06-15 21:00:00 2006-06-21 13:00:00	Rc:0.01 Tc:2 Qp:0.03	NDF	0.09 10 0.06	0.21 29.79 0.18	NDF
2006-06-21 09:00:00 2006-06-24 03:00:00	Rc:0.01 Tc:3 Qp:0.03	NDF	0.06 3 0.14	0.04 4 0.14	0.05 6 0.16
2006-06-27 15:00:00 2006-06-30 17:00:00	Rc:0.02 Tc:3 Qp:0.1	0.02 4 0.07	0.02 2 0.09	0.07 4 0.24	NDF
2006-07-01 11:00:00 2006-07-02 22:00:00	Rc:0.03 Tc:2 Qp:0.02	NP	NP	NP	NP
2006-07-06 07:00:00 2006-07-09 10:00:00	Rc:NP Tc:NP Qp:NP	NDF	NP	0.05 3 0.16	0.36 4 1.36

Appendix A3

Event start Event end (yyyy-mm-dd hh)	HOAL	Wimitzbach	Perschling	Gail	Dornbirnerach
2006-07-11 22:00:00 2006-07-12 13:00:00	Rc:NP Tc:NP Qp:NP	0.08 5 0.08	NP	NP	0.09 1 2.09
2006-07-14 08:00:00 2006-07-16 06:00:00	Rc:0.01 Tc:1 Qp:0.03	NDF	0.05 5 0.05	NP	NP
2006-07-23 13:00:00 2006-07-24 12:00:00	Rc:NP Tc:NP Qp:NP	NDF	0.06 13 0.02	0.03 2 0.15	NP
2006-07-28 10:00:00 2006-07-30 17:00:00	Rc:NP Tc:NP Qp:NP	NDF	NDF	0.04 4 0.12	0.05 2 0.18
2006-07-31 16:00:00 2006-08-02 22:00:00	Rc:0.02 Tc:1 Qp:0.04	NDF	NDF	NDF	0.24 4 0.62
2006-08-02 19:00:00 2006-08-05 23:00:00	Rc:0.01 Tc:2 Qp:0.04	0.03 3 0.08	0.02 2 0.11	0.15 3 0.72	0.49 3 2.2
2006-08-05 15:00:00 2006-08-06 22:00:00	Rc:0.02 Tc:3 Qp:0.03	NP	0.05 6 0.1	NP	1 1 11.06
2006-08-06 16:00:00 2006-08-09 15:00:00	Rc:0.02 Tc:4 Qp:0.06	NP	0.18 1 1.72	NP	1 3 4.18
2006-08-11 04:00:00 2006-08-15 14:00:00	Rc:0.02 Tc:3 Qp:0.07	0.04 15 0.04	0.08 9 0.1	NDF	0.45 9 1.03
2006-08-20 00:00:00 2006-08-21 22:00:00	Rc:0.01 Tc:1 Qp:0.02	NDF	0.03 5 0.13	0.44 10 0.14	0.24 6 0.55
2006-08-22 02:00:00 2006-08-24 03:00:00	Rc:NP Tc:NP Qp:NP	NP	NDF	NP	0.51 20 0.18
2006-08-24 09:00:00 2006-08-26 15:00:00	Rc:0.01 Tc:3 Qp:0.02	NDF	NDF	0.07 6 0.17	0.38 10 0.42
2006-08-26 14:00:00 2006-08-28 14:00:00	Rc:NP Tc:NP Qp:NP	0.03 15 0.03	NP	0.24 20 0.23	0.35 4 0.93
2006-08-28 13:00:00 2006-09-01 22:00:00	Rc:0.02 Tc:2 Qp:0.02	0.02 10 0.04	NDF	0.55 40 0.23	0.59 3 3.68
2006-09-07 15:00:00 2006-09-10 14:00:00	Rc:0.01 Tc:1 Qp:0.03	NP	0.04 7 0.15	0.03 4 0.16	0.3 2 1.9
2006-09-15 04:00:00 2006-09-17 22:00:00	Rc:NP Tc:NP Qp:NP	NDF	NP	0.05 4 0.34	0.49 1 4.3
2006-09-17 23:00:00 2006-09-20 10:00:00	Rc:0.01 Tc:1 Qp:0.09	NDF	MP	NP	0.75 3 3.45
2006-09-25 14:00:00 2006-09-27 22:00:00	Rc:NDF Tc:NDF Qp:NDF	NP	NDF	NP	0.23 5 0.84
2006-10-29 01:00:00 2006-10-31 01:00:00	Rc:0.01 Tc:1 Qp:0.06	NP	NP	NP	0.33 15 0.29

Appendix A3

Event start Event end (yyyy-mm-dd hh)	HOAL	Wimitzbach	Perschling	Gail	Dornbirnerach
2006-10-31 23:00:00 2006-11-02 23:00:00	Rc:NDF Tc:NDF Qp:NDF	NP	NP	NP	0.27 10 0.45
2006-11-04 21:00:00 2006-11-11 09:00:00	Rc:0.04 Tc:10 Qp:0.06	NP	NP	NP	0.55 13.68 0.27
2006-11-11 17:00:00 2006-11-16 18:00:00	Rc:0.02 Tc:3 Qp:0.03	NP	NP	NP	0.48 7 0.82
2006-11-21 12:00:00 2006-11-25 06:00:00	Rc:0.08 Tc:38.32 Qp:0.03	0.04 25 0.04	0.07 55 0.02	NP	0.26 15 0.12
2006-12-04 18:00:00 2006-12-06 08:00:00	Rc:NP Tc:NP Qp:NP	NP	NP	NP	0.4 12 0.21
2006-12-06 05:00:00 2006-12-11 18:00:00	Rc:NDF Tc:NDF Qp:NDF	0.06 50 0.02	NDF	0.05 5 0.07	0.16 5 0.48
2006-12-17 02:00:00 2006-12-20 04:00:00	Rc:NDF Tc:NDF Qp:NDF	NDF	NP	NDF	1 15.35 0.25
2007-01-01 01:00:00 2007-01-04 01:00:00	Rc:0.06 Tc:10 Qp:0.06	NDF	NDF	NDF	0.66 1 1.84
2007-01-06 21:00:00 2007-01-11 03:00:00	Rc:NDF Tc:NDF Qp:NDF	NDF	NDF	NDF	0.67 5 1.66
2007-01-18 16:00:00 2007-01-25 06:00:00	Rc:0.08 Tc:4 Qp:0.21	NDF	0.05 45 0.02	NDF	strange flow
2007-02-07 23:00:00 2007-02-10 17:00:00	Rc:NDF Tc:NDF Qp:NDF	NDF	NDF	NDF	0.39 15 0.13
2007-02-10 15:00:00 2007-02-14 01:00:00	Rc:NDF Tc:NDF Qp:NDF	NDF	NP	NDF	0.43 8 0.52
2007-02-14 19:00:00 2007-02-16 18:00:00	Rc:NDF Tc:NDF Qp:NDF	NP	NDF	NP	0.48 4 1.81
2007-02-27 17:00:00 2007-03-01 13:00:00	Rc:0.08 Tc:8 Qp:0.08	NDF	NDF	NDF	0.98 7 0.56
2007-03-01 14:00:00 2007-03-03 05:00:00	Rc:0.12 Tc:10 Qp:0.07	NDF	NDF	NDF	0.53 10 1.05
2007-03-03 00:00:00 2007-03-06 13:00:00	Rc:0.06 Tc:5 Qp:0.11	NP	NDF	NDF	1 5 1.27
2007-03-07 23:00:00 2007-03-12 13:00:00	Rc:0.08 Tc:16 Qp:0.07	0.12 80 0.02	0.11 50 0.03	NDF	NDF
2007-03-19 20:00:00 2007-03-22 05:00:00	Rc:0.06 Tc:15 Qp:0.05	NDF	NDF	NDF	NDF
2007-03-23 11:00:00 2007-03-28 17:00:00	Rc:0.09 Tc:8 Qp:0.13	NDF	0.27 15 0.29	NDF	NDF

Appendix A3

Event start Event end (yyyy-mm-dd hh)	HOAL	Wimitzbach	Perschling	Gail	Dornbirnerach
2007-05-06 01:00:00 2007-05-07 20:00:00	Rc:0.02 Tc:5 Qp:0.02	NP	NDF	NP	0.34 4 0.64
2007-05-08 10:00:00 2007-05-12 06:00:00	Rc:0.02 Tc:3 Qp:0.05	NP	0.04 11 0.1	NP	0.49 7 0.36
2007-05-23 04:00:00 2007-05-25 06:00:00	Rc:NP Tc:NP Qp:NP	0.13 11 0.03	NDF	NP	NP
2007-05-28 10:00:00 2007-06-08 01:00:00	Rc:0.01 Tc:1 Qp:0.02	0.02 10 0.05	0.02 15 0.03	0.18 20 0.22	0.98 5 3.17
2007-06-10 08:00:00 2007-06-14 13:00:00	Rc:0.01 Tc:2 Qp:0.08	NP	NP	NP	0.69 6.14 1.43
2007-06-13 15:00:00 2007-06-17 07:00:00	Rc:0.01 Tc:1 Qp:0.02	NP	NP	0.12 8 0.1	0.29 4 1.38
2007-06-22 02:00:00 2007-06-25 09:00:00	Rc:0.02 Tc:1 Qp:0.21	NP	NP	0.11 9 0.13	0.27 5 0.57
2007-06-25 11:00:00 2007-06-28 06:00:00	Rc:0.01 Tc:1 Qp:0.07	NP	NP	0.08 3 0.42	0.42 4 1.35
2007-07-02 04:00:00 2007-07-03 15:00:00	Rc:0.01 Tc:1 Qp:0.03	NP	NP	0.14 15 0.2	0.41 12 0.38
2007-07-03 13:00:00 2007-07-06 18:00:00	Rc:NDF Tc:NDF Qp:NDF	NDF	NDF	0.15 7 0.3	0.59 13 0.83
2007-07-09 01:00:00 2007-07-13 13:00:00	Rc:0.01 Tc:2 Qp:0.02	0.03 20 0.05	MP	0.19 10 0.49	0.54 4 1.85
2007-07-21 23:00:00 2007-07-23 00:00:00	Rc:NP Tc:NP Qp:NP	NP	NP	NP	0.15 7 0.34
2007-07-23 16:00:00 2007-07-25 10:00:00	Rc:0 Tc:1 Qp:0.01	NDF	0.01 8 0.01	NDF	0.29 2 1.47
2007-07-29 11:00:00 2007-08-01 10:00:00	Rc:0 Tc:1 Qp:0.01	0.02 10 0.04	0.01 2 0.01	NDF	0.59 2 6.45
2007-08-02 13:00:00 2007-08-05 05:00:00	Rc:0.01 Tc:1 Qp:0.02	NDF	NDF	NDF	0.23 2 1.16
2007-08-07 13:00:00 2007-08-10 15:00:00	Rc:0 Tc:1 Qp:0.04	NP	strange flow	0.06 7 0.17	0.81 2 8.15
2007-08-11 02:00:00 2007-08-13 07:00:00	Rc:0.01 Tc:2 Qp:0.05	NDF	0.01 2 0.05	NDF	NDF
2007-08-15 07:00:00 2007-08-19 15:00:00	Rc:0.01 Tc:2 Qp:0.02	NDF	NDF	0.05 3 0.15	0.35 10 0.76
2007-08-19 15:00:00 2007-08-22 11:00:00	Rc:0.01 Tc:1 Qp:0.01	NDF	0.01 12 0.01	0.15 12 0.36	NDF

Appendix A3

Event start Event end (yyyy-mm-dd hh)	HOAL	Wimitzbach	Perschling	Gail	Dornbirnerach
2007-08-29 02:00:00 2007-08-31 22:00:00	Rc:0.01 Tc:2 Qp:0.01	MP	NDF	NDF	0.49 4 1.27
2007-09-01 05:00:00 2007-09-02 14:00:00	Rc:0.01 Tc:1 Qp:0.03	NP	0.01 10 0.01	NP	NDF
2007-09-05 19:00:00 2007-09-08 22:00:00	Rc:0.09 Tc:2 Qp:0.75	NP	0.13 2 1.88	NP	NDF
2007-09-10 22:00:00 2007-09-13 11:00:00	Rc:0.14 Tc:2 Qp:0.84	NP	0.15 15 0.15	NP	0.33 5 0.55
2007-09-17 22:00:00 2007-09-20 07:00:00	Rc:0.01 Tc:2 Qp:0.02	0.02 15 0.03	NP	0.06 8 0.11	0.63 3 3.4
2007-09-26 06:00:00 2007-09-29 23:00:00	Rc:0.03 Tc:5 Qp:0.02	0.02 6 0.06	0.03 12 0.02	NDF	0.56 8 1.05
2007-10-23 00:00:00 2007-10-26 10:00:00	Rc:0.04 Tc:5 Qp:0.05	NP	0.12 10 0.21	NP	NDF
2007-10-27 12:00:00 2007-11-02 14:00:00	Rc:0.07 Tc:12 Qp:0.07	NP	0.27 8 1.04	0.07 6 0.1	0.31 15 0.26
2007-11-07 14:00:00 2007-11-09 21:00:00	Rc:0.11 Tc:5 Qp:0.19	NDF	NDF	NP	0.66 15 0.35
2007-11-11 00:00:00 2007-11-14 03:00:00	Rc:0.18 Tc:2 Qp:0.65	NDF	0.17 12 0.15	NDF	LRC
2007-11-24 03:00:00 2007-11-26 19:00:00	Rc:NDF Tc:NDF Qp:NDF	NDF	MP	0.14 9 0.28	strange flow
2007-12-02 18:00:00 2007-12-03 23:00:00	Rc:NDF Tc:NDF Qp:NDF	NP	NDF	NP	0.29 2 0.71
2007-12-11 15:00:00 2007-12-15 11:00:00	Rc:0.12 Tc:10 Qp:0.14	NDF	0.34 8 0.58	NP	NDF
2008-01-07 02:00:00 2008-01-09 06:00:00	Rc:NDF Tc:NDF Qp:NDF	NP	NDF	NP	1 8 1.5
2008-01-18 07:00:00 2008-01-23 06:00:00	Rc:0.18 Tc:15 Qp:0.06	NDF	0.27 20 0.08	NDF	strange flow
2008-01-22 01:00:00 2008-01-23 23:00:00	Rc:0.06 Tc:6 Qp:0.04	NP	NDF	NDF	0.16 12 0.18
2008-01-27 01:00:00 2008-01-29 15:00:00	Rc:0.09 Tc:15 Qp:0.06	NP	NDF	NDF	NDF
2008-02-06 01:00:00 2008-02-11 11:00:00	Rc:NDF Tc:NDF Qp:NDF	NP	NP	NP	0.75 25 0.18
2008-02-27 05:00:00 2008-02-28 11:00:00	Rc:NDF Tc:NDF Qp:NDF	NP	NP	NDF	0.95 5 0.96

Appendix A3

Event start Event end (yyyy-mm-dd hh)	HOAL	Wimitzbach	Perschling	Gail	Dornbirnerach
2008-03-01 00:00:00 2008-03-04 20:00:00	Rc:0.07 Tc:13 Qp:0.07	NDF	NDF	NDF	strange flow
2008-03-11 23:00:00 2008-03-13 15:00:00	Rc:0.03 Tc:3 Qp:0.04	NDF	NDF	NDF	1 4 1.63
2008-03-13 15:00:00 2008-03-16 19:00:00	Rc:0.08 Tc:12 Qp:0.08	NDF	0.11 3 0.2	NDF	0.84 5 0.97
2008-03-17 07:00:00 2008-03-18 22:00:00	Rc:0.03 Tc:5 Qp:0.04	NP	NDF	NP	0.61 5 1.53
2008-04-01 23:00:00 2008-04-05 10:00:00	Rc:0.03 Tc:5 Qp:0.05	NP	NDF	NDF	0.49 9.25 0.68
2008-04-21 10:00:00 2008-04-23 23:00:00	Rc:0.01 Tc:1 Qp:0.1	NDF	0.03 12 0.04	0.1 12 0.13	0.77 7 4.79
2008-04-22 12:00:00 2008-04-27 14:00:00	Rc:0.05 Tc:5 Qp:0.08	NDF	0.1 18 0.09	NDF	0.92 8 1.37
2008-04-28 10:00:00 2008-04-30 09:00:00	Rc:0.04 Tc:5 Qp:0.03	NDF	NP	0.48 35 0.14	0.59 5 2.32
2008-05-05 09:00:00 2008-05-07 20:00:00	Rc:0.03 Tc:4 Qp:0.06	NDF	0.03 6 0.05	NDF	melt wave
2008-05-17 09:00:00 2008-05-26 23:00:00	Rc:0.02 Tc:3 Qp:0.03	0.03 40 0.03	0.05 30 0.05	0.36 15 0.67	0.26 19.6 0.41
2008-06-02 08:00:00 2008-06-06 00:00:00	Rc:0.01 Tc:0.5 Qp:0.08	0.01 2 0.12	0.03 6 0.03	NDF	0.3 6 0.76
2008-06-07 05:00:00 2008-06-11 07:00:00	Rc:0.01 Tc:1.5 Qp:0.03	0.06 15 0.04	0.05 3 0.14	NDF	0.16 4 0.73
2008-06-11 09:00:00 2008-06-14 10:00:00	Rc:NDF Tc:NDF Qp:NDF	NDF	0.03 4 0.07	NDF	0.55 4 2.1
2008-06-23 16:00:00 2008-06-25 11:00:00	Rc:NP Tc:NP Qp:NP	0.04 7 0.05	0.01 4 0.03	0.26 9 0.18	NP
2008-06-25 17:00:00 2008-06-27 16:00:00	Rc:0.01 Tc:1 Qp:0.03	NDF	0.02 3 0.07	0.11 7 0.14	0.08 8 0.07
2008-06-26 13:00:00 2008-06-29 01:00:00	Rc:0.01 Tc:1 Qp:0.04	0.05 25 0.04	0.03 10 0.06	0.24 10 0.17	NP
2008-06-29 16:00:00 2008-07-02 14:00:00	Rc:0.01 Tc:2 Qp:0.05	NDF	0.02 6 0.04	0.1 8 0.22	NDF
2008-07-02 11:00:00 2008-07-05 09:00:00	Rc:0.01 Tc:3 Qp:0.02	NDF	NP	0.04 4 0.17	0.08 6 0.2
2008-07-06 12:00:00 2008-07-09 11:00:00	Rc:0.01 Tc:1 Qp:0.05	NDF	0.01 4 0.02	0.06 8 0.14	0.18 4 0.5

Appendix A3

Event start Event end (yyyy-mm-dd hh)	HOAL	Wimitzbach	Perschling	Gail	Dornbirnerach
2008-07-12 09:00:00 2008-07-14 02:00:00	Rc:0.02 Tc:1 Qp:0.16	NP	0.01 3 0.05	0.16 4 0.16	0.66 1 7.03
2008-07-13 14:00:00 2008-07-17 06:00:00	Rc:0.04 Tc:1 Qp:0.03	0.05 20 0.05	0.03 15 0.03	0.65 20 0.22	0.97 2 7.04
2008-07-16 15:00:00 2008-07-19 16:00:00	Rc:0.01 Tc:3 Qp:0.03	0.04 20 0.04	0.05 10 0.06	0.11 5 0.23	0.45 3 3.77
2008-07-19 23:00:00 2008-07-23 02:00:00	Rc:0.01 Tc:2 Qp:0.04	0.05 20 0.05	0.06 6 0.14	0.16 8 0.22	0.47 5 1.5
2008-07-23 06:00:00 2008-07-28 01:00:00	Rc:0.04 Tc:2 Qp:0.26	NDF	0.24 6 0.84	0.17 12 0.12	0.11 6 0.16
2008-07-30 16:00:00 2008-08-03 00:00:00	Rc:NP Tc:NP Qp:NP	NDF	strange flow	0.16 3 0.24	0.07 6 0.14
2008-08-04 17:00:00 2008-08-07 14:00:00	Rc:NDF Tc:NDF Qp:NDF	NP	NDF	0.04 2 0.16	0.12 8 0.21
2008-08-07 18:00:00 2008-08-14 08:00:00	Rc:0.01 Tc:1 Qp:0.03	0.03 20 0.04	0.04 10 0.04	0.08 6 0.24	0.2 4 0.67
2008-08-14 22:00:00 2008-08-17 18:00:00	Rc:0.03 Tc:2 Qp:0.15	0.04 19 0.07	0.07 4 0.37	0.14 15 0.23	0.47 5 2.88
2008-08-22 15:00:00 2008-08-23 12:00:00	Rc:NP Tc:NP Qp:NP	NP	NP	NP	0.25 10 0.33
2008-08-23 06:00:00 2008-08-25 08:00:00	Rc:NP Tc:NP Qp:NP	NDF	NP	0.07 5 0.24	0.54 5 1.01
2008-09-01 09:00:00 2008-09-02 14:00:00	Rc:0.02 Tc:2 Qp:0.02	NP	0.01 4 0.03	0.03 3 0.16	0.16 3 0.14
2008-09-06 20:00:00 2008-09-08 19:00:00	Rc:0.01 Tc:1 Qp:0.04	NDF	0.02 4 0.02	NDF	0.32 4 1.27
2008-09-12 14:00:00 2008-09-18 15:00:00	Rc:0.02 Tc:6 Qp:0.05	0.07 20 0.08	0.1 6 0.46	NDF	0.46 4 1.22
2008-09-25 01:00:00 2008-09-28 17:00:00	Rc:NDF Tc:NDF Qp:NDF	NP	0.18 14 0.09	NP	NP
2008-10-03 02:00:00 2008-10-06 12:00:00	Rc:0.03 Tc:2 Qp:0.05	0.04 30 0.05	0.04 1 0.14	0.1 20 0.1	0.22 10 0.25
2008-11-07 19:00:00 2008-11-09 18:00:00	Rc:0.03 Tc:15 Qp:0.02	NDF	strange flow	NP	NP
2008-11-11 13:00:00 2008-11-15 16:00:00	Rc:0.02 Tc:2 Qp:0.02	NDF	NDF	NDF	0.35 45 0.15
2008-11-16 13:00:00 2008-11-19 05:00:00	Rc:0.01 Tc:2 Qp:0.02	NP	NDF	NDF	0.45 9 0.43

Appendix A3

Event start Event end (yyyy-mm-dd hh)	HOAL	Wimitzbach	Perschling	Gail	Dornbirnerach
2008-11-20 04:00:00 2008-11-23 13:00:00	Rc:0.03 Tc:5 Qp:0.06	NP	0.06 13 0.07	NDF	0.35 8 0.64
2008-11-30 20:00:00 2008-12-03 15:00:00	Rc:NDF Tc:NDF Qp:NDF	0.13 15 0.07	NDF	NDF	0.22 30 0.1
2008-12-20 02:00:00 2008-12-22 16:00:00	Rc:0.12 Tc:5 Qp:0.26	NDF	strange flow	NDF	1 2 3.66
2009-01-19 19:00:00 2009-01-26 10:00:00	Rc:NDF Tc:NDF Qp:NDF	NDF	strange flow	0.54 40 0.09	0.12 9 0.14
2009-01-23 07:00:00 2009-01-26 04:00:00	Rc:NDF Tc:NDF Qp:NDF	NP	0.31 30 0.05	NP	0.65 10 0.29
2009-02-26 11:00:00 2009-03-05 03:00:00	Rc:0.44 Tc:8 Qp:0.44	NDF	strange flow	NDF	0.46 30 0.29
2009-03-06 14:00:00 2009-03-09 08:00:00	Rc:0.13 Tc:8 Qp:0.22	NDF	0.28 7 0.54	NP	NDF
2009-03-12 17:00:00 2009-03-18 22:00:00	Rc:0.15 Tc:10 Qp:0.18	NDF	MP	NDF	0.67 18 0.59
2009-03-23 17:00:00 2009-03-25 00:00:00	Rc:NDF Tc:NDF Qp:NDF	NP	0.35 20 0.14	NP	0.16 5 0.21
2009-03-28 21:00:00 2009-04-02 12:00:00	Rc:0.15 Tc:5 Qp:0.34	NDF	0.23 15 0.33	0.29 30 0.15	NDF
2009-05-03 22:00:00 2009-05-05 09:00:00	Rc:0.04 Tc:3 Qp:0.04	NP	NP	NDF	0.59 3 2.32
2009-05-11 13:00:00 2009-05-15 10:00:00	Rc:0.02 Tc:2 Qp:0.04	NDF	0.02 5 0.04	NDF	0.22 15 0.29
2009-05-18 13:00:00 2009-05-20 09:00:00	Rc:0.01 Tc:1 Qp:0.07	NDF	0.02 3 0.03	NDF	NDF
2009-05-26 13:00:00 2009-05-28 06:00:00	Rc:NP Tc:NP Qp:NP	NDF	0.01 7 0.02	NDF	0.29 3 1.93
2009-05-28 18:00:00 2009-05-29 17:00:00	Rc:0.03 Tc:4 Qp:0.03	NP	0.01 2 0.02	NP	0.1 6 0.16
2009-05-29 23:00:00 2009-05-31 12:00:00	Rc:0.01 Tc:1 Qp:0.03	NDF	0.08 6 0.25	NP	NP
2009-06-02 07:00:00 2009-06-04 16:00:00	Rc:NP Tc:NP Qp:NP	NDF	0.1 8 0.13	NDF	NDF
2009-06-06 06:00:00 2009-06-07 11:00:00	Rc:NP Tc:NP Qp:NP	NDF	NP	NDF	0.27 3 1.62
2009-06-07 16:00:00 2009-06-08 23:00:00	Rc:NP Tc:NP Qp:NP	NP	NP	NDF	0.31 4 0.51

Appendix A3

Event start Event end (yyyy-mm-dd hh)	HOAL	Wimitzbach	Perschling	Gail	Dornbirnerach
2009-06-15 16:00:00 2009-06-19 01:00:00	Rc:NP Tc:NP Qp:NP	0.05 25 0.05	NP	NP	0.48 2 5.25
2009-06-18 19:00:00 2009-06-23 05:00:00	Rc:0.01 Tc:2 Qp:0.07	0.04 50 0.05	0.02 5 0.05	0.09 5 0.47	0.33 3 1.47
2009-06-22 01:00:00 2009-06-25 16:00:00	Rc:0.1 Tc:1 Qp:0.94	0.06 25 0.05	0.28 2 2.68	NDF	0.57 3 2.74
2009-06-26 10:00:00 2009-06-28 19:00:00	Rc:0.04 Tc:3 Qp:0.18	NDF	0.28 2 1.1	NDF	0.38 5 0.55
2009-06-27 18:00:00 2009-06-30 07:00:00	Rc:0.09 Tc:2 Qp:0.64	NDF	0.43 5 1.44	NDF	NP
2009-07-04 21:00:00 2009-07-06 12:00:00	Rc:NP Tc:NP Qp:NP	NP	NP	0.08 6 0.13	0.25 1 5.01
2009-07-06 03:00:00 2009-07-07 09:00:00	Rc:0.01 Tc:1 Qp:0.04	NP	0.16 1 3.49	NP	0.31 5 0.59
2009-07-07 12:00:00 2009-07-09 13:00:00	Rc:0.02 Tc:3 Qp:0.04	0.04 8 0.05	0.2 8 0.43	0.07 8 0.15	0.6 4 1.26
2009-07-15 08:00:00 2009-07-16 15:00:00	Rc:0.01 Tc:1 Qp:0.06	NP	NP	NP	0.28 5 0.22
2009-07-17 05:00:00 2009-07-21 13:00:00	Rc:0.03 Tc:3 Qp:0.13	0.07 25 0.08	0.06 4 0.25	0.07 5 0.44	0.62 2 5.29
2009-07-23 09:00:00 2009-07-27 14:00:00	Rc:0.02 Tc:2 Qp:0.05	NDF	0.07 7.24 0.17	0.07 5 0.14	0.55 4.58 3.49
2009-07-27 19:00:00 2009-07-29 01:00:00	Rc:NP Tc:NP Qp:NP	NP	NP	NDF	0.55 2 4.97
2009-08-03 14:00:00 2009-08-06 07:00:00	Rc:0.02 Tc:3 Qp:0.06	NDF	0.04 12 0.08	0.04 7 0.14	0.5 2 6.43
2009-08-08 12:00:00 2009-08-09 17:00:00	Rc:NP Tc:NP Qp:NP	NP	NP	NP	0.21 2 0.94
2009-08-10 07:00:00 2009-08-12 09:00:00	Rc:0.03 Tc:8 Qp:0.11	NP	NP	0.12 25 0.09	0.22 6 0.52
2009-08-13 05:00:00 2009-08-15 13:00:00	Rc:0.02 Tc:2 Qp:0.04	NDF	0.05 15 0.03	0.15 27 0.09	NP
2009-08-21 16:00:00 2009-08-24 15:00:00	Rc:0.03 Tc:8 Qp:0.12	NDF	0.02 4 0.05	0.09 10 0.12	0.09 5 0.2
2009-08-28 13:00:00 2009-08-31 07:00:00	Rc:0.05 Tc:7 Qp:0.14	NDF	0.02 7 0.07	0.04 4 0.11	0.1 8 0.15
2009-09-01 20:00:00 2009-09-02 11:00:00	Rc:NP Tc:NP Qp:NP	NP	NP	NP	0.26 2 1.61

Appendix A3

Event start Event end (yyyy-mm-dd hh)	HOAL	Wimitzbach	Perschling	Gail	Dornbirnerach
2009-09-02 14:00:00 2009-09-03 12:00:00	Rc:NP Tc:NP Qp:NP	NP	NP	0.04 4 0.08	0.19 3 1.08
2009-09-03 10:00:00 2009-09-07 13:00:00	Rc:0.04 Tc:13 Qp:0.06	NDF	0.05 20 0.03	0.09 20 0.09	0.46 5 0.88
2009-09-13 18:00:00 2009-09-15 19:00:00	Rc:NDF Tc:NDF Qp:NDF	NDF	NDF	MP	0.13 6 0.22
2009-09-17 01:00:00 2009-09-19 08:00:00	Rc:0.02 Tc:4 Qp:0.06	NDF	NDF	0.36 15 0.3	NDF
2009-10-10 17:00:00 2009-10-11 19:00:00	Rc:MQ Tc:MQ Qp:MQ	MP	NP	0.09 7 0.08	0.27 3 0.61
2009-10-12 03:00:00 2009-10-14 22:00:00	Rc:MQ Tc:MQ Qp:MQ	MP	0.01 3 0.02	NP	0.39 3 1.39
2009-11-02 05:00:00 2009-11-06 07:00:00	Rc:MQ Tc:MQ Qp:MQ	NDF	0.05 16 0.04	NDF	0.5 5 1.36
2009-11-17 21:00:00 2009-11-19 08:00:00	Rc:MQ Tc:MQ Qp:MQ	NP	NP	NDF	0.36 4 1.82
2009-12-07 01:00:00 2009-12-09 23:00:00	Rc:MQ Tc:MQ Qp:MQ	NDF	NDF	NDF	1 7 1.55
2009-12-10 06:00:00 2009-12-14 23:00:00	Rc:MQ Tc:MQ Qp:MQ	NP	0.08 10 0.05	NP	1 5 1.55
2009-12-24 10:00:00 2009-12-27 09:00:00	Rc:MQ Tc:MQ Qp:MQ	0.11 30 0.07	strange flow	0.31 10 0.29	0.93 10 0.89
2009-12-29 16:00:00 2010-01-01 05:00:00	Rc:MQ Tc:MQ Qp:MQ	NP	NP	NP	0.66 4 1.91
2010-01-01 21:00:00 2010-01-03 17:00:00	Rc:0.24 Tc:25 Qp:0.04	NP	NP	NP	NDF
2010-02-05 06:00:00 2010-02-08 18:00:00	Rc:MQ Tc:MQ Qp:MQ	NP	NP	NP	0.07 7 0.17
2010-02-26 03:00:00 2010-02-28 08:00:00	Rc:0.62 Tc:3 Qp:0.57	NDF	melt wave	NDF	melt wave
2010-03-21 05:00:00 2010-03-23 08:00:00	Rc:NP Tc:NP Qp:NP	NP	NP	NDF	1 9 1.59
2010-03-30 18:00:00 2010-04-01 13:00:00	Rc:0.03 Tc:3 Qp:0.05	NDF	NDF	NDF	NDF
2010-04-13 16:00:00 2010-04-18 01:00:00	Rc:0.09 Tc:8 Qp:0.16	NDF	0.23 6 0.45	NDF	NDF
2010-05-01 10:00:00 2010-05-04 18:00:00	Rc:0.03 Tc:3 Qp:0.04	NDF	0.06 5 0.14	NDF	0.52 7 1.59

Appendix A3

Event start Event end (yyyy-mm-dd hh)	HOAL	Wimitzbach	Perschling	Gail	Dornbirnerach
2010-05-04 22:00:00 2010-05-08 15:00:00	Rc:NP Tc:NP Qp:NP	NDF	NDF	0.36 16 1.02	0.36 7 0.8
2010-05-13 06:00:00 2010-05-15 11:00:00	Rc:0.02 Tc:3 Qp:0.06	NDF	0.12 3 0.72	NDF	0.69 16 0.6
2010-05-15 11:00:00 2010-05-18 11:00:00	Rc:NDF Tc:NDF Qp:NDF	NP	0.3 6 0.98	NP	0.51 10 1.25
2010-05-17 23:00:00 2010-05-18 22:00:00	Rc:0.03 Tc:2 Qp:0.04	NP	NP	NP	0.47 6 0.75
2010-05-20 20:00:00 2010-05-22 12:00:00	Rc:NDF Tc:NDF Qp:NDF	NP	0.27 5 0.73	NP	NDF
2010-05-22 09:00:00 2010-05-24 19:00:00	Rc:0.01 Tc:1 Qp:0.04	NP	0.34 3 1.76	NP	NP
2010-05-26 10:00:00 2010-05-29 12:00:00	Rc:0.01 Tc:1 Qp:0.15	NP	0.02 3 0.12	0.67 45 0.36	0.28 5 0.84
2010-05-30 02:00:00 2010-05-31 22:00:00	Rc:0.03 Tc:4 Qp:0.03	NP	NP	NP	0.76 4 3.24
2010-06-01 18:00:00 2010-06-05 07:00:00	Rc:0.05 Tc:2 Qp:0.29	NP	0.28 4 0.95	NP	0.91 2 5.78
2010-06-12 17:00:00 2010-06-16 00:00:00	Rc:0.02 Tc:2 Qp:0.07	NP	0.06 2 0.76	0.25 20 0.19	0.22 5 0.59
2010-06-15 14:00:00 2010-06-17 19:00:00	Rc:0.05 Tc:6 Qp:0.11	NDF	0.26 5 0.67	0.16 10 0.24	NDF
2010-06-17 18:00:00 2010-06-23 13:00:00	Rc:0.07 Tc:10 Qp:0.07	0.04 20 0.06	0.31 10 0.31	0.29 40 0.22	0.58 1 5.39
2010-06-25 03:00:00 2010-06-26 06:00:00	Rc:0.04 Tc:3 Qp:0.09	NP	NDF	NP	NP
2010-07-11 13:00:00 2010-07-12 07:00:00	Rc:NP Tc:NP Qp:NP	NP	NP	0.03 2 0.13	NP
2010-07-12 14:00:00 2010-07-13 08:00:00	Rc:NP Tc:NP Qp:NP	NP	NP	0.26 8 0.13	NP
2010-07-12 19:00:00 2010-07-14 14:00:00	Rc:NP Tc:NP Qp:NP	NDF	NP	0.04 4 0.15	0.12 4 0.62
2010-07-15 20:00:00 2010-07-16 11:00:00	Rc:0.02 Tc:2 Qp:0.03	NP	0.02 3 0.03	NP	NP
2010-07-17 11:00:00 2010-07-19 12:00:00	Rc:0.01 Tc:2 Qp:0.08	NP	0.04 3 0.22	0.06 15 0.09	0.36 1 5.13
2010-07-23 07:00:00 2010-07-24 23:00:00	Rc:0.01 Tc:2 Qp:0.07	NDF	0.03 3 0.12	0.06 8 0.11	0.5 3 3.39

Appendix A3

Event start Event end (yyyy-mm-dd hh)	HOAL	Wimitzbach	Perschling	Gail	Dornbirnerach
2010-07-24 03:00:00 2010-07-27 06:00:00	Rc:0.04 Tc:4 Qp:0.03	NP	0.08 7 0.16	NP	1 3 5.45
2010-07-27 00:00:00 2010-07-28 05:00:00	Rc:NP Tc:NP Qp:NP	NP	NP	NP	0.66 3 1.63
2010-07-28 19:00:00 2010-07-31 22:00:00	Rc:0.02 Tc:2 Qp:0.06	0.03 40 0.03	0.06 2 0.47	0.06 13 0.08	0.64 3 4.31
2010-08-01 20:00:00 2010-08-02 14:00:00	Rc:NP Tc:NP Qp:NP	NP	NP	NP	0.2 8 0.4
2010-08-02 10:00:00 2010-08-05 10:00:00	Rc:0.04 Tc:15 Qp:0.06	NP	NP	NP	0.59 8 1.01
2010-08-05 06:00:00 2010-08-07 19:00:00	Rc:NP Tc:NP Qp:NP	0.05 23 0.04	0.03 6 0.06	0.04 5 0.13	0.8 2 8.4
2010-08-06 17:00:00 2010-08-09 13:00:00	Rc:0.07 Tc:5 Qp:0.18	NDF	0.24 6 0.77	NDF	NDF
2010-08-12 01:00:00 2010-08-14 18:00:00	Rc:0.02 Tc:2 Qp:0.06	0.03 12 0.05	0.02 3 0.07	0.07 6 0.15	0.18 15 0.18
2010-08-14 14:00:00 2010-08-16 15:00:00	Rc:NP Tc:NP Qp:NP	0.05 10 0.05	NP	0.13 3 0.68	0.31 9 0.45
2010-08-16 10:00:00 2010-08-18 22:00:00	Rc:0.03 Tc:1 Qp:0.03	NP	NP	NP	0.45 6 1.05
2010-08-20 20:00:00 2010-08-21 16:00:00	Rc:NP Tc:NP Qp:NP	NP	NP	NP	1 1 10.37
2010-08-23 12:00:00 2010-08-25 20:00:00	Rc:0.02 Tc:4 Qp:0.06	0.03 15 0.03	0.03 7 0.07	0.04 5 0.18	0.26 5 0.81
2010-08-27 07:00:00 2010-08-29 22:00:00	Rc: Tc: Qp:	0.06 35 0.03	0.11 15 0.04	0.08 5 0.18	0.52 2 4.58
2010-08-28 06:00:00 2010-08-31 23:00:00	Rc:0.04 Tc:5 Qp:0.13	0.08 35 0.03	0.12 35 0.04	0.12 12 0.15	0.74 2 3.02
2010-08-30 01:00:00 2010-09-01 18:00:00	Rc:0.09 Tc:15 Qp:0.05	NP	0.1 15 0.08	NP	1 2 3.25
2010-09-08 11:00:00 2010-09-09 21:00:00	Rc:NP Tc:NP Qp:NP	NP	0.06 15 0.03	NP	0.26 4 0.67
2010-09-12 20:00:00 2010-09-14 23:00:00	Rc:NDF Tc:NDF Qp:NDF	NP	NDF	NDF	0.49 8 1.19
2010-09-16 02:00:00 2010-09-20 10:00:00	Rc:NDF Tc:NDF Qp:NDF	0.03 8 0.12	0.03 8 0.02	0.08 6 0.14	0.15 12 0.16
2010-09-24 16:00:00 2010-09-28 03:00:00	Rc:0.02 Tc:3 Qp:0.05	0.05 25 0.05	0.04 6 0.09	0.14 20 0.39	0.51 3 2.84

Appendix A3

Event start Event end (yyyy-mm-dd hh)	HOAL	Wimitzbach	Perschling	Gail	Dornbirnerach
2010-09-29 10:00:00 2010-10-02 09:00:00	Rc:0.08 Tc:8 Qp:0.03	NP	NP	NP	0.13 8 0.14
2010-10-16 05:00:00 2010-10-19 00:00:00	Rc:0.03 Tc:3 Qp:0.03	0.14 30 0.04	0.05 28 0.02	MP	0.24 8 0.2
2010-10-19 22:00:00 2010-10-22 07:00:00	Rc:0.03 Tc:3 Qp:0.03	NP	NP	NP	0.29 18 0.35
2010-10-24 04:00:00 2010-10-27 10:00:00	Rc:0.03 Tc:3 Qp:0.03	0.04 18 0.06	0.15 20 0.03	NDF	0.45 25 0.28
2010-11-07 14:00:00 2010-11-12 01:00:00	Rc:NDF Tc:NDF Qp:NDF	0.06 18 0.1	0.18 6 0.02	NDF	0.12 15 0.13
2010-11-11 20:00:00 2010-11-14 21:00:00	Rc:0.02 Tc:2 Qp:0.03	NP	strange flow	NDF	0.64 6 1.07
2010-11-15 17:00:00 2010-11-18 17:00:00	Rc:NDF Tc:NDF Qp:NDF	NDF	NP	0.22 20 0.33	0.23 6 0.56
2011-01-12 14:00:00 2011-01-16 00:00:00	Rc:0.25 Tc:3 Qp:0.48	NDF	0.18 5 0.21	NDF	1 3 3.05
2011-02-26 19:00:00 2011-03-04 03:00:00	Rc:NP Tc:NP Qp:NP	NDF	NP	NDF	0.44 20 0.13
2011-03-16 09:00:00 2011-03-20 08:00:00	Rc:0.06 Tc:12 Qp:0.07	0.06 20 0.06	0.12 5 0.23	NDF	0.64 5 3.59
2011-04-04 06:00:00 2011-04-05 11:00:00	Rc:NDF Tc:NDF Qp:NDF	NDF	NP	0.22 15 0.27	0.66 1 4.07
2011-04-12 07:00:00 2011-04-14 11:00:00	Rc:NP Tc:NP Qp:NP	NDF	NDF	NDF	0.32 4 0.44
2011-05-01 04:00:00 2011-05-05 13:00:00	Rc:0.03 Tc:4 Qp:0.02	NDF	NDF	NDF	0.12 15 0.13
2011-05-12 16:00:00 2011-05-14 02:00:00	Rc:MQ Tc:MQ Qp:MQ	NDF	0.01 5 0.02	NDF	NDF
2011-05-14 11:00:00 2011-05-17 05:00:00	Rc:MQ Tc:MQ Qp:MQ	0.04 35 0.03	0.02 9 0.02	0.25 35 0.31	0.43 5 1.96
2011-05-26 22:00:00 2011-05-30 08:00:00	Rc:0.02 Tc:5 Qp:0.08	0.03 17 0.05	0.01 2 0.07	0.19 20 0.52	0.4 9 0.73
2011-05-31 14:00:00 2011-06-04 04:00:00	Rc:0.02 Tc:3 Qp:0.02	NDF	0.02 7 0.06	NDF	0.41 3 2.8
2011-06-06 10:00:00 2011-06-07 13:00:00	Rc:NP Tc:NP Qp:NP	NDF	NP	0.42 18 0.28	0.36 8 0.27
2011-06-07 12:00:00 2011-06-10 14:00:00	Rc:0.02 Tc:4 Qp:0.02	0.02 10 0.04	0.03 15 0.02	0.29 20 0.42	0.36 4 0.9

Appendix A3

Event start Event end (yyyy-mm-dd hh)	HOAL	Wimitzbach	Perschling	Gail	Dornbirnerach
2011-06-17 19:00:00 2011-06-20 21:00:00	Rc:0.01 Tc:4 Qp:0.02	0.02 12 0.08	0.03 15 0.03	0.12 12 0.38	0.81 2 6.67
2011-06-22 16:00:00 2011-06-25 15:00:00	Rc:NP Tc:NP Qp:NP	NDF	0.03 4 0.13	0.17 8 0.56	0.25 8 0.6
2011-06-29 23:00:00 2011-07-01 03:00:00	Rc:NP Tc:NP Qp:NP	NP	NP	NP	0.45 1 6.94
2011-07-05 01:00:00 2011-07-09 12:00:00	Rc:0.01 Tc:1 Qp:0.03	NDF	NDF	NDF	0.17 5 0.54
2011-07-10 21:00:00 2011-07-13 12:00:00	Rc:0.01 Tc:1 Qp:0.02	0.05 10 0.06	NP	0.08 9 0.12	MP
2011-07-13 04:00:00 2011-07-17 13:00:00	Rc:NDF Tc:NDF Qp:NDF	0.07 10 0.07	NP	0.07 6 0.22	0.86 3 4.43
2011-07-17 11:00:00 2011-07-18 18:00:00	Rc:NDF Tc:NDF Qp:NDF	NDF	NDF	NDF	0.31 4 1.08
2011-07-19 15:00:00 2011-07-21 12:00:00	Rc:NP Tc:NP Qp:NP	NDF	NDF	NDF	0.74 4 2.13
2011-07-21 00:00:00 2011-07-23 17:00:00	Rc:0.01 Tc:2 Qp:0.02	NDF	0.02 10 0.01	0.24 25 0.11	0.36 6 0.89
2011-07-23 06:00:00 2011-07-27 11:00:00	Rc:0.01 Tc:3 Qp:0.03	0.04 20 0.07	0.03 10 0.03	0.24 30 0.19	0.59 3 2.1
2011-07-30 17:00:00 2011-08-03 02:00:00	Rc:NDF Tc:NDF Qp:NDF	NP	0.04 25 0.03	NP	NP
2011-08-03 11:00:00 2011-08-06 01:00:00	Rc:0.02 Tc:4 Qp:0.06	0.05 20 0.04	0.07 22 0.02	0.11 10 0.1	0.11 7 0.18
2011-08-05 13:00:00 2011-08-06 21:00:00	Rc:NP Tc:NP Qp:NP	NP	NP	0.09 10 0.11	0.16 15 0.08
2011-08-07 00:00:00 2011-08-11 12:00:00	Rc:0.01 Tc:2 Qp:0.03	0.05 4 0.22	strange flow	0.12 6 0.36	0.47 3 2.47
2011-08-14 18:00:00 2011-08-18 02:00:00	Rc:NDF Tc:NDF Qp:NDF	NDF	0.03 24 0.02	0.09 6 0.15	0.29 6 0.82
2011-08-27 00:00:00 2011-08-29 14:00:00	Rc:0.01 Tc:2 Qp:0.02	NDF	NDF	0.11 14 0.09	0.18 4 0.57
2011-09-02 15:00:00 2011-09-03 17:00:00	Rc:NP Tc:NP Qp:NP	0.07 9 0.06	NP	NP	NDF
2011-09-04 15:00:00 2011-09-07 06:00:00	Rc:NP Tc:NP Qp:NP	NDF	0.01 4 0.03	NDF	0.45 3 2.61
2011-09-08 19:00:00 2011-09-13 09:00:00	Rc:0.01 Tc:2 Qp:0.02	NP	NDF	NP	0.19 4 0.58

Appendix A3

Event start Event end (yyyy-mm-dd hh)	HOAL	Wimitzbach	Perschling	Gail	Dornbirnerach
2011-09-14 05:00:00 2011-09-16 02:00:00	Rc:NP Tc:NP Qp:NP	0.05 15 0.04	0.03 17 0.01	0.04 12 0.08	0.43 12 0.27
2011-09-16 22:00:00 2011-09-17 16:00:00	Rc:NP Tc:NP Qp:NP	NP	NP	NP	0.26 4 0.88
2011-09-17 16:00:00 2011-09-18 06:00:00	Rc:NP Tc:NP Qp:NP	NP	NP	NP	0.31 4 1.49
2011-09-18 04:00:00 2011-09-23 15:00:00	Rc:0.01 Tc:2 Qp:0.05	MP	0.03 10 0.05	0.09 4 0.78	1 4 4.19
2011-10-06 16:00:00 2011-10-07 17:00:00	Rc:0.01 Tc:1 Qp:0.03	MP	MP	MP	MP
2011-10-10 02:00:00 2011-10-11 17:00:00	Rc:0.02 Tc:4 Qp:0.02	NP	MP	NDF	MP
2011-10-12 09:00:00 2011-10-14 17:00:00	Rc:0.03 Tc:3 Qp:0.11	NP	MP	NP	MP
2011-11-06 10:00:00 2011-11-13 03:00:00	Rc:NP Tc:NP Qp:NP	NP	NP	0.8 65 0.19	NP
2011-12-05 01:00:00 2011-12-06 15:00:00	Rc:NDF Tc:NDF Qp:NDF	NDF	NDF	NP	0.19 4 0.39
2011-12-07 07:00:00 2011-12-09 13:00:00	Rc:0.02 Tc:2 Qp:0.04	NP	NDF	NDF	1 8 0.56
2011-12-12 11:00:00 2011-12-14 09:00:00	Rc:0.01 Tc:2 Qp:0.02	NDF	NDF	NDF	0.22 10 0.15
2011-12-16 04:00:00 2011-12-19 14:00:00	Rc:0.1 Tc:25 Qp:0.03	NDF	0.1 1 0.05	NDF	0.86 4 1.18
2011-12-21 09:00:00 2011-12-24 04:00:00	Rc:NDF Tc:NDF Qp:NDF	NP	NDF	NP	1 2 2.06
2011-12-31 03:00:00 2012-01-02 13:00:00	Rc:NDF Tc:NDF Qp:NDF	NP	NDF	NP	1 4 3.04
2012-01-02 13:00:00 2012-01-03 19:00:00	Rc:NDF Tc:NDF Qp:NDF	NDF	NDF	NDF	0.51 8 0.73
2012-01-04 05:00:00 2012-01-05 11:00:00	Rc:NDF Tc:NDF Qp:NDF	NDF	NDF	NP	0.37 6 0.39
2012-01-05 01:00:00 2012-01-08 00:00:00	Rc:0.1 Tc:31.99 Qp:0.03	NDF	NDF	NDF	0.11 7 0.26
2012-01-19 04:00:00 2012-01-21 15:00:00	Rc:0.14 Tc:5 Qp:0.27	NP	0.2 12 0.13	NP	strange flow
2012-01-20 21:00:00 2012-01-23 20:00:00	Rc:0.14 Tc:10 Qp:0.15	NP	0.19 6 0.25	NP	0.92 12 0.7

Appendix A3

Event start Event end (yyyy-mm-dd hh)	HOAL	Wimitzbach	Perschling	Gail	Dornbirnerach
2012-02-25 11:00:00 2012-02-27 22:00:00	Rc:MP Tc:MP Qp:MP	NDF	NDF	NDF	0.61 10 0.74
2012-04-11 04:00:00 2012-04-13 14:00:00	Rc:0.01 Tc:2 Qp:0.02	0.03 20 0.03	NDF	NDF	0.21 13 0.41
2012-04-15 21:00:00 2012-04-19 09:00:00	Rc:NDF Tc:NDF Qp:NDF	NDF	0.14 10 0.15	NDF	NDF
2012-05-03 17:00:00 2012-05-05 08:00:00	Rc:0.01 Tc:2 Qp:0.04	NDF	0.01 5 0.04	NDF	NDF
2012-05-12 01:00:00 2012-05-14 03:00:00	Rc:0.01 Tc:2 Qp:0.02	0.02 15 0.04	NDF	NDF	0.33 5 1.1
2012-05-22 19:00:00 2012-05-25 13:00:00	Rc:0.01 Tc:1 Qp:0.03	NDF	NDF	NDF	0.29 5 0.69
2012-05-31 20:00:00 2012-06-02 15:00:00	Rc:0.01 Tc:2 Qp:0.03	NDF	NDF	NDF	NDF
2012-06-03 15:00:00 2012-06-06 14:00:00	Rc:0.01 Tc:2 Qp:0.03	NDF	NDF	0.07 7 0.19	0.52 2 5.45
2012-06-07 18:00:00 2012-06-11 12:00:00	Rc:0.01 Tc:3 Qp:0.02	NP	0.01 3 0.03	NP	0.39 4 1.6
2012-06-11 10:00:00 2012-06-14 16:00:00	Rc:0.01 Tc:2 Qp:0.04	NP	0.08 3 0.51	0.1 15 0.19	0.49 3 2.2
2012-06-20 12:00:00 2012-06-21 14:00:00	Rc:0.01 Tc:1 Qp:0.03	NP	0.03 2 0.17	0.05 4 0.16	NDF
2012-06-21 18:00:00 2012-06-23 20:00:00	Rc:NP Tc:NP Qp:NP	0.02 10 0.02	NP	0.04 6 0.13	0.12 13 0.14
2012-06-22 16:00:00 2012-06-24 13:00:00	Rc:0.01 Tc:2 Qp:0.03	NDF	0.02 12 0.03	0.06 8 0.11	NP
2012-06-24 16:00:00 2012-06-26 14:00:00	Rc:0.01 Tc:2 Qp:0.02	0.04 18 0.02	0.03 8 0.03	NDF	0.37 4 2.06
2012-07-03 16:00:00 2012-07-05 19:00:00	Rc:NP Tc:NP Qp:NP	NP	0.02 3 0.05	NP	0.18 4 1.33
2012-07-06 22:00:00 2012-07-09 00:00:00	Rc:NP Tc:NP Qp:NP	NP	0.01 15 0.02	NP	0.3 6 0.54
2012-07-08 19:00:00 2012-07-10 13:00:00	Rc:NP Tc:NP Qp:NP	NDF	NDF	0.03 2 0.13	0.29 7 0.54
2012-07-11 11:00:00 2012-07-12 09:00:00	Rc:NDF Tc:NDF Qp:NDF	NDF	NP	0.05 3 0.2	NP
2012-07-12 18:00:00 2012-07-14 16:00:00	Rc:NDF Tc:NDF Qp:NDF	0.02 15 0.04	NDF	0.13 5 0.32	NDF

Appendix A3

Event start Event end (yyyy-mm-dd hh)	HOAL	Wimitzbach	Perschling	Gail	Dornbirnerach
2012-07-14 17:00:00 2012-07-18 00:00:00	Rc:0.02 Tc:2 Qp:0.01	0.03 22 0.07	NDF	NDF	0.2 5 0.32
2012-07-19 14:00:00 2012-07-20 08:00:00	Rc:0 Tc:1 Qp:0.03	NDF	NDF	NDF	NP
2012-07-20 07:00:00 2012-07-24 05:00:00	Rc:0.01 Tc:2 Qp:0.03	strange flow	0.02 7 0.04	0.23 12 0.76	0.21 12 0.15
2012-07-25 04:00:00 2012-07-26 22:00:00	Rc:0.01 Tc:2 Qp:0.02	NDF	0.04 5 0.15	NDF	NP
2012-07-26 03:00:00 2012-07-26 16:00:00	Rc:0.01 Tc:2 Qp:0.04	NP	NP	NP	NP
2012-07-26 12:00:00 2012-07-27 19:00:00	Rc:0.01 Tc:3 Qp:0.04	NP	NP	NP	NP
2012-07-28 09:00:00 2012-07-31 14:00:00	Rc:0.02 Tc:12 Qp:0.03	NDF	NP	0.11 4 0.17	0.09 5 0.16
2012-07-30 15:00:00 2012-08-01 07:00:00	Rc:NP Tc:NP Qp:NP	NDF	NP	0.06 4 0.21	NP
2012-08-02 19:00:00 2012-08-05 19:00:00	Rc:0.01 Tc:2 Qp:0.03	NDF	0.01 6 0.03	0.06 8 0.13	0.1 8 0.09
2012-08-06 12:00:00 2012-08-07 20:00:00	Rc:NDF Tc:NDF Qp:NDF	NDF	NDF	NDF	0.27 3 1.7
2012-08-20 12:00:00 2012-08-21 16:00:00	Rc:NP Tc:NP Qp:NP	NP	NP	NP	0.07 4 0.23
2012-08-22 20:00:00 2012-08-23 15:00:00	Rc:NDF Tc:NDF Qp:NDF	NDF	NDF	NDF	0.06 4 0.23
2012-08-23 15:00:00 2012-08-24 21:00:00	Rc:0 Tc:1 Qp:0.02	NP	NP	NP	0.18 10 0.27
2012-08-24 21:00:00 2012-08-25 14:00:00	Rc:NP Tc:NP Qp:NP	NP	NP	NP	0.32 3 1.73
2012-08-25 14:00:00 2012-08-27 13:00:00	Rc:0.01 Tc:1 Qp:0.03	NDF	0.01 4 0.01	0.04 4 0.13	0.56 2 5.62
2012-08-30 12:00:00 2012-09-04 03:00:00	Rc:0.01 Tc:1 Qp:0.03	0.05 20 0.07	0.02 10 0.02	0.1 6 0.28	0.36 4 1.19
2012-09-05 11:00:00 2012-09-07 13:00:00	Rc:0.02 Tc:6 Qp:0.04	NP	0 2 0.03	NP	0.1 5 0.13
2012-09-12 00:00:00 2012-09-17 09:00:00	Rc:0.02 Tc:4 Qp:0.07	0.08 100 0.06	0.03 8 0.07	0.07 6 0.37	0.58 8 1.98
2012-09-18 18:00:00 2012-09-21 15:00:00	Rc:0.01 Tc:1 Qp:0.03	NDF	0.03 7 0.1	0.06 5 0.2	0.33 3 2.06

Appendix A3

Event start Event end (yyyy-mm-dd hh)	HOAL	Wimitzbach	Perschling	Gail	Dornbirnerach
2012-09-21 21:00:00 2012-09-23 21:00:00	Rc:NDF Tc:NDF Qp:NDF	NP	NP	NP	0.44 6 1.28
2012-09-24 09:00:00 2012-09-26 09:00:00	Rc:NDF Tc:NDF Qp:NDF	NDF	NDF	0.06 3 0.27	0.31 15 0.3
2012-09-26 10:00:00 2012-09-28 16:00:00	Rc:NP Tc:NP Qp:NP	NDF	NP	0.18 15 0.26	0.32 4 1.23
2012-10-07 04:00:00 2012-10-08 10:00:00	Rc:0.01 Tc:1 Qp:0.03	NP	MP	NP	MP
2012-10-12 11:00:00 2012-10-15 07:00:00	Rc:0.02 Tc:2 Qp:0.02	NP	MP	NP	MP
2012-10-16 00:00:00 2012-10-19 18:00:00	Rc:0.02 Tc:2 Qp:0.03	MP	NP	MP	MP
2012-11-04 15:00:00 2012-11-08 06:00:00	Rc:0.01 Tc:2 Qp:0.02	NDF	0.05 8 0.08	0.37 6 0.96	0.33 4 1.16
2012-11-10 21:00:00 2012-11-14 23:00:00	Rc:0.04 Tc:32.35 Qp:0.02	NDF	NDF	0.25 15 0.93	0.5 4 1.43
2012-12-22 19:00:00 2012-12-26 01:00:00	Rc:0.1 Tc:10 Qp:0.13	NDF	strange flow	NDF	0.91 6 2.28
2012-12-27 12:00:00 2012-12-30 11:00:00	Rc:0.02 Tc:3 Qp:0.03	NP	0.17 12 0.09	NP	0.36 8 0.41
2013-01-03 20:00:00 2013-01-09 14:00:00	Rc:0.17 Tc:10 Qp:0.25	NP	0.23 7 0.48	NDF	0.71 7 0.91
2013-01-29 08:00:00 2013-01-31 16:00:00	Rc:0.27 Tc:5 Qp:0.74	NDF	0.52 10 0.68	NDF	1 2 1.63
2013-02-01 04:00:00 2013-02-04 00:00:00	Rc:0.09 Tc:10 Qp:0.08	NDF	0.11 15 0.12	NP	0.54 2 2.49
2013-02-04 08:00:00 2013-02-07 11:00:00	Rc:0.17 Tc:15 Qp:0.07	NP	NP	NP	strange flow
2013-04-18 20:00:00 2013-04-22 19:00:00	Rc:0.04 Tc:3 Qp:0.13	NP	0.18 15 0.21	melt wave	melt wave
2013-05-02 14:00:00 2013-05-04 23:00:00	Rc:NDF Tc:NDF Qp:NDF	NP	0.02 4 0.06	melt wave	0.33 6 1.03
2013-05-07 00:00:00 2013-05-08 12:00:00	Rc:0.01 Tc:1 Qp:0.05	NDF	0.03 6 0.04	NDF	melt wave
2013-05-11 07:00:00 2013-05-13 13:00:00	Rc:0.04 Tc:2 Qp:0.07	NDF	strange flow	NDF	0.57 8 0.64
2013-05-17 17:00:00 2013-05-20 01:00:00	Rc:0.03 Tc:1 Qp:0.15	NDF	NP	0.21 12 0.49	NDF

Appendix A3

Event start Event end (yyyy-mm-dd hh)	HOAL	Wimitzbach	Perschling	Gail	Dornbirnerach
2013-05-21 17:00:00 2013-05-24 23:00:00	Rc:NDF Tc:NDF Qp:NDF	NDF	NDF	NDF	0.41 4 1.48
2013-05-26 15:00:00 2013-05-29 22:00:00	Rc:0.06 Tc:10 Qp:0.04	NDF	NDF	NDF	0.55 12 0.72
2013-05-30 17:00:00 2013-06-02 00:00:00	Rc:0.19 Tc:2 Qp:0.46	NDF	0.17 12 0.15	NDF	0.98 2 7.77
2013-06-01 09:00:00 2013-06-06 04:00:00	Rc:0.24 Tc:1 Qp:1.3	NDF	0.24 2 0.89	NDF	1 2 11.15
2013-06-09 15:00:00 2013-06-12 08:00:00	Rc:0.05 Tc:1 Qp:0.21	NP	MP	0.35 25 0.28	MP
2013-06-22 10:00:00 2013-06-23 03:00:00	Rc:0.03 Tc:0.5 Qp:0.51	NDF	NDF	NDF	NDF
2013-06-23 16:00:00 2013-06-27 06:00:00	Rc:0.33 Tc:1 Qp:3.05	NDF	0.17 4 1.81	0.12 10 0.39	0.48 3 2.63
2013-06-27 12:00:00 2013-06-29 03:00:00	Rc:NP Tc:NP Qp:NP	NP	NP	0.19 16 0.22	0.17 6 0.51
2013-06-29 09:00:00 2013-07-01 05:00:00	Rc:NP Tc:NP Qp:NP	NP	NDF	NP	0.5 4 1.8
2013-07-02 17:00:00 2013-07-03 12:00:00	Rc:NP Tc:NP Qp:NP	NDF	NDF	NDF	0.18 7 0.35
2013-07-03 11:00:00 2013-07-05 10:00:00	Rc:0.03 Tc:2 Qp:0.08	NDF	NDF	NDF	0.42 6 0.89
2013-07-05 14:00:00 2013-07-07 12:00:00	Rc:NDF Tc:NDF Qp:NDF	NP	0.06 12 0.06	NP	NP
2013-07-10 18:00:00 2013-07-12 06:00:00	Rc:0.03 Tc:1 Qp:0.23	NDF	0.05 3 0.21	NP	NP
2013-07-23 17:00:00 2013-07-24 18:00:00	Rc:NP Tc:NP Qp:NP	NP	NP	NDF	0.11 2 1.84
2013-07-29 08:00:00 2013-07-31 00:00:00	Rc:NP Tc:NP Qp:NP	NP	0.02 5 0.04	NP	0.17 2 1.36
2013-08-04 10:00:00 2013-08-06 15:00:00	Rc:0.01 Tc:1 Qp:0.09	NP	0.02 10 0.03	NP	0.07 5 0.06
2013-08-08 19:00:00 2013-08-11 00:00:00	Rc:0.02 Tc:1 Qp:0.06	NP	0.03 6 0.09	NDF	0.2 5 0.56
2013-08-12 19:00:00 2013-08-15 20:00:00	Rc:NDF Tc:NDF Qp:NDF	NDF	0.01 10 0.02	0.04 8 0.1	strange flow
2013-08-19 07:00:00 2013-08-21 05:00:00	Rc:0.01 Tc:1 Qp:0.04	NDF	0.02 5 0.1	0.04 4 0.21	0.21 4 0.74

Appendix A3

Event start Event end (yyyy-mm-dd hh)	HOAL	Wimitzbach	Perschling	Gail	Dornbirnerach
2013-08-24 22:00:00 2013-08-27 06:00:00	Rc:0.02 Tc:1 Qp:0.1	NDF	NDF	0.06 6 0.17	0.21 4 0.68
2013-08-27 08:00:00 2013-08-31 05:00:00	Rc:0.04 Tc:1 Qp:0.17	NDF	0.06 4 0.23	0.32 30 0.1	0.31 3 2.62
2013-09-08 17:00:00 2013-09-10 02:00:00	Rc:NP Tc:NP Qp:NP	NDF	NP	NDF	0.18 2 1.08
2013-09-11 20:00:00 2013-09-14 15:00:00	Rc:NDF Tc:NDF Qp:NDF	MP	0.04 15 0.02	MP	0.76 3 3.18
2013-09-16 11:00:00 2013-09-18 01:00:00	Rc:0.02 Tc:2 Qp:0.07	NDF	0.04 5 0.13	NDF	0.73 4 3.38
2013-09-17 21:00:00 2013-09-18 17:00:00	Rc:NP Tc:NP Qp:NP	NP	NDF	NP	0.34 4 0.99
2013-09-18 00:00:00 2013-09-20 09:00:00	Rc:0.03 Tc:2 Qp:0.05	NP	0.11 10 0.13	NP	0.96 2 6.34
2013-09-25 22:00:00 2013-09-28 10:00:00	Rc:0.02 Tc:3 Qp:0.03	NP	NP	NP	0.08 3 0.2
2012-10-12 11:00:00 2012-10-15 07:00:00	Rc:0.02 Tc:2 Qp:0.02	NP	MP	NP	MP
2013-11-03 02:00:00 2013-11-05 00:00:00	Rc:0.02 Tc:2 Qp:0.04	NDF	NDF	NDF	0.36 3 1
2013-11-04 23:00:00 2013-11-05 19:00:00	Rc:NDF Tc:NDF Qp:NDF	NDF	NDF	NDF	0.31 10 0.38
2013-11-05 19:00:00 2013-11-08 12:00:00	Rc:0.03 Tc:7 Qp:0.04	NDF	NDF	NDF	0.81 4 1.25
2013-11-08 22:00:00 2013-11-13 05:00:00	Rc:0.04 Tc:11 Qp:0.04	MP	0.07 15 0.08	strange flow	0.38 4 1.06
2013-11-23 14:00:00 2013-11-26 04:00:00	Rc:0.08 Tc:8 Qp:0.15	NDF	0.23 4 0.75	NP	NDF